SINGLE-STEP ANALYSIS BY CAPILLARY ELECTROPHORESIS

Single-step Analysis of Metabolites by Capillary Electrophoresis using On-line Sample Preconcentration with Chemical Derivatization

By

ADAM S. PTOLEMY, BSc.

A Thesis

Submitted to the School of Graduate Studies

In Partial Fulfilment of the Requirements

for the Degree

Doctorate of Philosophy

McMaster University

DOCTORATE OF PHILOSOPHY (2008) McMaster University

(Chemistry) Hamilton, Ontario

TITLE: Single-step Analysis of Metabolites by Capillary Electrophoresis using On-line Sample Preconcentration with Chemical Derivatization

AUTHOR: Adam S. Ptolemy, B.Sc. (Brock University)

SUPERVISOR: Dr. Philip Britz-McKibbin

NUMBER OF PAGES: xxii, 161

Abstract

New strategies for integrating sample pretreatment with chemical analyses under a single format is required for rapid, sensitive and enantioselective analyses of low abundance metabolites in complex biological samples. Capillary electrophoresis (CE) offers a unique environment for controlling analyte/reagent band dispersion and electromigration properties using a discontinuous electrolyte system allowing for highly efficient separations to be achieved. A fundamental study of the thermodynamic and electrokinetic parameters influencing enantioselectivity in chiral CE separation is first examined. A new strategy for single-step analysis of low abundance metabolites via on-line sample preconcentration with chemical derivatization by CE (SPCD-CE) is then detailed within. In-capillary sample preconcentration serves to enhance concentration sensitivity via electrokinetic focusing of long sample injection volumes for lower detection limits, whereas chemical derivatization by zone passing of single or multiple reagents is used to expand detectability and selectivity, notably for enantiomeric resolution of metabolites lacking intrinsic chromophores. Together, on-line SPCD-CE can provide over a 100-fold improvement in concentration sensitivity, shorter total analysis times, reduced sample handling and improved reliability for a variety of biologically relevant amino acid and amino sugar metabolites, which is also amenable to automated high-throughput screening. The basic method development and optimization parameters relevant to SPCD-CE, including applications to bacterial metabolite flux and biomarker analyses are discussed. Insight into the mechanism of analyte focusing and

labelling during electromigration by SPCD-CE is also presented, as well as future directions for continued research using this unique integrated analytical platform.

Acknowledgments

I would first like to acknowledge my supervisor Dr. Philip Britz-McKibbin for imparting his knowledge and support during the course of this thesis. His patience, friendship and wisdom facilitated my growth both professionally and personally. I thank him for proving me this opportunity to study and mature under his supervision.

The assistance of all present (Jennilee Gavina, Richard Lee and Ken Chalcraft) and past (Sheeba Samson, Giselle Segui-Lines, Kathryn Chan, Tenisha Mitchell, Lara Tran, Elyse Bernard, Jason D'Amaral, Kiran Lad, Mohamed Al Husseiny, Liliana Niewczas, Cassendra Mills, Marianne LeBihan, Nicolas Gernigon, Claire Kaiser and Audrey Kerdudo) group members were instrumental in the scientific advancements achieved in this thesis. As was the guidance of my PhD Advisory Committee Members; Dr. Paul Berti and Dr. Brian McCarry.

McMaster University and the federal and provincial governmental agencies providing; OGSST, OGS, PREA and NSERC scholarships are thanked for their financial support.

I am convinced that this thesis would not have been completed without the support of my family, graduate student colleagues and friends (too numerous to mention by name).

To each and every one of you, I will be forever indebted for your assistance.

Thank you.

The following *Chapter* material has been published previously and is reprinted with the written permission:

Chapter I:

- Reprinted in part from: *J. Chromatogr. A*, **1106**, A. S. Ptolemy and P. Britz-McKibbin, *Sample preconcentration with chemical derivatization in capillary electrophoresis: Capillary as preconcentrator, microreactor and chiral selector for high-throughput metabolite* screening, 7-18, Copyright (2006) with permission from Elsevier.

- Reproduced in part with permission from: *Anal. Chem.*, **79**, R. Lee, A. S. Ptolemy, L. Niewczas and P. Britz-McKibbin, *Integrative metabolomics for characterizing unknown low-abundance metabolites by capillary electrophoresis-mass spectrometry with computer simulations*, 403-415, Copyright (2007) American Chemical Society.

- Reprinted in part from: *submitted work*, *Analyst*, A.S. Ptolemy and P. Britz-McKibbin, *New advances in on-line sample preconcentration by capillary electrophoresis using dynamic pH junction*, copyright (2008) with permission from the Royal Society of Chemistry.

Chapter III:

- Reprinted from: *Analyst*, **130**, A. S. Ptolemy and P. Britz-McKibbin, *Single-step analysis of low abundance phosphoamino acids via on-line sample preconcentration with chemical derivatization by capillary electrophoresis*, 1263-1270, Copyright (2005) with permission from the Royal Society of Chemistry.

Chapter IV:

- Reprinted from: *Electrophoresis*, **26**, A. S. Ptolemy, M. L. Bihan and P. Britz-McKibbin, *On-line sample preconcentration with chemical derivatization of bacterial biomarkers by capillary electrophoresis: A dual strategy for integrating sample pretreatment with chemical analysis*, 4206-4214, Copyright (2005) with permission from Wiley InterScience.

Chapter V:

- Reprinted from: *Anal. Biochem.*, **354**, A. S. Ptolemy, L. Tran and P. Britz-McKibbin, *Single-step enantioselective amino acid flux analysis by capillary electrophoresis using on-line sample preconcentration with chemical derivatization*, 192-204, Copyright (2006) with permission from Elsevier.

Chapter VI:

- Reprinted in part from: *submitted work*, *Analyst*, A.S. Ptolemy and P. Britz-McKibbin, *New advances in on-line sample preconcentration by capillary electrophoresis using dynamic pH junction*, copyright (2008) with permission from the Royal Society of Chemistry.

Table of Contents

List of Figures

List of Tables

List of Abbreviations

2D	-	Two-dimensional
α	-	Separation selectivity factor
σ	-	Mean of the standard deviation of two analyte peaks
A	-	Analyte
AC	-	Analyte-additive complex
ACE	-	Affinity capillary electrophoresis
ACN	-	Acetonitrile
Ala	-	Alanine
$\mu_{ep}{}^{A}$	-	Apparent electrophoretic mobility
Asp	-	Aspartic acid
β-CD	-	β-cyclodextrin
BGE	-	Background electrolyte
C	-	Additive complexing agent
CBI	-	Cyanobenz[*f*]isoindole
CE	-	Capillary electrophoresis
CEC	-	Capillary electrochromatography
CGE	-	Capillary gel electrophoresis
CZE	-	Capillary zone electrophoresis
Δx	-	Distance between two analyte peak centers
D	-	Diffusion coefficient
DAP	-	Diaminopimelic acid
DIBR	-	Detector-to-injection bandwidth ratio
ε	-	Dielectric constant

E	-	Electric field strength
EOF	-	Electroosmotic flow
ESI-MS	-	Electrospray ionization-mass spectrometry
μ_{eo}	-	Electroosmotic mobility
$\mu_{ep,A}$	-	Electrophoretic mobility of free analyte
$\mu_{ep,AC}$	-	Electrophoretic mobility of the analyte-additive complex
FMOC	-	9-fluorenylmethyloxycarbonyl chloride
GC	-	Gas chromatography
GlcN	-	Glucosamine
GlcN-6P	-	Glucosamine-6-phosphate
Glu	-	Glutamic acid
HPLC	-	High-performance liquid chromatography
HP-β-CD	-	Hydroxypropyl-β-CD
i.d.	-	Internal capillary diameter
IEF	-	Isoelectric focusing
K	-	Apparent association constant
L_d	-	Effective capillary length to the detector
LED	-	Light-emitting diode
LIF	-	Laser-induced fluorescence
LOD	-	Limit of detection
L_t	-	Total capillary length
MA	-	Muramic acid
MALDI	-	Matrix-assisted laser desorption ionization
MCE	-	Microchip electrophoresis

ME	-	2-mercaptoethanol
MEKC	-	Micellar electrokinetic chromatography
μ-TAS	-	Micro-total analysis systems
MPA	-	3-mercaptopropionic acid
MS	-	Mass spectrometry
η	-	Viscosity of the buffer solution
N	-	Number of theoretical plates
NaOH	-	Sodium hydroxide
NDA	-	Naphthalene-2,3-dicaboxaldehyde
NMR	-	Nuclear magnetic resonance
o.d.	-	Outside capillary diameter
OPA	-	*O*-phthalaldehyde
PG	-	Peptidoglycan
pI	-	Isoelectric point
P-Ser	-	*o*-phosphoserine
P-Thr	-	*o*-phosphothreonine
P-Tyr	-	*o*-phosphotyrosine
Q_{eff}	-	Effective charge of the analyte
R_H	-	Hydrodynamic radius of the analyte
Rs	-	Resolution
S-β-CD	-	Sulfated β-cyclodextrin
SDS	-	Sodium dodecyl sulphate
Ser	-	Serine

SPCD-CE	-	Sample preconcentration with chemical derivatization capillary electrophoresis
t_A	-	Apparent migration time of the analyte
t_{eo}	-	Apparent migration time of the electroosmotic flow
t-ITP	-	Transient isotachophoresis
TOF-MS	-	Time-of-flight mass spectrometry
UPLC	-	Ultra-performance liquid chromatography
UV	-	Ultraviolet absorbance spectroscopy
σ_A^2	-	Analyte peak variance produced by adsorption
σ_D^2	-	Analyte peak variance produced by diffusion
σ_E^2	-	Analyte peak variance produced by electrophoretic dispersion
σ_I^2	-	Analyte peak variance produced by injection length
σ_J^2	-	Analyte peak variance produced by Joule heating
σ_O^2	-	Analyte peak variance produced by other effects
σ_T^2	-	Total apparent peak variance
σ_W^2	-	Analyte peak variance produced by width of detection zone
ν	-	Velocity of an ion
V	-	Applied voltage
W	-	Analyte base peak widths
w_{det}	-	Analyte detector bandwidths
w_{inj}	-	Sample injection length
$w_{1/2}$	-	Peak width at half height for an analyte band
ζ	-	Zeta potential

Chapter I

Introduction to Separation Science and Capillary Electrophoresis

I. Introduction to Separation Science and Capillary Electrophoresis

1.1. Separation theory

For a complex sample mixture to be separated into its individual components, solutes must possess unique physicochemical properties which allow them to be distinguished from one another. This diversity of traits that exist among atomic, molecular, polymer and cellular constituents (*i.e.,* analytes) ultimately permits their separation, assuming that the natural law of entropy which promotes diffusion can be overcome.

Fundamentally, there are two active transport processes that govern any separation system: separative and dispersive transport[1]. Dispersive transport, also referred to as band broadening, results from the additive contributions of diffusion, resistance to mass transfer and convection during separation. Separative transport describes the differential velocity of analytes as a result of interaction with their local environment. The specific mechanism of this transport translates unique analyte physiochemical properties into differences in energetic and/or kinetic interaction processes. For instance, differences in densities, boiling points, polarity, molecular size and effective charge can all be exploited to realize separation. Separative transport is fundamental to modern chromatographic, centrifugal and electrophoretic techniques, which take advantage of differences in equilibria (a thermodynamic process) and/or mobility (a kinetic process) to achieve resolution of discrete analytes in a complex mixture. However, a solute must possess significantly different transport properties in order to fully counteract dispersion. Thus, one can holistically view the art and science of separation as the pursuit of a set of

experimental conditions that simultaneously enhance and minimize separative and dispersion transport processes, respectively. Under these optimal conditions, maximum selectivity and high efficiency are achieved to generate high resolution separations. However, a compromise must often be struck between the extent of resolution desired and the total separation time required. Thus, analytical chemists often strive for rapid separations with adequate resolution that is ultimately dependent on sample complexity.

Capillary electrophoresis (CE) currently represents one of the most powerful analytical microseparation techniques available, in terms of its ability to produce high efficiency separations under optimal transport conditions. These features are directly correlated to the physical dimensions of the electrophoretic system and the unique separative mechanisms operative in CE. For instance, the absence of an immobilized stationary phase and the efficient heat dissipation of the narrow bore capillary eliminate the resistance to mass transfer while minimizing heat convection within the electrophoretic separation, both which would contribute to band broadening. In addition, the unique flat profile of the electroosmotic flow (EOF) serves to minimize axial diffusion and enhance separation efficiency compared to pressure-driven chromatographic techniques. Dispersive transport can be further minimized in CE by development of on-line sample preconcentration techniques, such as sample stacking, transient isotachophoresis (t-ITP), sweeping and dynamic pH junction[2]. These techniques serve to minimize and/or counter dispersion by electrokinetic focusing of long sample plugs in a discontinuous electrolyte system, which can also significantly improve detector concentration sensitivity. A fundamental investigation of these techniques and their

application in CE separations will be presented in *Chapter's III, IV* and *V* of the thesis. CE is also unique amongst modern separation platforms as it can simultaneously exploit differences in thermodynamic (equilibria) and electrokinetic (mobility) processes for enhanced selecitivity. This feature exists in capillary electrochromatography (CEC), as well as free solution CE when using soluble additives in the separation buffer, such as surfactants in micellar electrokinetic chromatography (MEKC). The inherent versatility of CE, in terms of optimizing multiple separation parameters by simple changes in electrolyte properties permits the separation of a wide class of analytes, ranging from discrete metal ions to whole organisms, such as bacteria[3]. The advantages of optimal separative transport mechanisms for high efficiency separation of chiral molecules will be discussed in *Chapter's II* and *V*. The history, general principles and separation parameters fundamental to CE will be introduced within the remaining sections of this chapter of the thesis.

1.2. History of capillary electrophoresis

Electrophoresis is defined as the differential movement of charged analytes under an applied electric field. In 1897 Kohlrausch first described the principle of electrophoresis and ionic migration in an electrolyte solution, however it was Tiselius who first experimentally demonstrated the technique in his doctoral thesis in 1930[4, 5]. In this work, Tiselius showed that under an applied electric field, a partial separation of the sample components in a protein mixture contained in a buffer filled tube could be achieved[4, 5]. In a paper published later that year, Svedberg detailed the significance of this electrophoretic work, including the ability to determine the isoelectric point (p*I*) of

several proteins and that the observed relative migration was directly related to a p*I* of a protein under the conditions employed[6]. Interestingly, Svedberg also noted that this electrophoretic technique could be seen as complementary to emerging centrifugation techniques that he himself developed, "The electrophoresis technique worked out by Tiselius has proved very useful for defining the electrochemical difference of such proteins which have the same molecular weight as determined by means of the ultracentrifugal methods."[6] However, despite the intriguing potential of the technique this initial electrophoresis separation system suffered from significant dispersive processes, caused by both convection and thermal diffusion, related to the use of free solutions as the separative medium.

In the following two decades researchers developed several different anti-convection media, which were designed to overcome this limitation by reducing the extent of Joule heating as the major source of band broadening generated within the electrophoretic system. For instance, paper electrophoresis was initially investigated for the separation of small molecules and polyacrylamide and agrose-based gel electrophoresis were also developed at this time. The latter gels permitted the separation of charged polymers based on their differential migration rate via a selective sieving mechanism. Ultimately, gel electrophoresis became a fundamental preparative separation technique for biochemical research, as it permitted the separation of complex samples mixtures derived from protein and nucleic acid sources. However, despite the high separation capacity of two-dimensional (2D) gel electrophoresis, the technique itself is limited by the time-consuming and labour-intensive processes associated with gel

preparation, sample application, staining and quantification.

Parallel to these electrophoretic developments, extensive chromatographic research related to new analytical procedures and modern instrumentation was being conducted. This ultimately resulted in the production of fully automated, commercially available HPLC and GC instruments. The widespread use and general acceptance of these analytical techniques, in a sense, stunted the development of analogous electrophoretic systems. However, one can also view the introduction of the narrow capillaries used in GC and the on-line detectors of HPLC as the basic foundation of analytical technology for which CE was ultimately developed. The emergence of biotechnology also spurred the development of CE as scientists sought new micro-separation platforms, which were capable of analyzing small volumes of complex biological samples to compliment the more established chromatographic techniques. For example, recent developments of automated multiplexed capillary gel electrophoresis systems later revolutionalized high-throughput gene sequencing efforts that contributed to the early completion of the *Human Genome Project*[7].

In 1967, Hjertén, who was a student of Tiselius, performed free solution electrophoresis in methylcellulose coated quartz tubes with internal diameters of 1-3mm[8]. The coating was applied to suppress the electroosmotic flow and the tubes themselves were longitudinally rotated upon the induction of electrophoresis to reduce the thermal convection generated. This work introduced the concept of performing electrophoretic separations in a narrow tubular format, which in 1979 was expanded upon by Mikkers *et al.* who employed narrow inert Teflon tubes[9]. These authors referred to their technique as

"high performance zone electrophoresis" and effectively illustrated that the apparatus was capable of minimizing the relative amount of dispersion seen in previous electrophoretic formats[9]. Two years later, Jorgensen and Lukas performed electrophoresis in fused-silica capillaries with internal diameters on the micron scale (*i.e.*, 75 μm) in what can be considered the inaugural report of *capillary* electrophoresis (CE)[10]. Despite the application of high voltages up to 30 kV, the small internal diameter employed provided efficient heat dissipation due to the large surface-to-volume-ratio of the capillary tube itself. This property permitted rapid separations of high efficiency with apparent theoretical plate numbers (N) exceeding 400,000, as reported for fluorescent derivatives of different amino acids, amines and dipeptides when using CE with laser-induced fluorescence detection[10]. In addition, the small internal capillary diameter required only nanolitre amounts of sample while using inexpensive and non-hazardous aqueous buffer reagents, which is conducive to the quantification of volume-limited biological samples with excellent mass sensitivity. On-line detection was achieved by burning off a small portion of the polyamide capillary coating, which imparts additional flexibility of the otherwise fragile glass column, near the distal end of the capillary. It should be noted that CE when using UV absorbance detection suffers from poor concentration sensitivity due to the small optical pathlength and limited sample volume injected. Regardless, the work by Jorgensen and Lukas[10] represents the beginning stages of CE emerging as a viable analytical format for the separation of complex sample mixtures.

After this initial report, the development of CE flourished in the 1980's with the first automated and commercial CE instrument introduced by Beckman Inc. in 1989. CE

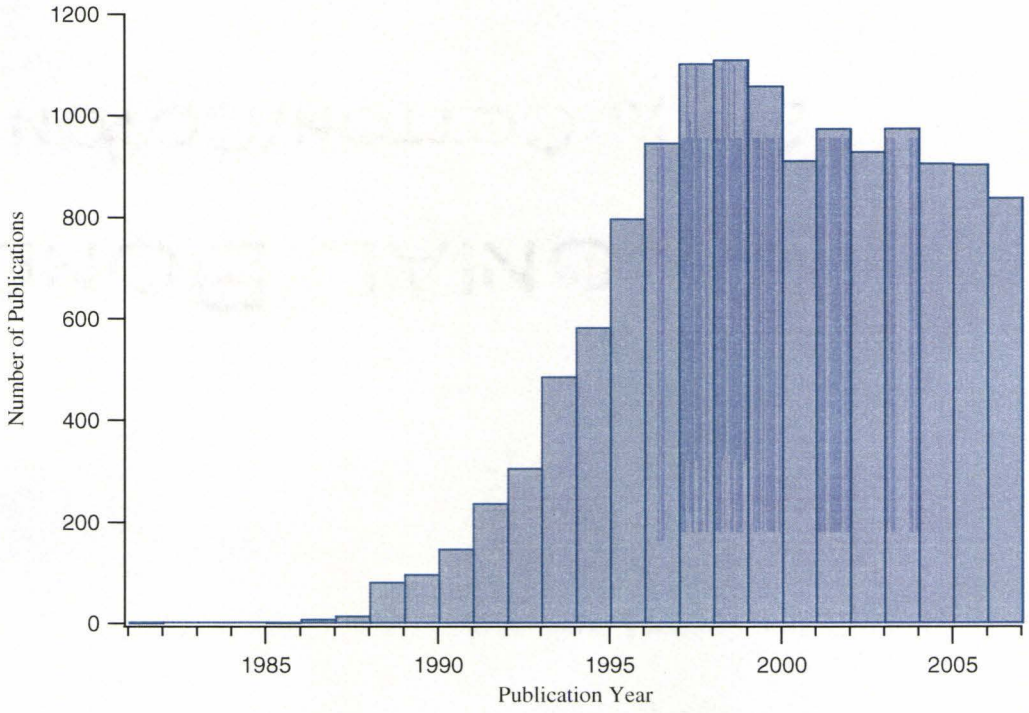

Figure 1.1: Plot of the total publications using CE from 1981 to 2007 from the Web of Science.

research has continued to rapid expand in the twenty-six years since it first appeared in the literature. For instance, a search of the different published research articles cited in the Web of Science (http://apps.isiknowledge.com) containing the words "capillary", "zone" and "electrophoresis" in the article title yielded a total of 13,992 publications from 1981 to 2007. By organizing and analyzing these manuscripts in terms of publication year it is clear that academic CE research peaked in the late 1990's and has remained relatively constant over the early part of the twenty-first century as depicted in *Figure 1.1*. Much of the research efforts today are focused on improving the separation performance, robustness, reliability, concentration sensitivity and selectivity of this powerful analytical technique in order to ultimately expand its applicability to emerging post-genomic

initiatives, drug development, environmental and forensic analyses and clinical screening.

1.3. CE instrumental set-up

A schematic design of a typical CE instrumental set-up is depicted in *Figure 1.2*. The design of a CE instrument is relatively simple and consists of a polyimide-coated fused-silica capillary whose ends are immersed in an inlet and outlet buffer reservoir. After rinsing and conditioning the capillary with a buffer solution, a sample reservoir is typically placed at the inlet side of the capillary and sample is injected via the application of a positive pressure (hydrodynamic injection) or electric potential (electrokinetic injection) for a fixed period of time. Following sample injection, the buffer reservoir is returned to the capillary inlet and electrophoresis is induced through the application of an electric potential supplied by a high voltage power supply connected to the buffer reservoirs via two platinum electrodes. The buffer contained within these reservoirs serves several important purposes; conduction of electricity through electrolyte carriers, providing buffering capacity for pH control due to electrolysis, and tuning the selectivity of the separation. In all work contained within this thesis, detection was performed on-capillary using UV absorbance (*Figure 1.2*). By using narrow bore fused-silica capillaries with internal diameters ranging from 25 to 100 μm, efficient dissipation of Joule heating as a result of buffer ion conduction can be achieved allowing for the use of high applied voltages (0-30 kV) for rapid and highly efficient separations. The small capillary dimensions are also advantageous in terms of buffer consumption (< 0.5 mL) and total sample volume requirements (< 10 nL). In fact, this desire for high efficiency separations has driven the recent development of "ultra-performance" liquid

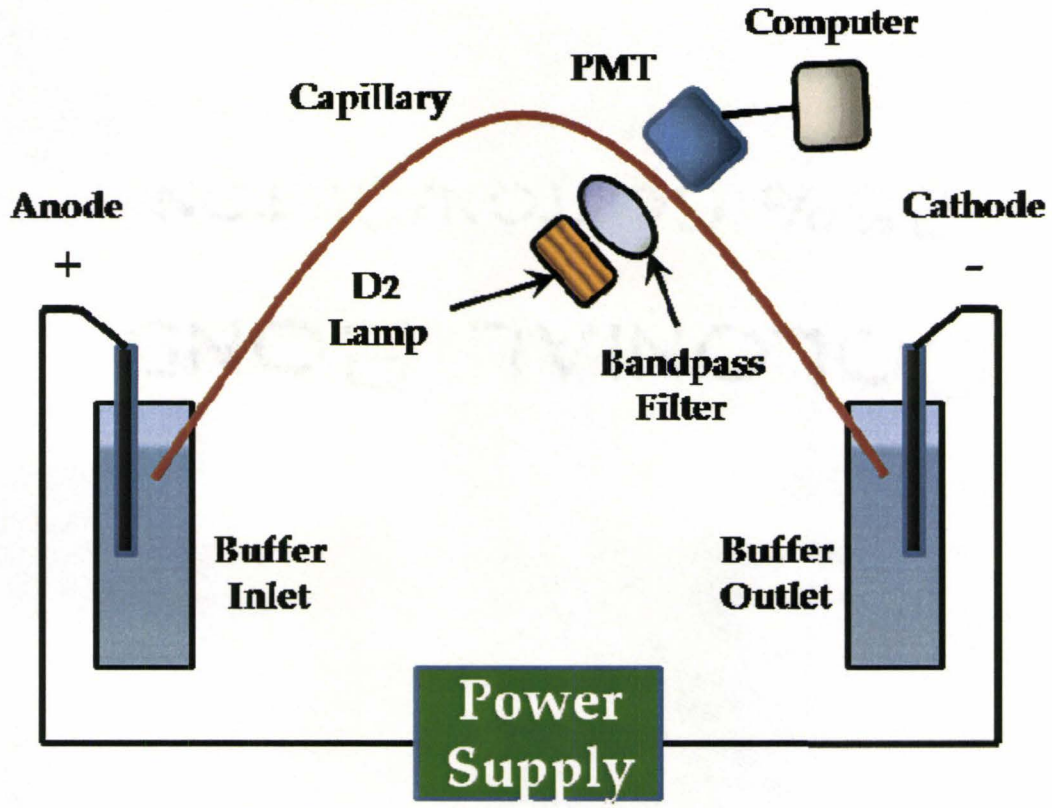

Figure 1.2: Instrumental set-up of capillary electrophoresis with UV absorbance detection

chromatography (UPLC), which employs sub-micron sized chromatographic column packings under higher pressures to achieve improved separation performance relative to conventional HPLC[11]. It should be noted that in CE, a natural electrokinetic pumping mechanism exists that does not suffer from backpressure constraints while providing reduced axial diffusion.

1.4. Electrokinetic phenomena in CE

Separations in CE are governed by two fundamental electrokinetic phenomena namely the electrophoretic mobility of the analyte ($\mu_{ep,A}$) and the electroosmotic mobility (μ_{eo}) or flow (EOF) of the bulk solution. The EOF represents the natural electrokinetic

pumping mechanism of the system that is associated with the properties of the capillary wall and the buffer system employed in the separation, whereas $\mu_{ep,A}$ is directly related to the intrinsic physiochemical properties of the analyte in its local environment. The summation of these two phenomena contributes to the apparent electrophoretic mobility (μ_{ep}^{A}) of an analyte. Provided there is sufficient differences in μ_{ep}^{A}, resolution of a complex mixture can be achieved.

1.4.1. Electrophoretic mobility

Electrophoretic mobility is defined as the velocity of an ion (v) per unit of electric field strength (E). When considering an ion with a spherical shape, $\mu_{ep,A}$ can be correlated to the balance between the viscous drag force of the ion in the bulk solution and the EOF as described by:

$$\mu_{ep,A} = \frac{v}{E} = \frac{Q_{eff}}{6 \cdot \pi \cdot \eta \cdot R_H} \qquad (1)$$

where Q_{eff} represents the effective charge of the analyte, η is the viscosity of the buffer solution, and R_H describes the hydrodynamic radius of the analyte[12]. Selectivity in CE is related to the differences in the direction and magnitude (vector) of $\mu_{ep,A}$. *Equation (1)* shows this property is correlated to the effective charge to size ratio of the analyte in the buffer solution. For instance, small highly charged cations will have a positive high $\mu_{ep,A,}$ whereas large anions with minimal charge have a negative low $\mu_{ep,A}$. Analytes lacking any formal charge (*i.e.*, neutral species) will co-migrate with the EOF without resolution unless charged additives are included in the buffer. Given that the mobility of an analyte in CE is directly related to its charged state, changes in the composition of the buffer

system, such as buffer type, ionic strength and pH can effectively alter the mobility of weakly ionic analytes in order to improve selectivity. For instance, buffer pH represents the most important parameter for achieving resolution in CE and is especially relevant when separating polar species, such as amino acids, whose effective charge is dependent on the characteristic pK_a of the functional groups present.

1.4.2. Electroosmotic flow

The EOF is an electrokinetic phenomenon which can be defined as the bulk flow of solution through the capillary upon voltage application. When the walls of a fused-silica capillary are exposed to water, weakly acidic silanol groups ($pK_a \approx 6.5$) are generated[13]. Thus, the surface of the capillary essentially possesses a net negative charge when a aqueous solution is in contact with the capillary wall above a pH > 3. According to the Debye-Huckle-Stern theory[12] an electric double layer of electrolytes is formed within a short distance (~ 10 - 50 nm) of the negatively charged capillary wall. This layer consists of an initial rigid layer of adsorbed cations (*i.e.,* Stern layer) followed by a mobile layer of cations and anions (*i.e.,* diffuse double layer) as shown in *Figure 1.3.* It should be noted that an excess of cations is present in the Stern layer to effectively neutralize the large negative charge associated with the silanol groups of the capillary wall. *Figure 1.3(a)* represents the electric double layer formed when the pH > 3, however when strongly acidic buffers (pH < 2) are employed, the silanol surface becomes protonated (*i.e.,* neutral) and the EOF is suppressed. In general, the EOF is directly related to the polarity and magnitude of the zeta potential (ζ) near the capillary surface.

Zeta potential is defined as the potential at the slipping plane between the

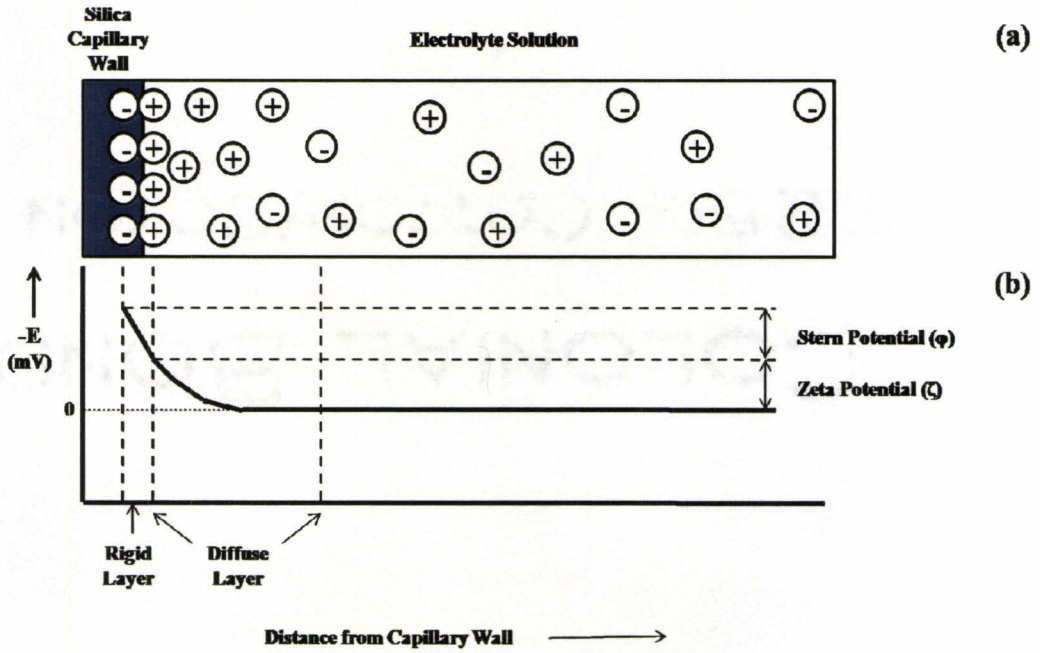

Figure 1.3: Debye-Huckle-Stern model of the electric double layer showing: (a) the diffuse double layer and (b) the zeta potential that generates EOF near the capillary surface under an applied voltage.

adsorbed and diffuse layers coating the inner capillary and decreases exponentially away from the capillary surface, as depicted in *Figure 1.3(b)*, which is directly associated with to the charge density near capillary wall. Upon application of an external voltage perpendicular to the ζ of the capillary surface (in normal polarity: cathode at buffer outlet) a net migration of the cations contained within the diffuse double layer migrates towards the cathode. Since these cations are hydrated, the transfer of bulk water due to the cohesive nature of hydrogen bonding with this migration is a consequence. Once generated within a narrow capillary, the stable EOF acts as an intrinsic electrokinetic pump which typically transports all analytes (including cations, anions and neutrals) past a fixed detector since its magnitude is greater than analyte mobility under most electrolyte conditions:

$$\mu_{eo} = \frac{\varepsilon \cdot \zeta}{6 \cdot \pi \cdot \eta} \qquad (2)$$

where ε represents the dielectric constant, ζ described the zeta potential of the double layer and η is the viscosity of the buffer solution. ζ is primarily dependent on buffer pH and ionic strength conditions since they influence the net capillary surface charge density. In general, low ionic strength alkaline buffer conditions generate a high ζ and thus a strong EOF, whereas high ionic strength acidic buffer conditions suppress EOF.

When capillaries with narrow internal diameters (< 200 μm) are employed, a stable EOF with a flat flow profile is generated, as the uniform charge distribution along of the assembled capillary wall creates a uniform flow velocity across the capillary. This linear flow minimizes analyte band broadening caused by axial diffusion, which leads to higher separation efficiency (*e.g.*, theoretical plate numbers > 10^5) and improved resolution. This flat flow profile is also in direct contrast to the parabolic profiles generated with conventional HPLC systems employing an external pump for sample and solvent delivery, as the differential friction forces along column surface create pressure drops and non-uniform parabolic flow as depicted in *Figure 1.4*.

1.5. Apparent mobility

The apparent electrophoretic mobility (μ_{ep}^{A}) of an analyte within an electrophoretic separation is the vector summation of both $\mu_{ep,A}$ and μ_{eo} as described by:

$$\mu_{ep}^{A} = \mu_{ep,A} + \mu_{eo} \qquad (3)$$

The electrophoretic mobility of an ionic species can be determined experimentally by measuring both the apparent migration time of the analyte and the migration time of a

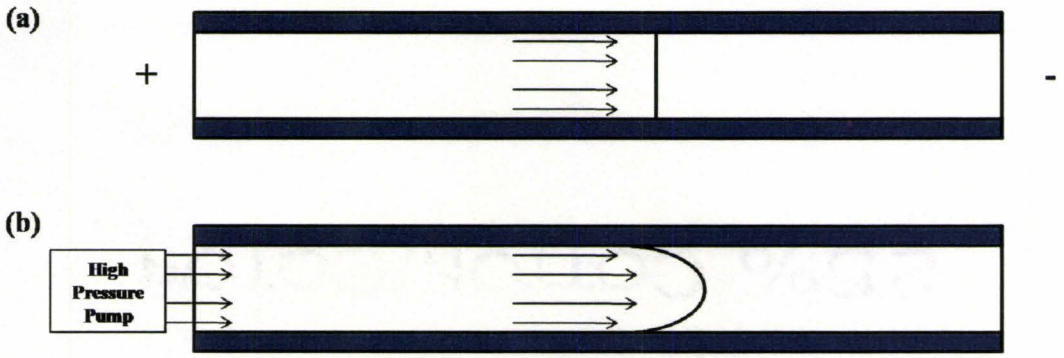

Figure 1.4: Comparison of fluid transport properties (a) a flat electrokinetic EOF profile in CE and (b) a parabolic flow profile generated by a pressure-driven HPLC pump system.

neutral marker, referred to as an EOF marker. Knowledge of these two experimental values and the separation conditions used in CE permits accurate determination of $\mu_{ep,A}$:

$$\mu_{ep,A} = \mu_{ep,A} - \mu_{eo} = \frac{L_t \cdot L_d}{V} = \left(\frac{1}{t_A} - \frac{1}{t_{eo}} \right) \qquad (4)$$

where L_t represents the total capillary length, L_d is the effective length to the detector, V in the applied voltage, and t_A and t_{eo} represent the apparent migration time of the analyte and EOF, respectively. It should be emphasized that $\mu_{ep,A}$ represents a fundamental physicochemical parameter characteristic of an analyte that is a function of the electrolyte conditions such as buffer type, pH, ionic strength, viscosity and temperature. Although apparent migration times in CE typically have larger variability than HPLC or GC due to changes in EOF, $\mu_{ep,A}$ can be measured precisely with a coefficient of variance often under 1 %.

1.6. Capillary zone electrophoresis

Capillary zone electrophoresis (CZE) uses a single continuous buffer for analyte separations and represents the most common operating mode in CE due to its widespread

applicability, versatility and ease of use. The major drawback of CZE is that it suffers for poor concentration sensitivity when detecting low abundance or poorly responsive analytes. To counteract this effect, different on-line sample preconcentration techniques have been developed which employ discontinuous electrolytes to induce analyte focusing within long sample injection plugs. The design, optimization and benefits of these approaches will be discussed in detail later in the thesis. It should be noted that historically many researchers use the acronyms "CZE" and "CE" interchangeably to describe this analytical platform designed to separate of analytes zones prior to detection, which is distinct from other separation modes in CE, such as isotachophoresis (ITP). CE does however, also encompass other modes based on zonal separation conducted under an electrophoretic format, including micellar electrokinetic chromatography (MEKC), affinity capillary electrophoresis (ACE), capillary gel electrophoresis (CGE) and isoelectric focusing (IEF). Indeed, the recent emergence of microfluidic systems has now spurred the development of microchip electrophoresis (MCE) as a convenient format for separation.

A typical CE separation process and electropherogram depicting the separation of a mixture of cationic, neutral and anionic analytes is depicted in *Figure 1.5*. Preceding the detection of these analytes: (A) the capillary was rinsed with a background electrolyte (BGE), (B) a sample was then hydrodynamically or electrokinetically injected and (C) an external voltage was applied across the capillary. Upon voltage application, ionic species in the original sample plug migrate with their characteristic $\mu_{ep,A}$ towards the corresponding electrode, namely cations to the cathode and anions to the anode. Provided

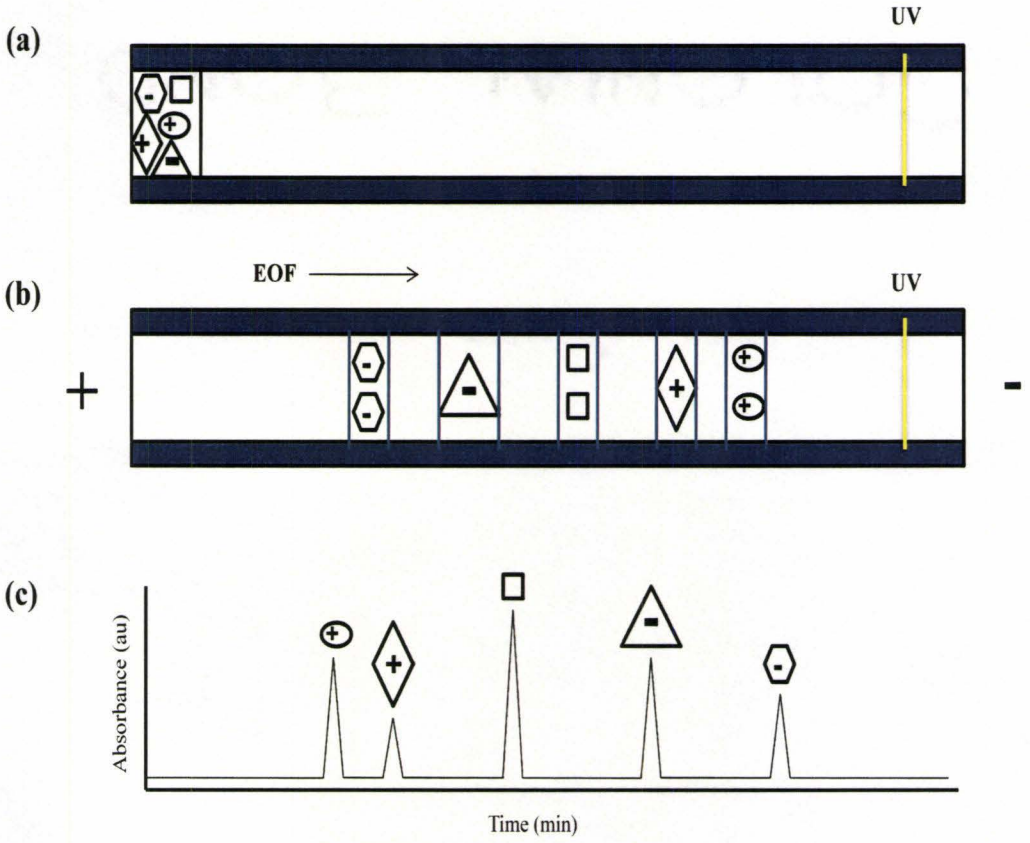

Figure 1.5: Schematic representation of an electrophoretic separation of cationic, neutral and anionic species using CE. (a) sample injection, (b) zonal separation, and (c) representative electropherogram of different sized and charged analytes using UV detection.

that the magnitude of the EOF is greater than $\mu_{ep,A}$, it will transport all analytes (including anions) from the capillary inlet past a fixed detector window towards the outlet. The apparent mobility (μ_{ep}^{A}) of analytes represents the vector sum of the EOF and their characteristic $\mu_{ep,A}$. Zonal separation of analytes in a sample mixture can be achieved if there exists sufficient differences in $\mu_{ep,A}$ without excessive band broadening, An electropherogram is generated by monitoring the detector signal response as a function of time. The relative migration time order in CE of different charged analytes is typically small cations < large cations < neutral analytes < large anions < small anions.

Conventional CE is unable to separate neutral analytes as they co-migrate with the EOF, which was addressed by Terabe *et al.* with the introduction of MEKC using charged surfactants as additives in the buffer that serve as migrating pseudo-stationary phases, such as sodium dodecyl sulphate (SDS)[14, 15]. Differential partitioning of neutral analytes with charged micelles during electromigration provides an electrokinetic mechanism for their separation. Similarly, enantiomers that possess identical mobilities in an achiral environment can be resolved in CE if they undergo differential interaction with specific chiral selectors added to the background electrolyte, such as cyclodextrins.

1.7. Capillary electrophoresis performance

1.7.1. Separation efficiency

Similar to chromatography, the efficiency of a separation in CE as reflected by the extent of band broadening can be assessed by determination of the number of theoretical plates (N). In order to properly quantify N for a given analyte, one must first consider the different sources of band broadening that contribute to total peak variance. The total apparent peak variance in CE, σ_T^2, is the summation of several distinct processes that contribute to the spreading of an analyte peak:

$$\sigma_T^2 = \sigma_D^2 + \sigma_I^2 + \sigma_J^2 + \sigma_E^2 + \sigma_A^2 + \sigma_W^2 + \sigma_O^2 \qquad (5)$$

where σ_D^2, σ_I^2, σ_J^2, σ_E^2, σ_A^2, σ_W^2, and σ_O^2 represent the variance produced by diffusion, injection length, Joule heating, electrophoretic dispersion, adsorption, width of detection zone and other effects, respectively. Through careful design of CE operation conditions, most of these variance contributions can be significantly minimized, with the dominant band broadening process remaining longitudinal diffusion. The Stokes-Einstein equation

describes this contribution as:

$$\sigma_T^2 \approx \sigma_D^2 = 2 \cdot D \cdot t \qquad (6)$$

where σ_D^2 represents the peak variance due to diffusion, t is the migration time of the analyte and D is its diffusion coefficient. In general, larger molecules (small D) that migrate through the capillary quickly show less variance than smaller molecules (large D) which reside in the system for an extended period of time. Assuming a symmetric Gaussian peak distribution with the development of the rate theory of band broadening in chromatography, separation efficiency, N can be defined as:

$$N = \frac{L_d^2}{\sigma_T^2} \qquad (7)$$

where L_d is the capillary length to the detector. Assuming that the major source of band broadening in a CE separation is from longitudinal diffusion, then the separation efficiency can be expressed by the following:

$$N = \frac{L_d^2}{2 \cdot D \cdot t} = \frac{L_d^2}{2 \cdot D \cdot \left[\dfrac{L_d^2}{\left(\mu_{ep,A} + \mu_{eo}\right) \cdot V} \right]} = \frac{\left(\mu_{ep,A} + \mu_{eo}\right) \cdot V}{2 \cdot D} \qquad (8)$$

From *Equation (8)* it is clear that high applied voltages (V), low sample diffusion coefficients (D) and fast analyte mobilities ($\mu_{ep,A}$) or rapid EOF (μ_{eo}) enhance separation efficiency in CE by reducing the extent of band broadening caused by diffusion. Given that $\mu_{ep,A}$ and D are dependent on the characteristic physiochemical properties of the analyte itself, the most direct way of enhancing separation efficiency is to increase the voltage applied across the capillary. In doing this, one must consider the impact of Joule heating associated with higher voltages due to higher ion conduction, which can lower

efficiency by increasing peak dispersion. In practice, applied electric potential can easily be optimized through the generation of an Ohm plot which relates the current generated with a specific buffer to the applied voltage. The highest voltage within the linear region of the Ohm plot provides good estimate of the optimum voltage to be used. In addition, the use of electrolytes with low conductivity and good buffer capacity along with capillary devices with active liquid or air cooling processes can permit the use of high voltages without Joule heating.

N can be experimentally determined from an electropherogram by the following expression:

$$N = 5.54 \cdot \left(\frac{t}{w_{1/2}} \right)^2 \qquad (9)$$

with $w_{1/2}$ representing the peak width at half height for an analyte band. Under optimal conditions efficiencies in CE often range from 10^5 to 10^6 theoretical plates which are comparable to typical GC separations.

1.7.2. Selectivity

Separation selectivity (α) is another measure of separation efficiency and describes the ratio of the migration velocities of two migrating components, A and B (where $\nu_A > \nu_B$) by the equation:[16]

$$\alpha = \frac{\nu_A}{\nu_B} \qquad (10)$$

When considering a CE system under a constant applied electric field and devoid of additives that specifically interact with an analyte during electromigration, the relative analyte migration velocities can be replaced by their apparent mobility:

$$\alpha = \frac{\mu_{ep,A}^{A}}{\mu_{ep,B}^{A}} = \frac{\mu_{ep,A} + \mu_{eo}}{\mu_{ep,B} + \mu_{eo}} \qquad (11)$$

To alter the selectivity of a separation in CE, the electrolyte conditions are most often optimized in terms of changes in the buffer type, pH and ionic strength. Each of these modifications can affect the effective charge to size ratio of analytes, thus altering their respective mobilities. Organic modifiers are water-miscible solvents (*e.g.*, methanol, acetonitrile and dimethylsulfoxide) that may also be employed for improving selectivity, as their addition to the run buffer can also enhance sample solubility. A major area of current CE research is focused on the development and application of new classes of soluble additives for modifying separation selectivity based on specific intermolecular interactions. Additives ranging from glycopeptides to aptamers can be added to the background electrolyte during separation in order to selectively alter analyte mobility for improved selectivity and resolution. The use of cyclodextrins for chiral CE separations, based on dynamic inclusion complexation during electromigration, is based on this principle and discussed in *Chapter's II* and *V* of this thesis.

1.7.3. Resolution

The quality of a separation in CE may also be evaluated in terms of the resolution between two adjacent migrating peaks. This is a useful measure of analytical performance as the apparent resolution takes into account the effects of both separative and dispersive transport. Resolution (Rs) is defined as the quotient of the distance between two peak centers (Δx) and the mean of the peaks standard deviation (σ) and is a function of both the column efficiency (band broadening) and separation selectivity as given by:

$$Rs = \frac{\Delta x}{4 \cdot \sigma} \tag{12}$$

Resolution can be experimentally measured by difference in migration times (t) of two adjacent peaks and the average of their base peak widths (w) as described by the following equation:

$$Rs = \frac{2 \cdot (t_2 - t_1)}{(w_1 + w_2)} \tag{13}$$

1.8. Improving separation efficiency and concentration sensitivity in CE

Analyte dispersion remains a fundamental obstacle in separation science for achieving separations of high resolution and peak capacity that is critical to bioanalytical chemistry. Strategies to minimize and/or counter dispersion are also relevant for improving detector concentration sensitivity, which is limited due to the small sample injection volumes, when employing CE or MCE.

Although nanolitre sampling is a boon to mass sensitivity, this presents a major challenge for detecting low abundance or poorly responsive analytes when using optical, electrochemical and electrospray ionization-mass spectrometry (ESI-MS) detection. For instance, conventional separations in CE are typically performed using a continuous background electrolyte, where the sample is injected as a discrete small plug (< 1% capillary length or ≈ 10 nL) in order to maintain high separation efficiency without sample overloading. The injection of larger sample plugs often results in increased band broadening due to the reduction in separation efficiency. Early fundamental electrophoretic studies revealed that by exploiting the conductivity difference between the a relatively large sample plug and the background electrolyte one can improve the

detector response of an analyte, while maintaining high separation efficiency based on field-amplified sample stacking[17]. Electrokinetic focusing of long sample plugs can also be mediated by differences in other electrolyte properties in a discontinuous electrolyte system, such as co-ion mobility, additive concentration and buffer pH. To date, four major on-line sample preconcentration techniques have been developed for sensitivity enhancement in CE, including sample stacking, transient isotachophoresis, sweeping and dynamic pH junction[18]. Other strategies for on-line sample preconcentration in electrophoresis using sorption, counter-flow balancing and electrokinetic membrane trapping processes are often considered separately from these modalities as they are not readily compatible to commercial instrumentation. Several comprehensive reviews that compare on-line sample preconcentration techniques in CE have recently been published[18-23].

1.8.1. Dynamic pH junction

Buffer pH represents one of the most important experimental variables influencing selectivity in electrophoretic-based separations since it influences the degree of ionization and thus the effective mobility of weakly ionic species. Simple yet effective means to generate pH gradients in electrophoresis without ampholytes have been used to improve selectivity in CE separations, however their applicability for sample enrichment were not initially recognized[24, 25]. Aebersold and Morrison[26] first reported a five-fold preconcentration of zwitter-ionic peptides without loss in resolution by CE when using a simple buffer pH junction composed of a hydrodynamically injected alkaline sample plug and a capillary-filled acidic buffer. Schwer and Lottspeich[27] demonstrated a modified on-

line sample preconcentration procedure by sandwiching a dilute peptide solution between concentrated acidic and alkaline plugs in a discontinuous electrolyte system. Britz-McKibbin *et al.* later introduced a selective assay for epinephrine determination in dental anesthetic solutions, which revealed an unusual pH-mediated sample self-stacking phenomenon[28, 29]. The focusing mechanism was later investigated and introduced as an effective on-line preconcentration technique for weakly ionic analytes in CE referred to as dynamic pH junction[30]. Subsequent studies[31, 32] supported a mechanism where weakly ionic analytes are electrokinetically focused at the interface of a moving pH boundary due to significant differences in pH-dependent analyte mobilities. This process continues until the sample discontinuity is dissipated by acid-base neutralization reactions with the background electrolyte, after which concentrated analyte bands separate by conventional zonal electrophoresis prior to detection. Analogous preconcentration methods have also been reported in the literature under different acronyms, such as transient-moving chemical reaction boundary[33]. In general, the pH of sample and background electrolyte segments are selected to maximize mobility changes of analytes based on their characteristic pK_a in the case of weakly acidic or basic solutes, or *pI* for zwitter-ions, including amino acids, catecholamines, peptide and protein[2]. Additional factors, such as ionic strength, electrolyte co-ion and sample injection length can also impact the rate of sample focusing and efficiency of sample enrichment that is applicable to biological samples in a high salt matrix[32, 34]. Although sensitivity enhancement factors over three orders of magnitude have been reported by CE with dynamic pH junction[35-40] this is ultimately dictated by the specific context of the assay, such as sample complexity,

resolution requirements, analysis time constraints and method reproducibility. Since the same capillary is used for both preconcentration and separation purposes under a single format, the effective capillary length needed for adequate resolution may be compromised when using full-capillary sample injections unless operating under specific conditions.

To date, CE using dynamic pH junction has been applied for improved detection of a wide class of analytes, including polar metabolites, peptides and protein[41-48]. Chang *et al.* reported a new method for riboflavin determination using on-line preconcentration by CE via dynamic pH junction with UV LED-based native fluorescence detection[49]. About a 60-fold improvement in concentration sensitivity without loss in separation efficiency was achieved using this strategy when using a sample injection length equivalent to 25 % of the effective capillary length. Fan *et al.* reported a flow-injection system for sample introduction with dynamic pH junction for on-line sample preconcentration of trimethoprim and sulfamethoxazole using MCE[50]. This system provided continuous sample introduction, resulting in a five-fold improvement in concentration sensitivity with shorter separation times and higher sample throughput. Sahlin demonstrated the applicability of dynamic pH junction for improving both sensitivity and resolution in two-dimensional CE separations[51]. The author demonstrated that co-migrating metabolites, mesityl oxide and *m*-nitrophenol, in the first-dimension separation were effectively preconcentrated and resolved upon transfer to the second capillary. Recently, Imami *et al.* demonstrated the benefit of using dynamic pH junction with CE-ESI-MS for improved identification of low abundance protein[37]. Under optimal conditions, a 1000-fold enhancement in peptide peak intensities was achieved without loss in resolution for

enhanced peptide mass fingerprinting. This method was directly applied to tryptic digests of cytochrome c to reveal low abundance peptide fragments thus allowing for increased protein coverage. Li *et al.* developed a negatively charged sol-gel capillary coating allowing for the selective extraction and on-line preconcentration of zwitter-ionic analytes, using myoglobin and asparagine as model compounds[38]. The dynamic pH junction served to both preconcentrate and desorb analytes through local pH changes within the capillary resulting in up to a 7000-fold sensitivity enhancement factor. Han *et al.* reported a modified on-line preconcentration technique referred to as acid-barrage stacking for the analysis of 9-fluorenlymethylchloroformate (FMOC) derivatized-amino acids within high salt matrices by CE with UV detection[39]. The focusing mechanism is similar to dynamic pH junction, with the exception that during the injection sequence, a short plug of concentrated acid is injected after the sample to generate a moving pH boundary across an alkaline buffer that resulted in about a 1000-fold enhancement in sensitivity. An analogous procedure was also reported by Mayboroda *et al.* for amino acid profiling with nanomolar detection limits when using CE-TOF-MS under acidic conditions, where a short plug of alkaline solution was injected prior to a long hydrodynamic injection of an acidified urine sample[52]. On-line sample preconcentration by dynamic pH junction was also applied for improved detection of weakly acidic inorganic arsenic and organoarsenic species using CE with UV absorbance[47]. Up to a 800-fold improvement in sensitivity was achieved by this method which permitted low ppb detection of roxarsone in soil samples when used in conjunction with off-line solid-phase extraction.

1.8.2. Novel extensions to dynamic pH junction

Several researchers have developed novel extensions to dynamic pH junction using alternative injection sequences or multiple electrokinetic focusing processes as a way to further improve method performance. For example, on-line sample preconcentration via dynamic pH junction-sweeping has been introduced as a hyphenated technique to expand sensitivity enhancement to both weakly ionic and neutral species based on analyte mobility changes induced by buffer pH and additive partitioning in a discontinuous electrolyte system[53]. Yu *et al.* reported about a 90-fold boost in sensitivity for the detection of trace levels of toxic pyrrolizidine alkaloids in Chinese herbal medicine by CE with dynamic pH junction-sweeping[54]. Recently, Horáková *et al.* developed two novel on-line sample preconcentration techniques for the trace analysis of weakly acidic analytes by dynamic pH junction using MEKC[36, 40]. The first strategy utilized an extended electrokinetic injection (*e.g.,* 0.3 - 4 hrs) of anionic benzoic acid and sorbate in alkaline borate buffer (pH 9.5) into a capillary pre-filled with acidic phosphate (pH 2.5) as the background electrolyte[40]. After electrokinetic sample accumulation at the interface of this buffer junction, the inlet buffer was replaced with a reservoir of phosphate buffer containing 150 mM SDS, allowing for immobilization and separation of the stacked neutral (*i.e.,* protonated) analytes by MEKC. Up to a 4,800-fold enhancement in concentration sensitivity was achieved by this method when using a two-hour electrokinetic accumulation time allowing for low nanomolar detection of trace levels of benzoic acid in sunflower oil samples to be achieved when using CE with UV detection. The same authors also reported an alternative on-line sample preconcentration strategy

using large volume sample stacking with dynamic pH junction in CE[36]. A hydrodynamic injection of the sample was used to fill the entire capillary (≈ 6 μL) in an alkaline buffer, whereas separation was performed under a reversed polarity voltage using acidic phosphate with 150 mM SDS as the background electrolyte. Focused neutral analyte zones at the buffer junction co-migrate with the electroosmotic flow until reaching the inlet side of the capillary, where migrating SDS micelles immobilize the stacked zones with normal separation by MEKC[36]. About a 2000-fold improvement in concentration sensitivity for benzoic acid was achieved while avoiding the long electrokinetic sample accumulation times required in their previous method.

Shih and Lin also reported a full-capillary sample stacking procedure for naphthalene-2,3-dicaboxaldehyde (NDA) labelled-amino acids using dynamic pH junction by MEKC with laser-induced fluorescence (LIF) detection[55]. Initially the entire capillary was filled with the weakly anionic analytes dissolved in a low conductivity sample electrolyte with an apparent pH 4.6. A moving pH boundary towards the inlet buffer was generated to electrokinetically focus analytes under a reversed polarity voltage while using a high conductivity background electrolyte with an apparent pH 2.0. This process was continued until the buffer reservoirs were switched after a fixed time interval (*e.g.,* 25 min) with the addition of SDS in the background electrolyte in order to mobilize and separate stacked neutral analytes by MEKC. Under optimal conditions the authors reported about a 400-fold improvement in concentration sensitivity for NDA-labelled tryptophan and leucine relative to conventional sample injections. However, the low conductivity sample matrix and buffer switching step after analyte stacking were later demonstrated not to be

required as a way to simplify the technique[36]. Kirschner *et al.* proposed a similar method for trace chiral analysis of cyanobenz[*f*]isoindole (CBI) labelled-amino acids by CE-LIF[56]. A mixed mode on-line preconcentration procedure combining field-amplified stacking, dynamic pH junction with sweeping under reversed polarity voltage was proposed to induce analyte focusing[56]. In contrast to similar approaches using SDS micelles[55, 56], a sulfated β-cyclodextrin (S-β-CD) was used as an anionic chiral selector for immobilization of stacked analyte zones with enantioselective resolution of CBI-labelled amino acid enantiomers that was favored under acidic conditions to minimize electrostatic repulsion. However, since the focusing mechanism relied primarily on stacking involving samples of low conductivity, it was not directly applicable to high salt microdialysates.

Arnett and Lunte developed an hyphenated on-line sample preconcentration method applicable to high ionic strength samples by CE with dynamic pH junction to enhance both the sensitivity and resolution of weakly acidic nucleosides[57]. Initially a small plug of acidic buffer (*i.e.,* conjugate acid of a weak base) was hydrodynamically injected into the capillary followed by electrokinetic injection of a high salt sample under reverse polarity. This process allowed electrolyte co-ions (*e.g.,* imidazole) in the front acidic plug to exchange with untitratable cations (*e.g.*, Na^+) in the injected sample. Upon electrokinetic injection of an alkaline solution of sodium hydroxide, an acid-base neutralization reaction creates a low-conductivity zone within the original sample segment. This novel in-capillary desalting procedure enabled selective removal of high salt in a biological sample while electrokinetically accumulating target nucleosides at the

interface of a buffer pH junction. Improved focusing of nucleosides in high salt samples was achieved using this protocol due to the combined effects of field-enhanced sample stacking with dynamic pH junction that also resulted in greater separation resolution with extremely sharp peak widths. Hsieh and Chang developed an on-line sample preconcentration method for simultaneous preconcentration of amines and organic acids using CE with laser-induced native fluorescence detection[58]. Electrokinetic focusing of both weakly acidic and basic classes of analytes was achieved by exploiting differences in multiple electrolyte properties, including solution viscosity, buffer pH and conductivity. Simultaneous focusing of amines and organic acids was achieved with about a 400- and 800-fold boost in sensitivity for 5-hydroxytryptamine and 5-hydroxyindole-3-acetate, respectively relative to conventional injections.

1.8.3. Sample pretreatment and integrated chemical analyses

A growing area of interest in CE is the development of strategies for integrating multiple sample pretreatment protocols during separation that allows for direct analysis of real-world samples. Off-line sample pretreatment steps represent critical features to the overall performance of an assay (*e.g.,* chemical labelling, desalting, extraction *etc.*), but they are often time-consuming, labor-intensive and contribute to overall bias and loss of precision.

Nesbitt *et al.* reported an integrated CE technique allowing for the selective extraction and preconcentration of a target protein based on its characteristic isoelectric point (p*I*)[35]. The authors demonstrated selective electrokinetic sampling and focusing of dilute myoglobin from a buffered protein mixture by CE in conjunction with off-line

MALDI-MS analyses. Recently, this technique was further expanded to allow for in-capillary trypsin digestion of myoglobin directly in-capillary for 2 h at an incubation temperature of 37°C[59]. Upon tryptic digest completion, voltage application refocused the peptide fragments by CE using a dynamic pH junction with partial separation of peptides prior to detection. Direct sample spotting of preconcentrated peptide zones from the capillary outlet provided a sample enrichment factor up to 20-fold with 82 % sequence coverage for a standard 0.05 $\mu g \cdot \mu L^{-1}$ myoglobin sample. Recently, Lee *et al.* examined the mechanism of dynamic pH junction in CE-ESI-MS by comparing experimental and computer simulations, which was also used for accurate prediction of the relative migration times of metabolites based on two fundamental physicochemical parameters, namely absolute mobility and pK_a[58]. The authors demonstrated that CE can provide important qualitative information to support MS characterization for *de novo* identification of unknown metabolites among several putative isomeric or isobaric candidates when commercial standards are unavailable.

Indeed, the ease of integrating sample pretreatment steps directly in-capillary represents a distinguishing feature of CE for realizing high-throughput and low cost analyses. Dynamic pH junction serves not only to lower detection limits, but also can be used to enhance separation resolution, as well as integrate several sample pretreatment steps directly in-capillary, such as selective extraction, sample desalting, and enzymatic reactions. Indeed, a major focus of this thesis is the development of integrated CE separations that combine several distinct sample pretreatment steps during chemical analyses. A large portion of the thesis is based on the development of a new CE

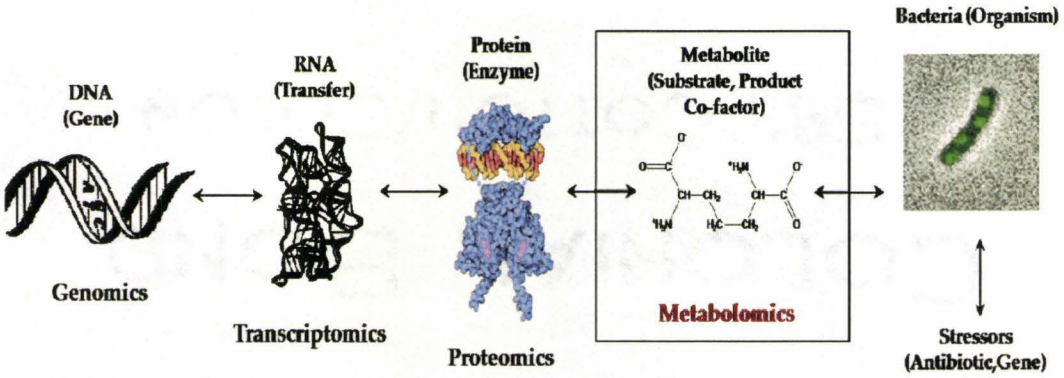

Figure 1.6: Schematic representing the "omic" levels of a biological system.

technique for single-step analysis of low abundance metabolites in biological samples, referred to as on-line sample preconcentration with chemical derivatization by CE (SPCD-CE), which permits enhanced detection of weakly ionic analytes that lack intrinsic chromophores. This work will be discussed in *Chapters III, IV* and *V* of this thesis.

1.9. Metabolomics

It has been suggested that metabolomics represents the greatest "omics" of all[60], in terms of the sheer size of "functional" information the metabolome yields[61]. This belief is derived from the difficulty and limitations in establishing a definitive correlation between changes in the transcriptome or proteome and observed perturbations in the phenotype of the organism[62]. In addition, the metabolome represents a real-world endpoint of a biological system (*Figure 1.6*) and thus is directly influenced by the environment of an organism and associated internal or external stressors. Thus, unbiased comprehensive metabolomic studies can provide insight into the pathological, physiological and biochemical states directly associated with the phenotype of an organism that is relevant to new developments in personalized medicine[63], drug

screening[64], drug toxicity[64], plant biotechnology[65], microbial engineering[66], human health[67], and protein discovery[68].

However, despite the enormous potential benefits of obtaining both a qualitative and quantitative understanding of an organisms' metabolome, this emerging field of research is not without its share of controversy[69] and challenges. The actual term "metabolome" was first introduced into the literature in 1998 by Oliver *et al.* to describe a set of metabolites that were synthesized by an organism[70]. These researchers defined this terminology as, " . . . the quantitative complement of all of the low molecular weight molecules present in cells in a particular physiological or developmental state."[70] In 1999 Nicholson *et al.* defined the term "metabonomics" as, "the quantitative measure of the dynamic multiparametric metabolic response of living systems to pathophysiological stimuli or genetic modification."[71] These researchers envisioned metabonomic studies to have the capacity to detect, identify, quantify and catalogue time-related metabolic changes in an integrated biological system[71]. Two years later, Fiehn defined the term "metabolomics" as the comprehensive analysis of all metabolites in a biological system in which the low molecular weight species are both identified and quantified[72]. In the approximately eight years of scientific literature following the introduction of these parallel concepts, the terms "metabonomics" and "metabolomics" have been used interchangeably by researchers quantifying low molecular weight metabolites. Compounding the confusion surrounding this terminology, metabolomics has been described as a subset of systems covered by metabonomics, and yet metabonomics can also be thought out of as a subset of metabolomics[60, 73, 74]. Given the historical

precedence, similarity in analytical methodologies, and common goal of metabolome analysis, the term "metabolomics" will be used throughout this thesis.

It should be noted that the analysis of biologically relevant metabolites is certainly not by any means a new concept. Small subsets of metabolites, often related to specific metabolic pathways, have traditionally been qualitatively identified and quantified. However, these individual pathways do not act in isolation and are often interconnected and/or act in concert with other biological processes within the organism. This fact has required scientists to undertake a more holistic view of the metabolome and develop robust techniques capable of truly global metabolite analyses. The analytical challenge of this later initiative is immense and to date no single analytical technique is a capable total metabolite analyses. The sheer number of metabolites, as well as their large dynamic range and chemical diversity are primarily responsible for this failure. Researchers have estimated dynamic range of the metabolome to extend of 7-9 orders on magnitude (pmol – mmol)[75] with claims of over 200,000 unique metabolites contained within the plant system being reported in the literature[76]. Thus given the enormous challenge of this quest, many researchers have instead focused on targeted metabolomic studies of specific classes or subsets of small molecules, such as different low abundance metabolites that can serve as biologically relevant biomarkers of disease.

Several different techniques have been reported for *directed* metabolomics primarily based on hyphenated chromatographic techniques coupled to MS or NMR detection[75]. Although multidimensional NMR methods offer a powerful format for structural elucidation of unknown metabolites, they are limited by poor concentration sensitivity.

GC-MS offers improved sensitivity for low-abundance metabolite detection, but requires chemical derivatization for polar metabolites that are thermally stable and nonlabile. Although LC-ESI-MS can be directly applied to polar metabolites without chemical labelling[77, 78], selection of a stationary phase with sufficient selectivity for both cationic and anionic metabolites is challenging[79]. Capillary electrophoresis-mass spectrometry (CE-MS) has also been applied to the analysis of small amounts of complex sample mixtures, ranging from protein to pharmaceuticals[80-83], although volatile buffer conditions compatible with ESI-MS detection may limit its applicability to specific classes of polar metabolites.

Given the challenges surrounding existing analytical procedures for directed metabolomics, new analytical strategies that improve detector sensitivity, increase the speed and reduce the cost of analyses, as well as enhance overall separation efficiency and peak capacity are urgently needed. Recently, metabolomic-based research initiatives related to understanding human health and diseases have been reported showing the promise of this initiative. For instance, Holmes *et al.* assessed the relationship between phenotype diversity within a population, diet and blood pressure[84], while Lan *et al.* identified molecular changes associated with the pathophysiology and drug treatment of bipolar disorder[85]. These recent studies illustrate that despite the enormous benefits of metabolomic applications for disease prognosis and drug development, similar efforts are also urgently needed in fundamental method development in separation science such that routine analyses can be performed directly on complex biological samples with minimal

off-line sample pre-treatment[86]. The latter process in fact represents one of the most important components to a successful and reliable analytical assay.

1.10. Research objectives

To enhance the applicability of CE for targeted metabolomic studies directed at low abundance metabolites, new analytical strategies must be rationally designed, optimized and properly validated. To aide in this endeavour two major research objectives are associated with the work performed during this doctoral thesis; (a) improvement in the understanding of the fundamental thermodynamic and electrokinetic parameters governing CE separations, and (b) development of single-step strategies for improved detection of low abundance metabolites by CE in complex biological samples without off-line sample pretreatment. The ultimate objective of these goals is the design of a superior separation platform for high-throughput and low cost analysis of minor, unnatural and/or unusual metabolites of biological significance with emphasis on enantioselective separations. The thesis can thus be viewed as two distinct yet complementary sections aimed at fulfilling this goal:

Section A: Fundamental studies of the thermodyanamics and electrokinetics of chiral separations by capillary electrophoresis: Minimum criteria for enantioselective resolution, *Chapter II.*

Section B: Development and application of on-line sample preconcentration with chemical derivatization by capillary electrophoresis (SPCD-CE) for single-step analysis of *o*-phosphoamino acids, *Chapter III*, bacterial biomarkers, *Chapter IV*, and *D/L*-amino acids, *Chapter V.*

The thesis will also conclude with a final chapter (*Chapter VI*) that will summarize the unique contributions of the thesis, as well as highlight future directions for research notably for the analysis of labile yet biologically relevant biomarkers of oxidative stress.

1.11. References

1. J. C. Giddings, *Unified Separation Science*, John Wiley & Sons, New York, NY., 1991.
2. P. Britz-McKibbin and S. Terabe, *J. Chromatogr. A*, 2003, **1000**, 917-934.
3. D. W. Armstrong, G. Schulte, J. M. Schneiderheinze and D. J. Westenberg, *Anal. Chem.*, 1999, **71**, 5465-5469.
4. A. Tiselius, *Inagural Dissertation Upsala*, 1930.
5. A. Tiselius, *Trans. Faraday Soc.*, 1937, **33**, 524-531.
6. T. Svedberg, *Trans. Faraday Soc.*, 1930, **26**, 737-760.
7. N. J. Dovichi and J. Z. Zhang, *Angew. Chem. Int. Ed.*, 2000, **39**, 4463-4468.
8. S. Hjerten, *Chromatogr. Rev.*, 1967, **9**, 122-219.
9. F. E. P. Mikkers, T. N. Everaerts and T. P. E. M. Verheggen, *J. Chromatogr.*, 1979, **169**, 11-20.
10. J. W. Jorgenson and K. D. Lucas, *Anal. Chem.*, 1981, **53**, 1298-1302.
11. I. D. Wilson, J. K. Nicholson, J. Castro-Perez, J. H. Granger, K. A. Johnson, B. W. Smith and R. S. Plumb, *J. Proteome Res.*, 2005, **4**, 591-598.
12. J. P. Landers, ed., *Handbook of Capillary Electrophoresis*, CRC Press, Boca Raton, FL. USA, 1997.
13. P. Camilleri, *Chem. Comm.*, 1996, **16**, 1851-1856.

14. S. Terabe, K. Otsuka, K. Ichikawa, A. Tsuchiya and T. Ando, *Anal. Chem.*, 1984, **56**, 111-113.

15. S. Terabe, *Anal. Chem.*, 2004, **76**, 240A-246A.

16. M. T. Bowser, G. M. Bebault, X. Peng and D. D. Y. Chen, *Electrophoresis*, 1997, **18**, 2928.

17. R. L. Chien and D. S. Burgi, *J. Chromatogr.*, 1991, **559**, 141-152.

18. P. Britz-McKibbin and S. Terabe, *J. Chromatogr. A*, 2003, **1000**, 917-934.

19. S. L. Simpson, J. P. Quirino and S. Terabe, *J. Chromatogr. A*, 2008, **1184**, 504-541.

20. C.-H. Lin and T. Kaneta, *Electrophoresis*, 2004, **25**, 4058-4073.

21. M. R. N. Monton and S. Terabe, *J. Chromatogr. B*, 2006, **841**, 88-95.

22. Z. Mala, L. Krivankova, P. Gebauer and P. Bocek, *Electrophoresis*, 2007, **28**, 243-253.

23. M. C. Breadmore, *Electrophoresis*, 2007, **28**, 254-281.

24. V. Sustacek, F. Foret and P. Bocek, *J. Chromatogr.*, 1989, **480**, 271-276.

25. W. E. Rae, J. E. Wong and C. A. Lucy, *J. Chromatogr. A*, 1997, **781**, 3-10.

26. R. Aebersold and H. D. Morrison, *J. Chromatogr.* , 1990, **516**, 79-88.

27. C. Schwer and F. Lottspeich, *J. Chromatogr. A*, 1992, **623**, 345-355.

28. P. Britz-McKibbin, A. R. Kranack, A. Paprica and D. D. Y. Chen, *Analyst*, 1998, **123**, 1461-1463.

29. P. Britz-McKibbin, J. Wong and D. D. Y. Chen, *J. Chromatogr. A*, 1999, **853**, 535-540.

30. P. Britz-McKibbin and D. D. Y. Chen, *Anal. Chem.*, 2000, **72**, 1242-1252.

31. J.-B. Kim, Y. Okamoto and S. Terabe, *J. Chromatogr. A*, 2003, **2003**, 251-256.

32. R. Lee, A. S. Ptolemy, L. Niewczas and P. Britz-McKibbin, *Anal. Chem.*, 2007, **79**, 403-415.

33. C.-X. Cao, W. Zhang, W.-H. Qin, S. Li, W. Zhu and W. Liu, *Anal. Chem.*, 2005, **77**, 955-963.

34. M. C. Breadmore, R. A. Mosher and W. Thormann, *Anal. Chem.*, 2006, **78**, 538-546.

35. C. A. Nesbitt, J. T.-M. Lo and K. K.-C. Yeung, *J. Chromatogr. A*, 2005, **1073**, 175-180.

36. J. Horakova, J. Petr, V. Maier, J. Znaleziona, A. Stanova, J. Marak, D. Kaniansky and J. Sevcik, *J. Chromatogr. A*, 2007, **1155**, 193-198.

37. K. Imami, M. R. N. Monton, Y. Ishihama and S. Terabe, *J. Chromatogr. A*, 2007, **1148**, 250-255.

38. W. Li, D. Fries and A. Malik, *J. Sep. Sci.*, 2005, **28**, 2153-2164.

39. Y. Han, M. Zuo, L. Qi, K. Liu, L. Mao and Y. Chen, *Electrophoresis*, 2006, **27**, 4240-4248.

40. J. Horakova, J. Petr, V. Maier, E. Tesarova, L. Veis, D. W. Armstrong, B. Gas and J. Sevcik, *Electrophoresis*, 2007, **28**, 1540-1547.

41. G. W. Xu, Q. H. Yao, Q. F. Weng, B. L. Su, X. Zhang and J. H. Xiong, *J. Pharma. Biomed. Analysis*, 2004, **36**, 101-104.

42. S.-R. Mei, Q.-H. Yao, L.-S. Cai, J. Xing, G.-W. Xu and C.-Y. Wu, *Electrophoresis*, 2003, **24**, 1411-1415.

43. C. Smadja, I. LePotier, P. Chaminade, C. Jacquot, J. H. Trouvin and M. Taverna, *Chromatographia*, 2003, **58**, 79-85.

44. M. R. N. Monton, K. Imami, M. Nakanishi, J.-B. Kim and S. Terabe, *J. Chromatogr. A*, 2005, **1079**, 266-273.

45. Y. Du, L. Jia, H. Liu and D. Xing, *Anal. Lett.*, 2007, **40**, 2005-2015.

46. E. A. Bessonova, L. A. Kartsova and A. U. Shmukov, *J. Chromatogr. A*, 2007, **1150**, 332-338.

47. J. Jaafar, Z. Irwan, R. Ahamad, S. Terabe, T. Ikegami and N. Tanaka, *J. Sep. Sci.*, 2007, **30**, 391-398.

48. C.-C. Wang, S.-S. Chiou and S.-M. Wu, *Electrophoresis*, 2005, **26**, 2637-2642.

49. Y.-S. Chang, C.-M. Shih and C.-H. Lin, *Anal. Sci.*, 2006, **22**, 235-240.

50. L. Fan, L. Liu, H. Chen, X. Chen and Z. Hu, *J. Chromatogr. A*, 2005, **1062**, 133-137.

51. E. Sahlin, *J. Chromatogr. A*, 2007, **1154**, 454-459.

52. O. A. Mayboroda, C. Neusub, M. Pelzing, G. Zurek, R. Derks, I. Meulenbelt, M. Kloppenburg, E. P. Slagboom and A. M. Deelder, *J. Chromatogr. A*, 2007, **1159**, 149-153.

53. P. Britz-McKibbin, K. Otsuka and S. Terabe, *Anal. Chem.*, 2002, **72**, 3736-3743.

54. L. Yu and S. F. Y. Li, *Electrophoresis*, 2005, **26**, 4360-4367.

55. C.-M. Shih and C.-H. Lin, *Electrophoresis*, 2005, **26**, 3495-3499.

56. D. L. Kirschner, M. Jaramillo and T. K. Green, *Anal. Chem.*, 2007, **79**, 736-743.

57. S. D. Arnett and C. E. Lunte, *Electrophoresis*, 2007, **28**, 3786-3793.

58. M.-H. Hsieh and H.-T. Chang, *Electrophoresis*, 2005, **26**, 187-195.

59. C. A. Nesbitt, K. Jurcic and K. K.-C. Yeung, *Electrophoresis*, 2008, **28**, 466-471.

60. D. Ryan and K. Robards, *Anal. Chem.*, 2006, **78**, 7954-7958.

61. L. W. Summer, P. Mendes and R. A. Dixon, *Phytochemistry*, 2003, **62**, 817-836.

62. O. Fiehn, L. Kopka, P. Dormann, T. Altmann, R. N. Trethewey and L. Willmitzer, *Nat. Biotechnol.*, 2000, **18**, 1157-1161.

63. J. N. Haselden and W. A. Nicholls, *Nat. Medicine*, 2006, **12**, 510-511.

64. J. K. Nicholson, J. Connelly, J. C. Lindon and E. Holmes, *Nat. Rev. Drug Discovery*, 2002, **1**, 153-161.

65. G. S. Catchpole, M. Beckmann, D. P. Enot, M. Mondhe, B. Zywicki, J. Taylor, N. Hardy, A. Smith, R. D. King, D. B. Kell, O. Fiehn and J. Draper, *Proc. Natl. Acad. Sci. USA*, 2005, **102**, 14458-14462.

66. B. Teusink and E. J. Smit, *Nat. Rev. Micrbiol.*, 2006, **4**, 46-56.

67. J. T. Brindle, H. Antti, E. Holmes, G. Tranter, J. K. Nicholson, H. W. L. Bethell, S. Clarke, P. M. Schofield, E. McKilligan, D. E. Mosedale and D. J. Grainer, *Nat. Medicine*, 2002, **8**, 1439-1444.

68. N. Saito, M. Robert, S. Kitamura, R. Baran, T. Soga, H. Mori, T. Nishioka and M. Tomita, *J. Proteome Res.*, 2006, **5**, 1979-1984.

69. S. G. Villas-Boas, S. Rasmussen and G. A. Lane, *Trends Biotechnol.*, 2005, **23**, 385-386.

70. S. G. Oliver, M. K. Winson, D. B. Kell and F. Banganz, *Trends Biotechnol.*, 1998, **16**.

71. J. K. Nicholson, J. C. Lindon and E. Holmes, *Xenobiotica*, 1999, **29**, 1181-1191.

72. O. Fiehn, *Comp. Funct. Genom.*, 2001, **2**, 155-168.

73. L. M. Raamsdonk, B. Teusink, D. Broadhurst, N. Zhang, A. Hayes, M. C. Walsh, J. A. Berden, K. M. Brindle, D. B. Kell, J. J. Rowland, H. V. Westerhoff, K. V. Dam and S. G. Oliver, *Nat. Biotechnol.*, 2001, **19**, 45-50.

74. O. Fiehn, *Plant Mol. Biol.* , 2002, **48**, 155-171.

75. W. B. Dunn and D. I. Ellis, *Trends Anal. Chem.*, 2005, **24**, 285-293.

76. T. Hartman, T. M. Kutchan and D. Stack, *Phytochemistry*, 2005, **66**, 1198-1199.

77. V. V. Tolstikov and O. Fiehn, *Anal. Biochem.*, 2002, **301**, 298-307.

78. V. V. Tolstikov, A. Lommen, K. Nakanishi, N. Tanaka and O. Fiehn, *Anal. Chem.*, 2003, **75**, 6737-6740.

79. S. U. Bajad, W. Lu, E. H. Kimball, J. Yuan, C. Peterson and J. D. Rabinowitz, *J. Chromatogr. A*, 2006, **78**, 76-88.

80. D. C. Simpson and R. D. Smith, *Electrophoresis*, 2005, **26**, 1291-1305.

81. C. W. Klampf, *Electrophoresis*, 2006, **26**, 3-34.

82. M. R. N. Monton and S. Terabe, *Anal. Sci.*, 2005, **21**, 5-13.

83. E. F. Smyth, *Electrophoresis*, 2005, **26**, 1334-1357.

84. E. Holmes, R. L. Loo, J. Stamler, M. Bictash, I. K. S. Yap, Q. Chan, T. Ebbels, M. D. Iorio, I. J. Brown, K. A. Veselkov, M. L. Daviglus, H. Kasteloot, H. Ueshima,

L. Zhao, J. K. Nicholson and P. Elliott, *Nature*, 2008, Published on-line: 20 April 2008. DOI: 2010.1038/nature06882

85. M. J. Lan, G. A. McLoughlin, J. L. Griffin, T. M. Tsang, J. T. J. Huang, P. Yuan, H. Manji, E. Holmes and S. Bahn, *Mol. Psychiatry*, 2008, Published on-line: 5 February 2008. DOI: 2010.1038/sj.mp.4002130.

86. O. Beckonert, H. C. Keun, T. M. D. Ebbels, J. Bundy, E. Holmes, J. C. Lindon and J. K. Nicholson, *Nat. Protocols*, 2007, **2**, 2692-2703.

Chapter II

Fundamental Studies of Chiral Separations for Racemic Drug Mixtures by Capillary Electrophoresis: Minimum Criteria for Enantioselective Resolution

II. Fundamental Studies of Chiral Separations for Racemic Drug Mixtures by Capillary Electrophoresis: Minimum Criteria for Enantioselective Resolution

2.1. Abstract

A fundamental study of the thermodynamic and electrokinetic parameters influencing chiral separations in CE was performed for the racemic adrenergic β-blocker drugs, *R/S*-propranolol and *R/S*-atenolol. Hydroxypropyl-β-cyclodextrin (HPβCD) was used as a chiral selector for the resolution of cationic drug enantiomers based on differences in their apparent binding constant (*K*) and complex mobility ($\mu_{ep,AC}$) during electromigration. The temperature-dependence of host-guest inclusion complexation revealed that the interaction was entropy-driven ($\Delta S° > 0$), however the selectivity of the separation was determined primarily by small differences in enthalpy change ($\Delta H°$). A minimum energy difference ($\Delta\Delta G°$) of about 50 cal·mol^{-1} as related to formation complex stability was determined to be required for ensuring baseline resolution of drug enantiomers, which is also dependent on the relative magnitude of $\mu_{ep,AC}$. ^2H_2O was investigated as an alternative solvent for enhancement of hydrophobic interactions to improve the resolution of weakly interacting atenolol at lower concentrations of chiral selector. Single-step analysis of micromolar levels of *R/S*-propranolol in urine by CE was also demonstrated, which provided a convenient format for differential metabolism studies of racemic drugs as normalized to creatinine without complicated sample handling.

2.2. Introduction

Chirality and molecular recognition play important roles in biological processes in

nature. It has been estimated that nearly half of all drugs and pesticides currently in use are chiral[1]. Since the toxicological and pharmacological properties of such chemicals are highly dependent upon their intrinsic stereochemistry, the development of selective methods for assessment of enantiomeric purity is important. Racemic (*R/S*)-propranolol is a classic non-selective β-antagonist which has been widely used for the treatment of hypertension and cardiac dysrhythmia[2]. Although the drug is still prescribed as a racemic mixture, *S*-propranolol has been reported to have over a 100-fold greater activity relative to its racemate[3]. Recently, there has been renewed interest in the therapeutic use of *R/S*-propranolol for the treatment of chronic post-traumatic stress syndrome by reducing the consolidation of emotional memory[4]. With growing concern of the impact of pharmaceutical products in the environment[5], the enantiomeric excess of propranolol has been shown to be a useful tracer for identification of untreated sewage discharges in surface waters[6]. Previous studies have demonstrated that the racemic drug undergoes higher clearance as the *S*-propranolol glucuronide relative to the *R*-propranolol conjugate in human urine[7]. Pharmacokinetic studies have also revealed differential enantiomer metabolism among a variety of ethnic groups[8, 9]. These results indicate non-uniform hepatic drug metabolism for *R/S*-propranolol among different races, which raises concerns about potential adverse health impacts with continued administration of the drug in its racemic form.

The small sample requirements and high separation efficiency of CE makes it an attractive technique for chiral separations of *R/S*-propranolol when using UV absorbance[10-13], electrochemical[14], and ESI-MS[15] detection. Unlike chiral GC

separations[16], CE allows for rapid analysis of polar drug enantiomers without time-consuming off-line chemical derivatization. In addition, the application of on-line sample preconcentration techniques in CE can greatly enhance concentration sensitivity for trace detection of low abundance chiral solutes[17]. A comprehensive review of different liquid-phase separation techniques for enantioselective analysis of adrenergic drugs has recently been reported[18]. Since the electrophoretic mobility ($\mu_{ep,A}$) of enantiomers is equivalent in an achiral environment, separations in free solution CE are most often performed via dynamic complexation using soluble chiral selectors in the background electrolyte. In contrast to chromatographic techniques that rely on costly immobilized chiral stationary phases, resolution can be readily tuned in CE based on changes in the composition of the buffer solution, including the use of single or multiple additives at different concentrations, as well as organic solvent modifiers and other types of additives[19]. A variety of different chiral selectors have been used in CE, including bile salt surfactants, crown ethers, ionic polymers, protein and oligosaccharides, glycopeptide antibiotics and copper-ligand exchange complexes[20]. However, cyclodextrins and their related cyclic oligosaccharide derivatives remain the most popular additives for enantioselective separations in CE because of their tendency to form stable inclusion complexes with small hydrophobic solutes, such as *R/S*-propranolol and other classes of drugs[21].

Chiral resolution in CE can be achieved provided that binding results in a significant change in the apparent mobility ($\nu \cdot \mu_{ep}^{A}$) of enantiomers prior to detection[22, 23]. Although most studies have emphasized the importance of differences in binding affinity[24], the relative magnitude in complex mobility ($\nu \cdot \mu_{ep,AC}$) as reflected by the

effective conformational size of the host-guest complex can also have a cooperative or anti-cooperative impact on overall resolution[25, 26]. Indeed, in cases where enantiomers have similar binding affinity to a chiral selector, differences in the electrokinetic properties of diastereomeric complexes can serve as a unique mechanism for chiral recognition in CE[23]. To date, there have been few rigorous studies examining the fundamental thermodynamic and electrokinetic processes influencing chiral separations in CE[27, 28]. In this study, the minimum criteria required for enantioselective resolution under a defined set of CE experimental conditions is investigated based on the dynamic complexation of *R/S*-propranolol and *R/S*-atenolol to HPβCD as a model system. Although the driving force for inclusion complexation was entropy-driven ($\Delta S^\circ > 0$), small differences in enthalpy change (ΔH°) influenced the selectivity and apparent migration order of the separation. In cases when the complex mobility for both enantiomers is similar in magnitude, a minimum relative energy difference ($\Delta\Delta G^\circ$) of about 50 cal·mol^{-1} was found to be sufficient for resulting in baseline resolution of *R/S*-propranolol, whereas only partial resolution of *R/S*-atenolol was achieved due to smaller differences in complex stability that approached experimental error. For entropy-driven processes involving weakly interacting solutes, ^2H_2O was used as an alternative solvent for enhancing hydrophobic interactions, which allowed for greater resolution of *R/S*-atenolol at lower HPβCD concentrations. Single-step analysis of micromolar levels of *R/S*-propranolol was also validated in this study, which provided a direct format for simultaneous determination of enantiomeric composition with normalization to creatinine in pooled urine samples.

2.3. Materials and methods

2.3.1. Chemicals and reagents

De-ionized water used for buffer and sample preparations was obtained using a Barnstead EASYpure®II LF ultrapure water system (Dubuque, Iowa, USA). ^2H_2O was obtained from Cambridge Isotope Laboratories, Inc. (Andover, MA. USA). Formate buffer was used in fundamental binding studies in CE, which was prepared from sodium formate (Sigma-Aldrich, St. Louis, MO. USA) with either H_2O or ^2H_2O as the solvent. The pH/p^{2}H of these buffers was adjusted to 4.0 with concentrated formic acid (Sigma-Aldrich, St. Louis, Mo. USA). Separate 200 mM stock solutions of HPβCD (Sigma-Aldrich, average degree of substitution of 7.0, average MWt: 1,540 Da were prepared in the 50 mM formate, pH 4.0 and p^{2}H 4.0 buffers respectively. HPβCD was used in this study because of its much greater water solubility compared to native β-CD in order to examine a wider concentration range for weakly interacting solutes. (*R*)-(+)-propranolol, (*S*)-(-)-propranolol, (*R*)-(+)-atenolol, (*S*)-(-)-atenolol and creatinine were all purchased from Sigma-Aldrich. 75 mM phosphate buffer was prepared from sodium dihydrogen phosphate from Alfa-Aesar (Ward Hill, MA., USA). The pH of this buffer was adjusted to 2.0 with concentrated phosphoric acid (Sigma-Aldrich), which was employed as the run buffer for *R/S*-propranolol determination in urine in order to suppress the electroosmotic flow (EOF) for improved chiral resolution. 1-naphthlenemethylamine (Sigma-Aldrich) was included as an internal standard for enhanced precision in quantification based on relative peak areas. Individual 50 mM stock solutions of 1-naphthlenemethylamine, caffeine (EOF marker) and the *R*- and *S*-enantiomers of

propranolol and atenolol were prepared in de-ionized water prior to analysis.

2.3.2. Urine samples

First morning mid-stream urine was collected from three healthy male individuals and kept on ice until analysis. Pooled samples (n = 3) were initially centrifuged at 10,000 r.p.m. for 10 min and then diluted 10-fold in de-ionized water prior to analysis by CE with UV detection.

2.3.3. Instrumentation

Automated P/ACE MDQ and P/ACE 5500 CE systems (Beckman-Coulter Inc., Fullerton, CA, USA) were used for all separations in which H_2O or ^2H_2O were used during buffer preparations. Uncoated fused-silica capillaries (Polymicro Technologies, Phoenix, AZ, USA) with 75 μm i.d., 362 μm o.d. were used for all separations. Capillary lengths were 90 cm (P/ACE MDQ) or 87 cm (P/ACE 5500) respectively. Separations were initiated by a 5 min rinse of the separation buffer followed by a 10 s injection of the sample. Electrophoresis was performed with an applied voltage of 30 kV and UV absorbance was monitored at 214 nm.

2.3.4. Theory and dynamic complexation model

A 1:1 dynamic complexation model was used in this study by measuring changes in apparent electrophoretic mobility (μ_{ep}^{A}) of enantiomers as a function of HPβCD concentration and temperature as depicted in *Figure 2.1*. The stoichiometry of reversible HPβCD:propranolol interactions, including other cyclodextrin derivatives was previously confirmed to be 1:1[29]. In order to accurately measure K and $\mu_{ep,AC}$ parameters, all non-specific changes in apparent solute mobility (μ_{ep}^{A}) with HPβCD addition need to be

corrected, such as solution viscosity. The relative viscosity correction factor (ν) at each HPβCD concentration was measured (n = 5) directly by CE as the time ratio required to push a 10 s sample plug past the detector under low pressure (0.5 psi) relative to a HPβCD-free solution[26]. A non-linear binding isotherm (Igor Pro 4.0, Wavemetrics Inc., Lake Oswego, USA) was used for determination of K and $\mu_{ep,AC}$ based on changes in viscosity-corrected apparent mobility ($\nu \cdot \mu_{ep}^{A}$) for each enantiomer at different HPβCD concentrations based on the following expression:

$$\nu \cdot \mu_{ep}^{A} = \frac{1}{1 + K \cdot [C]} \cdot \mu_{ep,A} + \frac{K \cdot [C]}{1 + K \cdot [C]} \cdot \mu_{ep,AC} \qquad (1)$$

where [C] represents the concentration of chiral selector, HPβCD. Similarly, the temperature-dependence of binding was assessed using a van't Hoff plot, which was performed for determination of thermodynamic parameters impacting chiral separations using temperatures ranging from 293.15 K to 313.15 K. Separations were performed in commercial CE instruments without significant Joule heating, as deduced by Ohm plots, with about 85% of the effective capillary length adequately thermostatted using a liquid coolant system. All mobility measurements were performed in triplicate (n = 3) with coefficient of variances (CV) typically under 2 %.

The enantioselectivity in CE is based on relative differences in apparent mobility ($\Delta\mu_{ep}^{A} = \mu_{ep}^{A}{}_{R} - \mu_{ep}^{A}{}_{S}$) for each enantiomer pair due to differential intermolecular interactions with a chiral selector during electromigration as described[30-32] by:

$$\Delta\mu_{ep}^{A} = \frac{\mu_{ep,A} + \mu_{ep,AC_R} K_R [C]}{1 + K_R \cdot [C]} - \frac{\mu_{ep,A} + \mu_{ep,AC_S} K_S [C]}{1 + K_S \cdot [C]} \qquad (2)$$

Equation (2) assumes that the magnitude of both binding affinity and complex mobility are different for each enantiomer. Four different scenarios can be deduced from this expression[23]. Maximum separation of cationic enantiomers when using a neutral chiral selector in CE occurs when $K_R > K_S$ and $\mu_{ep,AC,R} < \mu_{ep,AC,S}$, where both thermodynamic and electrokinetic processes are cooperative and additively contribute to chiral discrimination. This favourable case can occur whenever higher binding affinity results in complexes of larger average conformational size and/or lower effective charge. In contrast, if $K_R > K_S$ but $\mu_{ep,AC,R} > \mu_{ep,AC,S}$, then resolution gained by the enantiomer of higher affinity can be offset by its higher complex mobility resulting in lower resolution and in some cases a reversal in migration order as predicted by affinity alone[27], which is indicative of an anti-cooperative case. If the binding affinity is equivalent for each enantiomer such that $K_R \approx K_S$, then subtle differences in complex mobility based on conformational selectivity can induce chiral resolution[23]. In all four situations, the overall resolution in chiral CE separations is directly proportional to the magnitude of $\Delta\mu_{ep}{}^{A}$, which is enhanced under EOF suppressed conditions (*i.e.*, $\mu_{eo} \approx 0$) for cationic solutes as described by the equation below:

$$R_S = \frac{\sqrt{N}}{4} \cdot \left(\frac{\Delta \mu_{ep}{}^{A}}{\mu_{ep,A(Average)} + \mu_{eo}} \right) \qquad (3)$$

where N represents the number of theoretical plates. Strategies for enhancing separation efficiency (N) while minimizing dispersion can also improve chiral resolution, such as operation under high voltages without Joule heating and application of on-line sample preconcentration techniques that induce analyte band narrowing to counter diffusion[33].

2.4. Results and discussion

2.4.1. Chiral CE separations of racemic β-blocker drugs using HPβCD

The stability of inclusion complexes involving small hydrophobic solutes with cyclodextrins (CDs) depend on both steric and electronic complementarity. The former property is dependent on the dimensions of the cavity for the host relative to the specific size and shape of guest, which is illustrated by significant differences in binding affinity observed among different oligomeric CDs (*i.e.*, α, β, γ)[29]. For instance, propranolol has been observed not to interact with α-CD due to steric repulsion, whereas β-CD can accommodate the bulky apolar naphthyl moiety of propranolol due to its greater cavity diameter of about 7 Å[34]. Enantioselectivity in chiral CE separations is also dependent on the average degree of substitution and the regioselective position of substituent groups when using modified CD derivatives, which can significantly alter affinity[35]. In this work a heterogeneous mixture of HPβCD with an average degree of substitution of 7.0 was used as the chiral selector due to its high aqueous solubility. Bulky modifications to the chiral selector can result in complete loss in enantioselective resolution for *R/S*-propranolol, such as (2,6-di-O-methyl)-β-CD[11]. Although the fundamental driving forces associated with cyclodextrin inclusion complexation in aqueous solutions is still controversial, as it is dependent on specific electrolyte conditions, van der Waal and hydrophobic interactions, as well as hydration effects associated with rearrangement of original solvated water molecules around the host and guest[36]. In general, a simultaneous three-point interaction of the chiral selector with three different substituents on the stereogenic centre of a solute is necessary for chiral recognition[37]. *Figure 2.*1 highlights

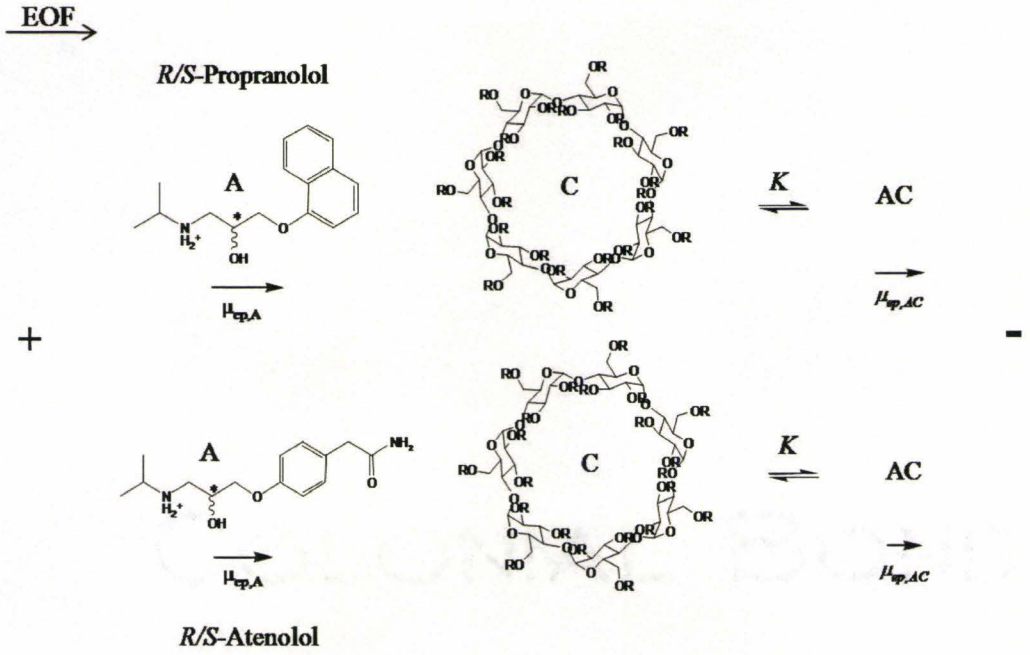

Figure 2.1: Schematic diagram of dynamic 1:1 inclusion complexation of cationic racemic drugs with neutral HPβCD (C) as the chiral selector in CE, where K, $\mu_{ep,A}$ and $\mu_{ep,AC}$ represent the apparent binding constant, free mobility and complex mobilities of drug enantiomers. Complex formation results in a significant reduction in mobility ($\mu_{ep,AC} < \mu_{ep,A}$) due to increased hydrodynamic size of the host-guest complex (AC) relative to free solute (A).

that propranolol and atenolol differ primarily in terms of the polarity of the ether substituent, which significantly reduces the hydrophobicity of atenolol relative to propranolol as related to their octanol-water partition coefficient values (logP) of 0.23 and 3.65, respectively[38]. Wren and Rowe[39] previously demonstrated that the relative magnitude of logP for related β-blockers analogues was correlated to their binding affinity when using CDs in chiral CE separations in the absence of significant steric hindrance. Note that the free mobility ($\mu_{ep,A}$) and complex mobility ($\mu_{ep,AC}$) of propranolol are both larger in magnitude relative to atenolol, which is indicative of its smaller average molecular volume and hydrodynamic radius. Thus, significant

differences in both steric and electronic properties of the guest solutes impact the apparent stability of complex formation with CDs.

2.4.2. Binding isotherms and limits of weak enantioselectivity

Figure 2.2 depicts a series of electropherograms highlighting changes in the migration and enantioselectivity for *R/S*-propranolol and *R/S*-atenolol as a function of HPβCD concentration in 50 mM formic acid, pH 4.0. It is apparent that the addition of 20 mM HPβCD was sufficient to resolve *R/S*-propranolol with significantly longer migration times (*i.e.,* slower μ_{ep}^{A}), in contrast to *R/S*-atenolol which remained unresolved. Higher concentrations of HPβCD failed to adequately baseline resolve *R/S*-atenolol (Rs ≈ 0.7) at the expense of a loss in resolution of *R/S*-propranolol. This resolution dependence on the specific concentration of chiral selector is related to the relative influences of both K and $\mu_{ep,AC}$ on the separation[40]. A maximum concentration of HPβCD not exceeding 100 mM was used in this study due to significant increases in background noise and baseline stability. Thus, simultaneous resolution of both racemic drugs under a single experimental condition is challenging due to their large differences in complex stability. *Figure 2.3* depicts non-linear binding isotherms by CE for *R/S*-propranolol and *R/S*-atenolol based on changes in $\nu \cdot \mu_{ep}^{A}$ as a function of [HPβCD] as described in *Equation (1)*, which clearly highlights the stronger affinity for inclusion complexation of propranolol. For both racemic cationic β-blocker drugs, the *R*-enantiomer was observed to have a higher relative affinity that is consistent with previous reports[21]. However, in the case of *R/S*-atenolol, the extent of enantioselective resolution as measured by $\Delta\mu_{ep}^{A}$ approached experimental error (CV < 2 %) in this study. For instance, optimum

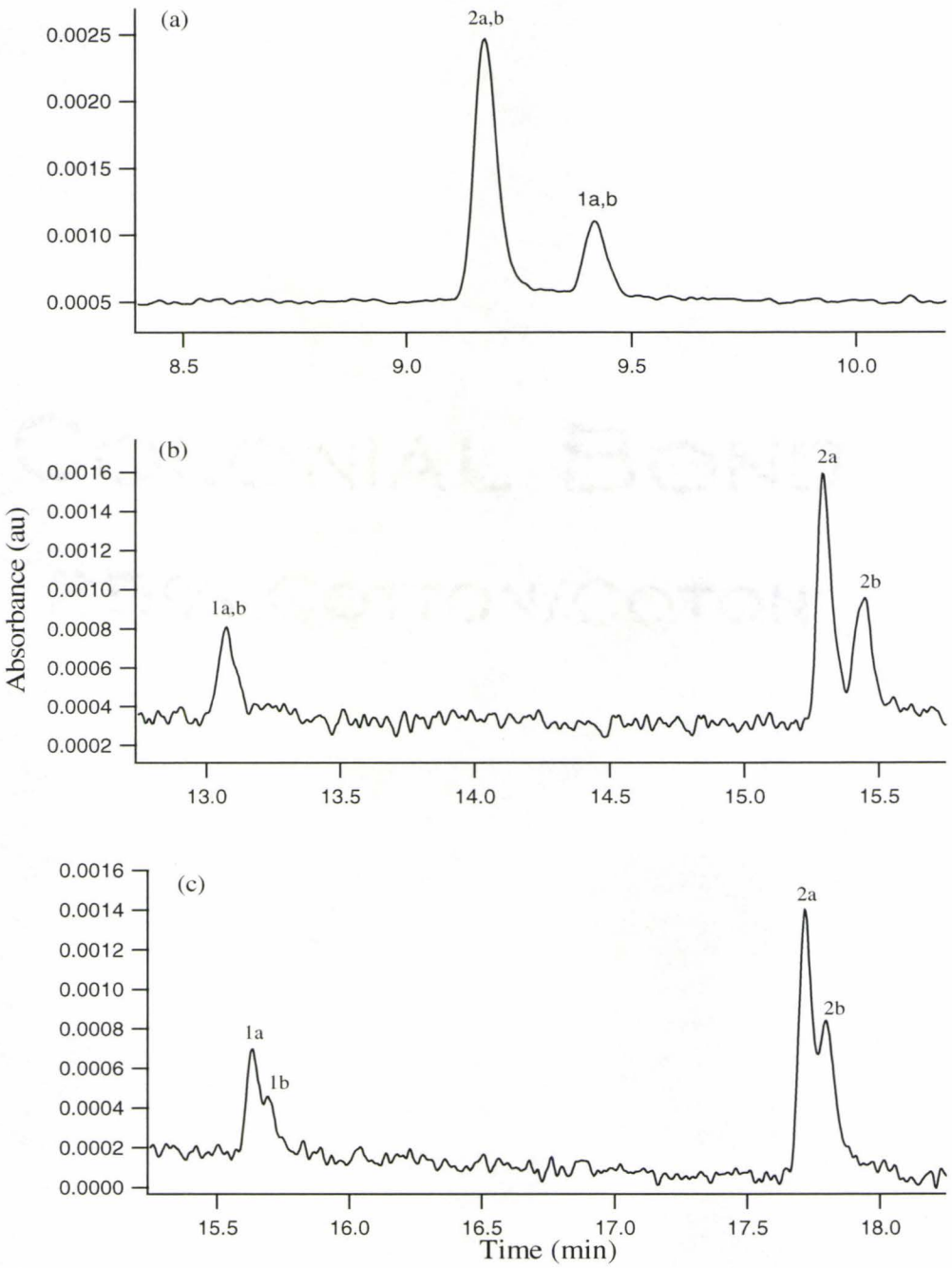

Figure 2.2: (a) Representative electropherograms for the separation of *R/S*-atenolol and *R/S*-propranolol at 25°C in 50 mM formate buffer, pH 4.0 containing (a) 0 mM, (b) 20 mM and (c) 70 mM HPβCD respectively. Conditions: 50 mM formate buffer, pH 4.0 containing varying concentrations (0 to 70 mM) of HPβCD; temperature 298.15 K; voltage 30 kV; capillary length 90 cm; capillary i.d. 75 μm; injection time 10 s; UV 214 nm. Analyte peak numbering; 1a, *S*-atenolol; 1b, *R*-atenolol; 2a, *S*-propranolol and 2b, *R*-propranolol.

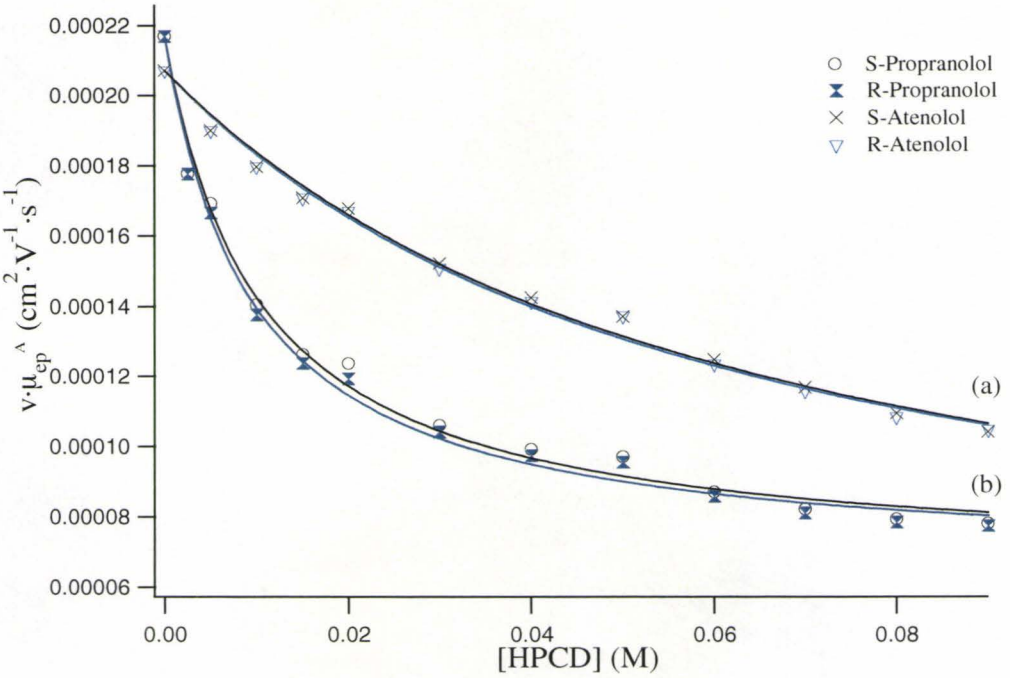

Figure 2.3: Non-linear binding isotherms of (a) *R/S*-atenolol and (b) *R/S*-propranolol based on changes in average (n=3) viscosity-corrected electrophoretic mobilities ($v \cdot \mu_{ep}{}^{A}$) as a function of [HPβCD]. Note that differences in apparent mobilities for *R/S*-atenolol ($v \cdot \mu_{ep}{}^{A}$) are within experimental error (CV < 2 %). Separation conditions for binding studies are the same as described in *Figure 2.2*.

resolution of *R/S*-atenolol at 90 mM HPβCD generated an average $\Delta\mu_{ep}{}^{A}$ difference of only 1.3 % in contrast to over 3.0 % for *R/S*-propranolol at 20 mM HPβCD as calculated using *:*

$$\Delta\mu_{ep}{}^{A} = \frac{\left(\mu_{ep}{}^{A}{}_{R} - \mu_{ep}{}^{A}{}_{S}\right)}{\left(\frac{\mu_{ep}{}^{A}{}_{R} + \mu_{ep}{}^{A}{}_{S}}{2}\right)} \cdot 100\ \% \qquad (4)$$

where $\mu_{ep}{}^{A}{}_{R}$ and $\mu_{ep}{}^{A}{}_{R}$ represent the apparent mobilities of the *R*- and *S*- drug enantiomers respectively. A recent study by Castronuovo *et al.*[34] noted that the enantioselectivity of *R/S*-propranolol interactions with β-CD was not detectable by

calorimetry due their weak and similar binding affinity despite chiral resolution greater than 1.0 reported by LC separations[21]. Thus, the excellent precision offered by CE permits the accurate determination of weak binding interactions in free solution[23, 41] that can be used to distinguish small differences in enantioselectivity as an aid to conventional spectroscopic and calorimetry protocols provided the relative difference in $\Delta\mu_{ep}^{A}$ for enantiomer pairs exceeds about 2 %.

2.4.3. Thermodynamics and electrokinetics of inclusion complexation

A fundamental understanding of the thermodynamic and electrokinetic factors governing chiral resolution in CE will ultimately aid in the design and rigorous optimization[40, 42] of effective chiral separations. *Table 2.*1 summarizes apparent *K* and $\mu_{ep,AC}$ parameters for *R/S*-propranolol and *R/S*-atenolol at 25°C, as well as enthalpy (ΔH^{o}) and entropy ($T\Delta S^{o}$) contributions to the overall free energy of complex formation. It is apparent that *R*-propranolol has a larger *K* of 105 M^{-1} relative to 97 M^{-1} for *S*-propranolol, whereas both *R/S*-atenolol enantiomers have much weaker and statistically equivalent binding affinity of about 16 M^{-1}. Both of these relative differences in *K* were not significant at the 95% confidence interval. The average formation constant for *R/S*-propranolol determined in this study is consistent with 120 M^{-1} as reported for the racemic mixture by calorimetry when using HPβCD with a degree of substitution of 6.3 in water[34]. *Table 2.1* also reveals that $\mu_{ep,AC}$ values were significantly different between propranolol and atenolol complexes as compared to their free mobilities (only 5 % difference in $\mu_{ep,A}$), which is associated with the greater depth of inclusion formation within the cavity of HPβCD that is favored for the napthyl substituent of propranolol[43].

Table 2.1: Thermodynamic and electrokinetic factors influencing chiral separations of *R/S*-propranolol and *R/S*-atenolol by CE using HPβCD in 50 mM formate, pH 4.0.

Analyte	K^a (M^{-1})	$\Delta H°$ [b] (kcal·mol^{-1})	$T\Delta S°$ [b] (kcal·mol^{-1})	$\mu_{ep,AC}$ x 10^{-5} [a] ($cm^2 \cdot V^{-1} \cdot s^{-1}$)
S-Propranolol	(97 ± 8)	(0.2 ± 0.2)	(2.9 ± 0.2)	(6.6 ± 0.3)
R-Propranolol	(105 ± 8)	-(0.02 ± 0.08)	(2.7 ± 0.1)	(6.6 ± 0.3)
S-Atenolol	(16 ± 2)	(1.4 ± 0.5)	(3.0 ± 0.5)	(3.6 ± 1)
R-Atenolol	(16 ± 2)	(1.2 ± 0.3)	(2.9 ± 0.3)	(3.7 ± 1)

[a] Parameter determined from non-linear regression of the 298.15 K HPβCD binding isotherm with error ± 1σ, where the average free mobility ($\mu_{ep,A}$) of *R/S*-propranolol and *R/S*-atenolol were 2.17×10^{-4} $cm^2 \cdot V^{-1} \cdot s^{-1}$ and 2.07×10^{-4} $cm^2 \cdot V^{-1} \cdot s^{-1}$ respectively.

[b] Thermodynamic properties derived from a van't Hoff plot using five experimental values from 293.15 - 313.15 K

However, the relative differences in $\mu_{ep,AC}$ for their respected enantiomers (*i.e.*, diasteromeric complexes) was not statistically significant within experimental error. This equivalence in $\mu_{ep,AC}$ translates into equivalence in the frictional drag of the formed complex during electromigration as dictated by its overall size, shape and degree of salvation. The thermodynamics of binding were determined to be largely entropy-driven indicative of the high positive values of $T\Delta S°$ (> 2.7 kcal·mol^{-1}) notably for *R/S*-propranolol. This data is consistent with hydrophobic interactions as being the major driving force associated with solvation effects and the relaxation of bulk water upon inclusion complexation. *Table 2.1* highlights that small differences in enthalpy ($\Delta H°$) for *R/S*-propranolol that is weakly endothermic or null ($\Delta H° \approx 0$) is the likely cause for the observed enantioselectivity, since the diastereomeric complex of *R*-propranolol is marginally more exothermic than *S*-propranolol. Similar findings also attributed minimum energy configurations for *R*-propranolol relative to *S*-propranolol with β-CD as

determined by X-ray crystallographic projections[21] and computer molecular modelling[43]. It is clear that the major cause for the weak affinity and reduced enantioselectivity of *R/S*-atenolol is related to its unfavourable energetics upon HPβCD complexation that is considerably endothermic with $\Delta H° > 1.2$ kcal·mol^{-1}. The relatively high error associated with $\mu_{ep,AC}$ determination for *R/S*-atenolol is related to the binding isotherm extending to only about 62 % of the fraction of complex formed due to its weak overall affinity and limitations in the experimental conditions. This work suggests that under these experimental conditions, in which $\mu_{ep,AC}$ is equivalent for both enantiomers, a relative minimum energy difference ($\Delta\Delta G°$) of about 50 cal·mol^{-1} in terms of complex stability was found to be sufficient to generate baseline resolution of enantiomers by chiral CE. It should be noted though that K, $\mu_{ep,AC}$ and peak efficiency all directly influence an observed chiral separation in CE[23]. Thus, this 50 cal·mol^{-1} difference in free energy should not be viewed as an absolute energy difference required for achieving chiral separation of *R/S*-propranolol under any electrophoretic system. For instance, a $\Delta\Delta G$ value of 50 cal·mol^{-1} may be sufficient for resolution if the ΔK of the enantiomers is small but if ΔK is large, this $\Delta\Delta G$ value is inconsequential and the relative influences of $\mu_{ep,AC}$ on the separation must also be considered[23].

It should also be noted that the thermodynamic and electrokinetic parameters derived in this study represent the average interactions with the multiple component HPβCD mixture. They do not reflect the complexation of the racemic drugs with HPβCD of a specific degree of substitution but are indicative of the average effects of analyte : HPβCD binding. Thus, the $\Delta\Delta G$ value derived in this study solely represents the relative

free energy of binding difference for *R*- and *S*-propranolol, as dictated by their respective apparent association constants with the heterogeneous HPβCD chiral selector mixture under the designed experimental conditions, responsible for the observed separation.

2.4.4. Enhancement of hydrophobic interactions using D_2O as solvent

To date, most chiral CE studies have examined the impact of different CD analogues and organic modifiers for improving enantioselectivity. For instance, over a two-fold improvement in resolution (Rs > 4) was achieved for determination of the enantiomeric purity of *R*-propranolol when using the anionic carboxymethyl-β-CD derivative relative to HPβCD presumably due to favorable electrostatic interactions upon complexation[11]. Significant improvements in chiral resolution was also reported by using achiral organic additives that form rigid ternary complexes with *R/S*-propranolol and β-CD[10]. However, the latter strategy is not suitable for weakly interacting solutes because of competitive displacement by organic additives that results in a significant loss in binding affinity notably when performing non-aqueous chiral CE separations[44]. Since the driving force for inclusion complexation in this study is based primarily on hydrophobic interactions, the impact of ^2H_2O as a solvent on the apparent enantioselectivity and binding affinity for the weakly interacting *R/S*-atenolol was investigated in this study. Due to the stronger bond energies and higher structural order of ^2H_2O relative to H_2O, previous reports have demonstrated higher apparent binding affinity for complex formation of different solutes with β-CD[45, 46]. *Figure 2.4* shows an overlay of three electropherograms for *R/S*-atenolol under different buffer conditions that highlights that an equivalent resolution of about 0.5 is achieved at a similar migration time when using

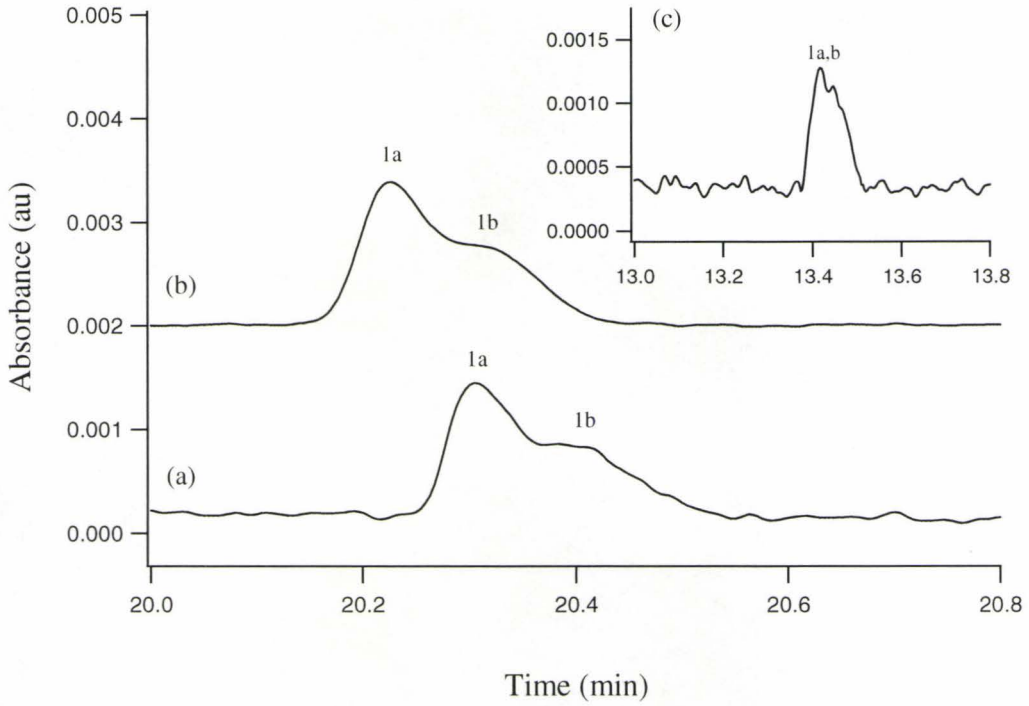

Figure 2.4: Impact of ^2H_2O as a useful solvent in chiral CE separations to enhance hydrophobic interactions with HPβCD involving weakly interacting solutes. Electropherograms demonstrate that equivalent resolution of *R/S*-atenolol can be achieved at lower [HPβCD] in ^2H_2O due to the combined effects of higher apparent guest affinity and increased solution viscosity. 50 mM formate buffer, pH 4.0 with (a) 100 mM HPβCD in H_2O, (b) 30 mM HPβCD in ^2H_2O and (c) 30 mM HPβCD in H_2O. Analyte peak numbering and other conditions are similar to *Figure 2.2*.

30 mM HPβCD in ^2H_2O relative to 90 mM HPβCD in H_2O. The inset of *Figure 2.4* is a control that depicts the loss in resolution and faster migration time (*i.e.,* higher $\mu_{ep}{}^{A}$) of *R/S*-atenolol when using 30 mM HPβCD in H_2O. An apparent K of 23 ± 3 M^{-1} for *R/S*-atenolol at 25°C for HPβCD was determined by this study, which is about 44% greater than in aqueous solution. It should be noted that the significant increase in *R/S*-atenolol migration time when using ^2H_2O in *Figure 2.4* was due to the combined effects of higher binding affinity and increased solution viscosity, which is about 23 % greater than H_2O at 25°C[46] that is reflected in the apparent decrease in $\mu_{ep,AC}$ for *R/S*-atenolol of 2.9 ± 0.7x10^{-5} $cm^2 \cdot V^{-1} \cdot s^{-1}$. Despite the advantage of obtaining greater resolution at lower chiral selector

concentrations in chiral CE separation when using deuterated solvents, there was no appreciable improvement in the enantioselectivity for *R/S*-atenolol. These results again confirm that molecular association of racemic drugs with CDs in this study is indeed entropy-driven that can be enhanced in $^{2}H_2O$ solvent, however enantioselectivity is dictated by enthalpy differences involving weak intermolecular interactions that are not associated with hydration effects.

2.4.5. Single-step enantioselective analysis of R/S-propranolol in urine

Urine spot sampling is a convenient and widely used method for clinical monitoring of drug and xenobiotic metabolism that depends on creatinine-adjusted solute concentrations to correct for urinary flow variability. Creatinine is typically measured independently by the standardized Jaffe reaction using colorimetric detection[47]. *Figure 2.5* depicts a single-step enantioselective method for determination of low micromolar levels of *R/S*-propranolol spiked in urine samples as normalized to creatinine by CE with UV detection. Pooled human urine samples were diluted 10-fold in de-ionized water prior to CE analyses without complicated sample handling. In this case, 75 mM phosphate, 17 mM HPβCD, pH 2.0 was used as the optimized buffer for separation in order to achieve baseline resolution of *R/S*-propranolol (Rs > 1.0) under EOF suppressed conditions while avoiding interferences from background cationic metabolites in the urine matrix. Simultaneous quantification of creatinine and propranolol in urine samples was feasible by CE despite over two-orders of magnitude difference in their respected concentrations. *Table 2.2* summarizes validation parameters for the optimized method that highlights

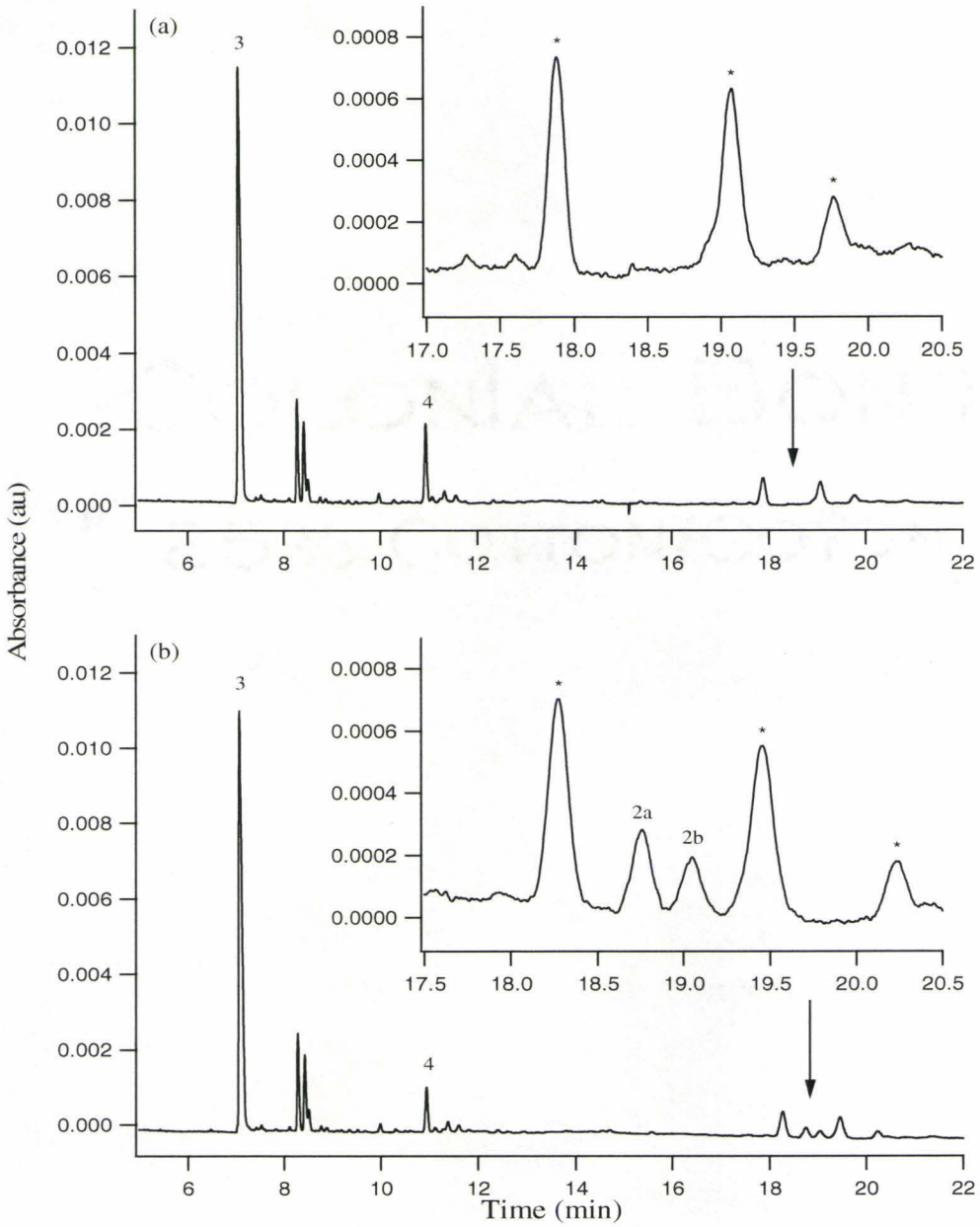

Figure 2.5: Single-step enantioselective analysis of *R/S*-propranolol in pooled human urine as normalized to creatinine. Electropherograms represent (a) pooled human urine spiked with 10 μM internal standard (I.S.) and (b) sample spiked with 3 μM *S*-propranolol and 2 μM *R*-propranolol. Urine samples were diluted 10-fold in de-ionized water prior to CE analysis. Conditions: 75 mM phosphate buffer, pH 2.0 containing 17 mM HPβCD; temperature 25°C; voltage 30 kV; capillary length 67 cm; sample injection 10 s; UV 214 nm. Analyte peak numbering; 2a, *S*-propranolol; 2b, *R*-propranolol; 3, creatinine; 4, naphthlenemethylamine (I.S.); and * denotes background urinary metabolites.

Table 2.2: Validation of single-step[a] enantioselective analysis of *R/S*-propranolol in urine as normalized to creatinine by CE with UV detection.

Validation Parameter	Creatinine	*S*-Propranolol	*R*-Propranolol
A. Interday precision (n = 5)			
Migration Time/CV	1.3	2.9	3.0
IS Normalized Peak Area[b]/CV	1.9	3.1	3.3
B. Calibration Curve[c]			
Linearity/R^2	0.9945	0.9958	0.9947
C. Detection Limit (S/N ≈ 3)			
Concentration/μM	1.0	0.1	0.1

a. Optimal conditions; Conditions: 75 mM phosphate buffer, pH 2.0 containing 17 mM HPβCD; temperature 25°C; voltage 30 kV; capillary length 67 cm; injection 10 s; UV 214 nm.
b. Precision measurements performed using 30 μM creatinine, 5 μM *R/S*-propranolol and 10 μM I.S.
c. Duplicate measurements of ten and fifteen solutions ranging from 5 μM to 12 mM for creatinine and 0.5 to 110 μM for *R/S*-propranolol respectively. All solutions contained 10 μM I.S.

excellent method reproducibility under 4% when using an internal standard, a wide linear dynamic range, as well as sub-micromolar detection limits of about 0.1 μM for *R/S*-propranolol. Although the majority of propranolol exists as its glucuronide, sulphate or hydroxide conjugate in urine[8, 9], acid hydrolysis pretreatment can be readily adopted to this method for future assessment of differential metabolism of racemic drugs.

2.5. Summary and conclusion

A fundamental study of the thermodynamic and electrokinetic factors influencing chiral separations was examined for model racemic drugs by CE. Enantioselectivity was influenced by small differences in enthalpy as related to the stability of complex formation despite molecular association being driven by high entropy changes indicative of hydrophobic interactions. The chiral resolution and apparent binding affinity for *R/S*-

propranolol was significantly greater than *R/S*-atenolol because of unfavorable endothermic processes associated with its lower hydrophobicity (logP) and reduced complex mobility ($\mu_{ep,AC}$). In this study, a minimum standard free energy difference ($\Delta\Delta G°$) of about 50 $cal \cdot mol^{-1}$ was determined to be necessary for adequate enantioselective resolution with accurate determination of binding constants for *R/S*-propranolol enantiomers under the experimental conditions employed. Enhanced binding of weakly interacting *R/S*-atenolol was enhanced by using ^2H_2O as a solvent during chiral CE separations that allows for improved resolution at lower chiral selector concentrations when hydrophobic interactions are dominant. A single-step method using single-spot urine samples for differential racemic drug metabolism studies was also demonstrated that offers a convenient and rapid format for enantioselective determination of low micromolar levels of *R/S*-propranolol adjusted to creatinine.

2.6. References

1. G. Gubitz and M. G. Schmid, *Molecular Biotechnology*, 2006, **32**, 159-180.
2. S. Nattel, G. Gagne and M. Pineau, *Clin. Pharmacokinet.*, 1987, **13**, 293-316.
3. B. Silber and S. Riegelman, *J. Pharmacol. Exp. Ther.*, 1980, **215**, 643-648.
4. G. Vaiva, F. Ducrocq, F. Jezequel, B. Averland, P. Lestavel, A. Brunet and C. R. Marmar, *Biological Psychiatry*, 2003, **54**, 947-949.
5. P. H. Roberts and K. V. Thomas, *Science Total Environ.* , 2006, **356**, 143-153.
6. L. J. Fono and D. L. Sedlak, *Environ. Sci. Technol.*, 2005, **39**, 9244-9252.

7. C. Pham-Huy, A. Sahui-Gnassi, V. Saada, J. P. Gramond, H. Galons, S. Ellouk-Achard, V. Levresse, D. Fompeydie and J. R. Claude, *J. Pharma. Biomed. Anal.*, 1994, **12**, 1189-1198.

8. K. M. Sowinski, J. J. Lima, B. S. Burlew, J. D. Massie and J. A. Johnson, *Br. J. Clin. Pharmacol.*, 1996, **42**, 339-346.

9. L.-J. Luan, Q. Shao, J.-Y. Ma and S. Zeng, *World J. Gastro.*, 2005, **11**, 1822-1824.

10. E. Billot, J. Wang and I. M. Warner, *J. Chromatogr. A*, 1997, **773**, 321-329.

11. M. Fillet, I. Bechet, P. Chiap, P. Hubert and J. Crommen, *J. Chromatogr. A*, 1995, **717**, 203-209.

12. J. J. Martinez-Pla, Y. Martin-Biosca, S. Sagrado, R. M. Villanueva-Camanas and M. J. Medina-Hernandez, *Anal. Chim. Acta*, 2004, **507**, 175-182.

13. J. J. B. Nevado, J. R. Flores, G. C. Penalvo and F. J. G. Bernardo, *Anal. Chim. Acta*, 2006, **559**, 9-14.

14. X. Bai, T. You, H. Sun, X. Yang and E. Wang, *Electroanalysis*, 2000, **12**, 1379-1382.

15. W. Lu and R. B. Cole, *J. Chromatgr. B*, 1998, **714**, 69-75.

16. V. Schurig, *Trends Anal. Chem.* , 2002, **21**, 647-661.

17. Sanchez-Hernandez, A. L. Crego, M. L. Marina and C. Garcia-Ruiz, *Electrophoresis*, 2008, **29**, 237-251.

18. Z. Wang, J. Ouyang and W. R. G. Baeyens, *J. Chromatogr. B*, 2008, **862**, 1-14.

19. X. J. Peng, M. T. Bowser, P. Britz-McKibbin, G. M. Bebault, J. R. Morris and D. D. Y. Chen, *Electrophoresis*, 1997, **18**, 706-716.

20. G. Gübitz and M. G. Schmid, *Electrophoresis*, 2007, **28**, 114-126.

21. D. W. Armstrong, T. J. Ward, R. D. Armstrong and T. E. Beesley, *Science*, 1986, **232**, 1132-1135.

22. Y. Tanaka and S. Terabe, *J. Chromatgr. B*, 2002, **769**, 81-92.

23. B. Chankvetadze, W. Lindner and G. K. E. Scriba, *Anal. Chem.*, 2004, **76**, 4256-4260.

24. R. Vespalee and P. Bocek, *Chem. Rev.* , 2000, **100**, 3715-3753.

25. B. Chankvetadze, *Electrophoresis*, 2002, **23**, 4022-4035.

26. S. Samson and P. Britz-McKibbin, *Electrophoresis*, 2006, **27**, 842-851.

27. C. Kaiser, G. Seguí-Lines, J. C. D'Amaral, A. S. Ptolemy and P. Britz-McKibbin, *Chem. Comm.* , 2008, **3**, 338-340.

28. J. C. Reijenga, B. A. Ingelse and F. M. Everaerts, *J. Chromatogr. A*, 1997, **792**, 371-378.

29. M. Plätzer, M. A. Schwartz and R. H. H. Neubert, *J. Microcol. Sep.*, 1999, **11**, 215-222.

30. S. A. C. Wren and R. C. Rowe, *J. Chromatogr. A*, 1992, **603**, 235-241.

31. S. A. C. Wren and R. W. Rowe, *J. Chromatogr. A*, 1993, **609**, 363-367.

32. N. D. Stepanova, A. V. Stepanov and J. Russion, *J. Appl. Chem. Engl. Ed.*, 1969, **42**, 1576-1578.

33. A. S. Ptolemy and P. Britz-McKibbin, *Analyst*, 2008, *submitted.*

34. G. Castronuovo and M. Niccoloi, *Bioorg. Med. Chem.*, 2006, **14**, 3883-3887.

35. K. W. Phinney, J. W. Jackson and L. C. Sander, *Electrophoresis*, 2002, **23**, 1308-1313.

36. L. Liu and Q.-X. Guo, *J. Inclu. Phenom. Macro. Chem.*, 2002, **42**, 1-14.

37. A. Berthod, *Anal. Chem.*, 2006, **78**, 2093-2099.

38. J. M. Cruikshank, *Am. Heart J.*, 1980, **100**, 160.

39. S. A. C. Wren and R. C. Rowe, *J. Chromatogr. A*, 1993, **635**, 113-118.

40. C.-E. Lin, W.-S. Liao and K.-H. Chen, *Electrophoresis*, 2003, **24**, 3139-3146.

41. P. Britz-McKibbin and D. D. Y. Chen, *Electrophoresis*, 2002, **23**, 880-888.

42. Y. Y. Rawje, R. L. Williams, L. A. Buckinghams and G. Vigh, *J. Chromatogr. A*, 1994, **688**, 273-282.

43. H. Kim, K. Jeong, S. Lee and S. Jung, *Bull. Korean Chem. Soc.*, 2003, **24**, 95-99.

44. F. Wang and M. G. Khaledi, *Anal. Chem.*, 1996, **68**, 3460-3467.

45. A. S. Wang and Y. Matsui, *Bull. Chem. Soc. Jpn.*, 1994, **67**, 2917-2920.

46. S. Hamai and H. Sakuri, *J. Chromatogr. A*, 1998, **800**, 327-332.

47. H. Husdan and A. Rapoport, *Clin. Chem.*, 1968, **14**, 222-238.

Chapter III

Single-step Analysis of Low Abundance Phosphoamino Acids *via* On-line Sample Preconcentration with Chemical Derivatization by Capillary Electrophoresis

III. Single-step Analysis of Low Abundance Phosphoamino Acids *via* On-line Sample Preconcentration with Chemical Derivatization by Capillary Electrophoresis

3.1. Abstract

New strategies for rapid, sensitive and high-throughput analysis of low abundance metabolites in biological samples are required for future metabolomic research. In this *Chapter*, a direct method for sub-micromolar analyses of phosphoamino acids was developed using on-line sample preconcentration with 9-fluorenylmethyloxycarbonyl chloride (FMOC) derivatization by CE with UV detection is presented. Analyte focusing by dynamic pH junction and FMOC labelling efficiency were influenced by several experimental factors including buffer pH, ionic strength, sample injection length and FMOC concentration. About a 200-fold enhancement in concentration sensitivity was achieved under optimal conditions relative to conventional off-line derivatization, as reflected by a detection limit (S/N $\approx$ 3) of 0.1 μM. In-capillary sample preconcentration with chemical labelling by CE offers a unique single-step analytical platform for high-throughput screening of low abundance metabolites without intrinsic chromophores.

3.2. Introduction

Metabolomics is an emerging area of functional genomic research that involves the comprehensive analysis of metabolites in a cell or biological fluid. Metabolites that exist at low concentrations often have critical biological functions as hormonal chemical mediators influencing protein activity and phenotype. Low abundance metabolites in complex biological samples offer significant challenges to analytical methods in terms of

adequate sensitivity and selectivity. Conventional analysis of low abundance metabolites normally requires several distinct sample pre-treatment procedures, such as off-line sample preconcentration, chemical derivatization and desalting. Sample enrichment and analyte labelling methods are often time-consuming, incur sample loss, reduce precision and are difficult to automate. This begs the question: "is it feasible to integrate sample pretreatment and analysis using a single analytical format without deterioration of separation performance?"

Capillary electrophoresis (CE) represents a sensitive and high resolution separation method that is well suited for analysis of trace levels of charged metabolites[1, 2], in comparison to other methods including direct infusion MS[3], GC-MS[4], LC-MS[5], LC-NMR[6], and NMR[7], techniques. The rapid analysis times, minimal band dispersion and small sample requirements afforded by CE make it ideally suited for biological analyses. Moreover, CE is based on both electrokinetic and thermodynamic parameters which permit effective control of analyte band separation and dispersion processes. Despite these advantages, CE suffers from poor concentration sensitivity when using conventional UV absorbance detection. The small sample injection volume (typically less than 10 nL) and the narrow optical path length of CE often results in micromolar detection limits. CE with absorbance detection is not capable of measuring sub-micromolar levels of analytes and thus it is necessary to use a more sensitive detector format such as laser-induced fluorescence[8] or sample pretreatment based on off-line sample preconcentration by solid-phase microextraction[9]. Alternatively, there are several "in-capillary" sample preconcentration procedures developed for CE which include sample stacking[10, 11],

transient isotachophoresis[12, 13], sweeping[14, 15], dynamic pH junction[16, 17], as well as dynamic pH junction-sweeping[18, 19]. On-line preconcentration technique induce electrokinetic focusing of large volumes of injected sample based on differences in local analyte velocity within two or more distinct buffer segments in a capillary. Selection of the most appropriate sample preconcentration technique in CE is based on several factors including analyte physiochemical properties, sample matrix and buffer type used for separation[20].

To date, there have been few publications that effectively combine on-line sample preconcentration with chemical derivatization in CE, which is required for analytes that lack intrinsic chromophores. On-line preconcentration with chemical derivatization is vital for labelling trace levels of metabolites with high yield and fast kinetics under a single capillary format. Reinhoud *et al.*[21] first reported the use of isotachophoresis (ITP) using an on-line reaction cell and LIF detection of glutathione and several amino acids with the chemical label *o*-phthalaldehyde (OPA) and naphthalene-2,3-dicarboxaldehyde. This technique allowed for careful control of the derivatization reaction provided the buffer co-ions used with the ITP are carefully selected. Latorre *et al.*[22] employed large volume sample stacking combined with in-capillary derivatization using 1,2-naphthoquinone-4-sulfonate for the determination of amino acids in pharmaceutical and feed samples. The authors reported a 1000-fold improvement in detection limit with respect to conventional analyses provided the samples are of low conductivity. Recently, Oguri *et al.*[23] reported a technique for preconcentrating biogenic amines using field-amplified sample stacking and gradient effect mode on column prior to their

derivatization with OPA using capillary electrochromatography (CEC) and fluorescence detection. However, there currently is no routine procedure on-line preconcentration with chemical derivatization in CE that can be applied to different classes of low abundance metabolites derived from real biological samples.

In this report, the optimization and validation of an integrated on-line preconcentration and chemical derivatization technique based on dynamic pH junction and 9-fluorenylmethyloxycarbonyl chloride (FMOC) labelling is examined by CE with UV detection for sub-micromolar analyses of the major low abundance *O*-phosphoamino acid metabolites: phosphoserine, phosphothreonine and phosphotyrosine. Phosphoamino acids represent important post-translationally modified amino acids in many regulatory proteins in the cell. Conventional analyses of phosphoamino acids are based on the use of immunoassays[24], ^{32}P radioactive labelling[25], MS[26], and HPLC[27]. Recently, Lui *et al.*[28] reported a method using CE with LIF detection for the determination of phosphoamino acids in a hydrolyzed sample of a protein kinase. Although detection limits below 75 nM were reported for the three amino acids, the technique required a relatively long chemical derivatization time for off-line labelling using 3-(2-furoyl)quinoline-2-carboxaldehyde. In such cases, off-line chemical derivatization is the longest and most critical step for reliable quantitative analysis. Shorter total analysis times, improved precision and enhanced sensitivity can be realized by combining chemical derivatization, sample preconcentration and high resolution separations in CE. In this report, over a 200-fold enhancement in concentration sensitivity was realized for phosphoamino acid analysis compared to conventional off-line methods using CE and UV detection with a LOD of

about 0.1 μM and intra-day precision under 5 %. Optimal band narrowing and chemical derivatization of analytes was influenced by several factors including sample/buffer pH, ionic strength, sample injection length and FMOC concentration. To the best of our knowledge, this work represents the first report that investigates the use of buffer pH junctions to simultaneously tune in-capillary analyte focusing and analyte reactivity via zonal passing by CE.

3.3. Experimental

3.3.1. Chemicals and reagents

Deionized water used for buffer and sample preparations was obtained using a Barnstead EASYpure®II LF ultrapure water system (Dubuque, Iowa, USA). The aqueous background electrolyte (BGE) of 140 mM borate was prepared using sodium tetraborate decahydrate (borax) from Sigma-Aldrich (St. Louis, Mo., USA). The pH of the borate buffer was modified by 0.1 M NaOH to obtain a pH of 9.6 unless otherwise noted. The 40 mM phosphate sample buffer, pH 6.5 was prepared using sodium dihydrogen phosphate from Alfa-Aesar (Ward Hill, Mo., USA). All amino acids, *O*-phosphoamino acids and FMOC reagents were obtained from Sigma-Aldrich. 20 mM standard solutions of the phosphoamino acids, *O*-phosphoserine (P-Ser), *O*-phosphothreonine (P-Thr) and *O*-phosphotyrosine (P-Tyr) were prepared in 1:1 MeOH and de-ionized water. Stock solutions of amino acids were then diluted in buffer prior to off-line derivatization or direct analysis by on-line preconcentration and derivatization. 100 mM FMOC solutions were prepared fresh in HPLC grade acetonitrile (Sigma-Aldrich) every two days and kept refrigerated at 4°C. This was performed due to the

limited solubility of FMOC in aqueous solutions and its propensity to hydrolyze in water[29].

3.3.2. Instrumentation and procedure

Separations were performed on a Beckman P/ACE 2100 automated capillary electrophoresis system (Beckman Instruments, Fullerton, CA., USA). Uncoated capillaries (Polymicro Technologies, Phoenix, AZ., USA) with 75 μm i.d., 365 μm o.d., and 87 cm length were used. Each separation was initiated with a 5 min rinse of 0.1 M NaOH, followed by a 5 min rinse with BGE. Off-line derivatization was performed by mixing 20 μM of each phosphoamino acid with 100 mM FMOC in acetonitrile, which was vortexed for 30 s prior to CE analysis. The sample was then introduced using a low pressure (0.5 psi or 3.5 kPa) hydrodynamic injection for 3 s. The low pressure rinse was measure in triplicate to have an average velocity of 5.1 $cm \cdot min^{-1}$, which was used to measured sample injection length (w_{inj}). On-line preconcentration and FMOC labelling was performed on-capillary by first directly injecting a plug of phosphoamino acid dissolved in phosphate buffer for 3 s to 300 s under low pressure. Next a 10 s low pressure injection of BGE immediately followed the sample injection, which is referred to as a spacer plug. A 100 mM FMOC solution in acetonitrile was then injected under low pressure to 5 s. All injection sequences were automated under computer control and separations were carried out thermostatted at 25°C using a voltage of 25 kV and UV absorbance monitored at 214 nm. The detector bandwidths (w_{det}) were measured by transforming the measured base peak width in the time to the distance domain by multiplying by the analyte migration velocity. The detector to injection band width ratio

(DIBR) was used as a measure of analyte band focusing[16]. The conductivity of the buffer solutions was measured with a MC 126 conductivity meter (Mettler-Toledo GmbH, Switzerland).

3.4. Results and discussion

3.4.1. On-line sample preconcentration *via* dynamic pH junction

Electrokinetic focusing is not only important for achieving sample enrichment by concentrating large volumes of an analyte within a narrow zone, but also for realizing extremely high separation efficiency needed for adequate resolution of complex mixtures. Various buffer properties (*e.g.*, conductivity, co-ion mobility, additive interaction) can be used to modify the local analyte electrophoretic mobility, however buffer pH represents one of the most effective ways to tune the focusing of weakly ionic metabolites in CE. Although synthetic ampholytes are typically used to generate pH gradients across the capillary for isoelectric focusing of zwitterionic proteins[30], discrete segments of conventional buffers (*i.e.*, buffer pH junction) can also be utilized. In contrast to conventional IEF, dynamic pH junction generates transient pH gradients within the sample plug without the need for a separate immobilization step since analyte focusing and analyte zone separation occur sequentially during electromigration. On-line preconcentration by dynamic pH junction represents a promising technique for enhancing the concentration sensitivity of CE that is applicable to several different classes of weakly ionic metabolites, ranging from catecholamines to estrogens[2] provided that the analyte mobility as determined by its pKa is sufficiently altered within the two buffer segments selected, namely the sample and background electrolyte.

As depicted in *Figure 3.1(a)*, when a continuous electrolyte system (sample is dissolved in borate, pH 9.6) is used with a large sample injection, both Tyr and P-Tyr migrate as extremely broad peaks with w_{det} of 16.2 cm and 17.8 cm, respectively, due to sample overloading. In contrast, *Figure 3.1(b)* demonstrates on-line preconcentration by dynamic pH junction of 20 μM of the two aromatic amino acids, tyrosine (Tyr) and *O*-phosphotyrosine (P-Tyr) using a sample injection of 150 s which is equivalent to a w_{inj} of about 12.8 cm or 16 % of the effective capillary length. The dynamic pH junction consists of a long sample injection of analytes dissolved in 40 mM phosphate, pH 6.5, whereas the background electrolyte is 140 mM borate, pH 9.6. Both Tyr and P-Tyr were observed to undergo significant band narrowing as reflected by a w_{det} of 0.50 cm and 2.6 cm, respectively. In general, a DIBR value of <1 demonstrates band narrowing, where as a DIBR > 1 indicates band broadening that is normally caused by several factors including longitudinal diffusion[16]. In this case, Tyr and P-Tyr peak in *Figure 3.1(a)* have a DIBR of 0.038 and 0.20, respectively, which corresponds to a 26- and 5-fold band narrowing relative to the initial injection plug. The greater band narrowing observed for Tyr relative to P-Tyr is due to its larger mobility difference at the of the buffer pH junction, as well as its higher apparent mobility (*i.e.*, shorter migration time) under these conditions to minimize broadening caused by diffusion. For example, the electrophoretic mobility of Tyr is only -1.24×10^{-5} $cm^2\cdot V^{-1}\cdot s^{-1}$ in phosphate, pH 6.5, whereas its mobility is increased to -1.57×10^{-4} $cm^2\cdot V^{-1}\cdot s^{-1}$ in borate, pH 9.6, as reflected by its p*I* of 5.6[31]. On the other hand, P-Tyr undergoes a more modest change in mobility from -2.92 to -3.02×10^{-4} $cm^2\cdot V^{-1}\cdot s^{-1}$ in phosphate, pH 6.5, relative to borate, pH 9.6, respectively due to the

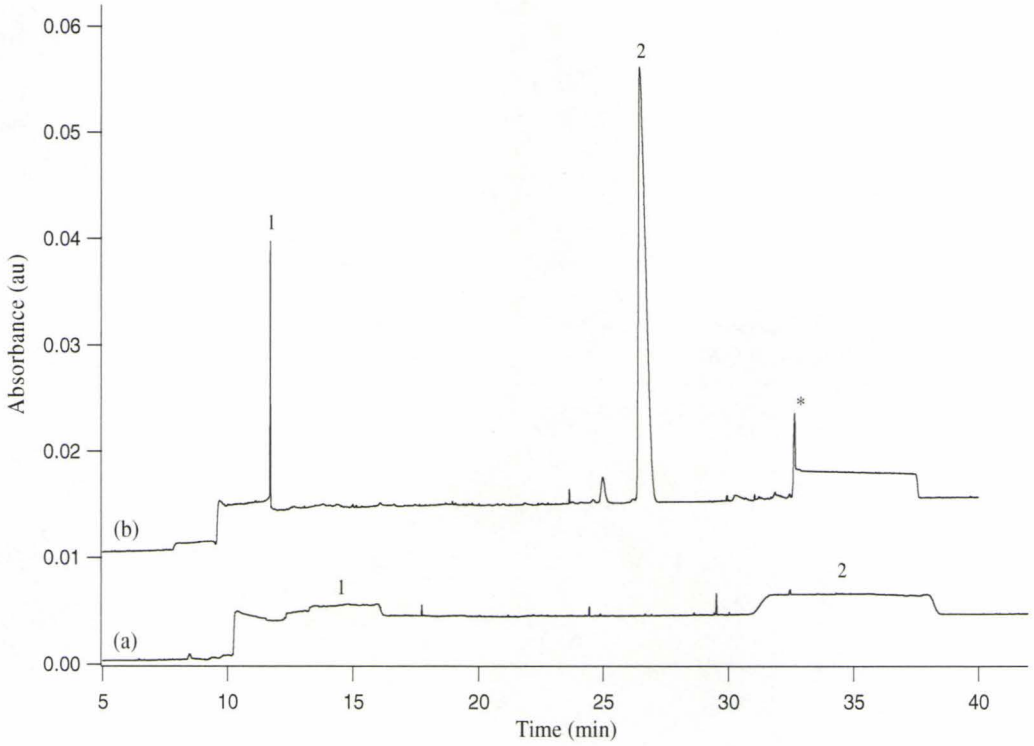

Figure 3.1: Electropherograms using large volume sample injections in CE which compare (a) normal band broadening caused by sample overloading and (b) on-line sample preconcentration by dynamic pH junction. Samples contained 20 µM Tyr and P-Tyr in either (a) 140 mM borate, pH 9.6, or (b) 40 mM phosphate, pH 6.5. Conditions: 140 mM borate buffer, pH 9.6; voltage, 25 kV; capillary length, 87 cm; injection, 150 s; UV, 214 nm. Analyte peak numbering corresponds to; 1, Tyr; 2, P-Tyr; where * denotes the focused front end of the phosphate zone derived from the sample.

presence of the weakly acidic diprotic phosphate moiety and lower p*I*. Recent computer modeling of analyte focusing by dynamic pH junction based on different buffer co-ions indicated that a co-operative transient isotachophoretic effect can result in stabilization of a sharp moving pH boundary that migrates across the sample zone[32]. This effect is indicated in *Figure 3.1(a)* by the sharpening of the front end of the phosphate sample zone (indicated by an asterisk) that migrates after P-Tyr when monitoring the absorbance at 214 nm. Dynamic pH junction methods based on differences in buffer pH and buffer co-ion mobility can also be used to enhance the focusing of weakly ionic analytes by

expanding the accessible pH range compared to a single homogenous buffer system. It should be noted that only Tyr and P-Tyr were detected at this concentration level as both amino acids contain aromatic moieties which strongly absorb at 214 nm. In order to detect trace levels of other non-aromatic phosphoamino acids (*i.e.*, P-Ser and P-Thr), chemical derivatization with a suitable chromophoric label is needed.

3.4.2. On-line sample preconcentration with chemical derivatization

There are several attributes to consider when selecting a chromophoric label applicable to on-line chemical derivatization in CE, such as analyte specificity (functional group), reactivity and useful absorbance or fluorescence properties. In addition, fast kinetics and quantitative yield to form the labelled product are also critical aspects for on-line derivatization based on zone-passing[33] of a concentrated chromophore zone through a slower-migrating analyte band. In this work, FMOC was selected as the label since it is an inexpensive that has rapid reactivity towards both 1^0 and 2^0 amines under alkaline conditions. *Figure 3.2* illustrates the general procedure for combining on-line sample preconcentration by dynamic pH junction with on-line chemical derivatization using FMOC in a single format. First, the capillary is rinsed and filled with borate buffer, pH 9.6, followed by hydrodynamic injection of a long sample plug of analyte (*e.g.*, P-Ser) in phosphate, pH 6.5, which constitutes the initial buffer pH junction. Next, an injection of a small spacer plug of borate buffer in then followed by a small yet concentrated plug of 100 mM FMOC in acetonitrile as shown in *Figure 3.2(a).* The spacer is included to prevent mixing of the sample and FMOC zones prior to separation, as well as to control the timing of the chemical derivatization. The advantage of on-line labelling by zone

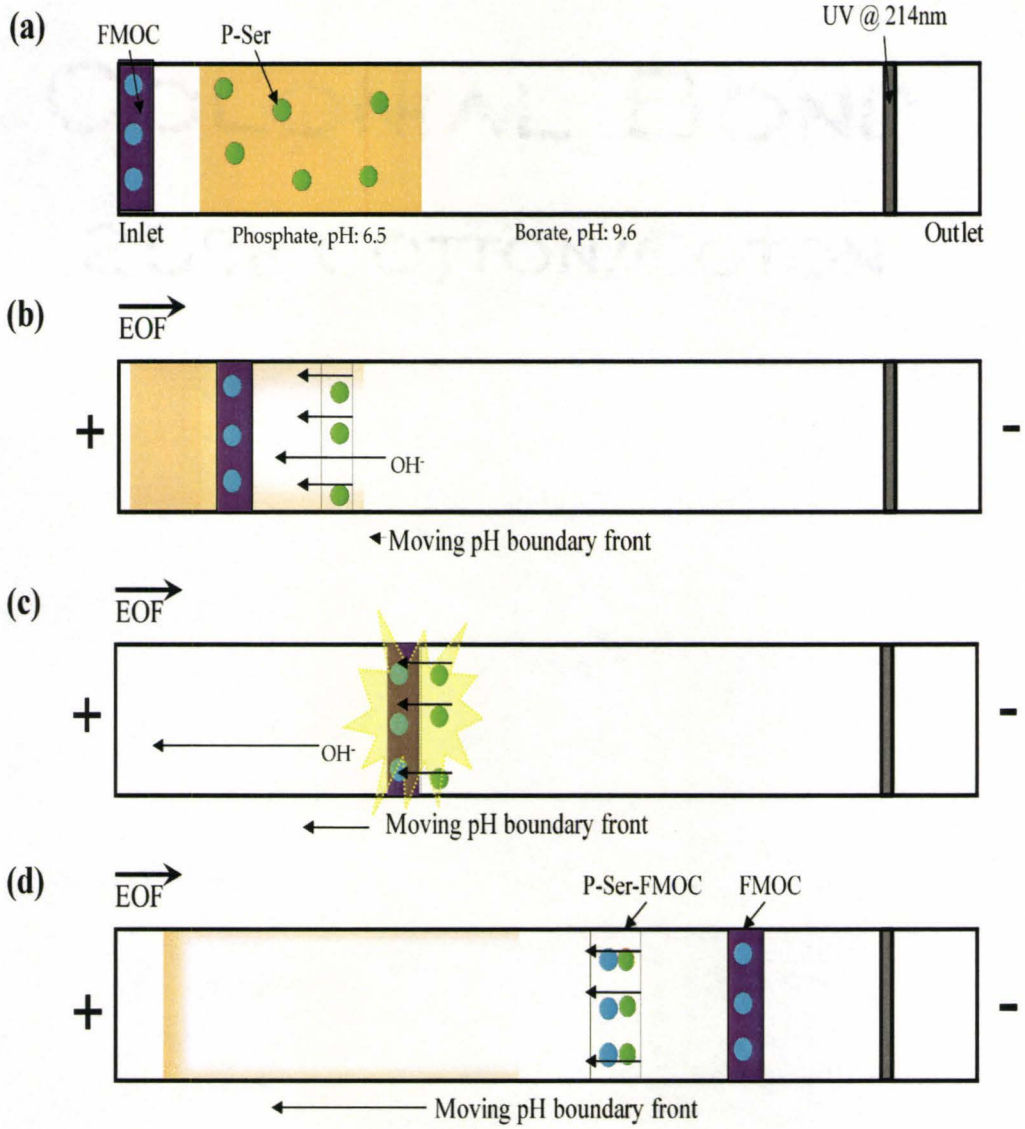

Figure 3.2: Schematic illustrating the four major processes involved with single-step on-line preconcentration of phosphoamino acids with FMOC derivatization by CE: (a) multiple injection sequence, (b) electrokinetic focusing of P-Ser by dynamic pH junction, (c) FMOC-labelling of P-Ser and (d) zone passing of excess FMOC.

passing in CE is that only a small volume (about 10 nL) of the reagent is used for analyte derivatization in contrast to through-capillary derivatization in which the label is added directly to the background buffer[34]. Application of the voltage generates a moving pH boundary that is formed and stabilized by a transient isotachophoretic process at the

interface of the borate and phosphate zones, resulting in electrokinetic focusing of the P-Ser band towards the front end of the sample zone as depicted in *Figure 3.2(b)*. The FMOC plug is injected after the sample zone because it is neutral and co-migrates with the EOF. Since P-Ser has a large negative mobility, FMOC soon migrates past the focused P-Ser zone (*i.e.*, zone passing), resulting in the formation of the P-Ser-FMOC adduct. It is important to emphasize that analyte focusing must precede chemical derivatization in order to take advantage of the favourable kinetic effects for reaction caused by the concentrated analyte present within a narrow zone of the capillary. Excess FMOC then migrates past the sample zone to the detector window followed by the negatively charged P-Ser-FMOC adduct.

Figure 3.3(a) depicts an electropherogram demonstrating on-line sample preconcentration with FMOC labelling of 20 μM of phosphoamino acids (P-Ser, P-Thr and P-Tyr) and their non-phosphorylated precursors by CE. Since the FMOC-labelled amino acids (Ser, Thr and Tyr) have a lower mobility than phosphoamino acids, their peaks were observed to co-migrate within the broad FMOC zone which made their quantification difficult. However all three FMOC-labelled phosphoamino acids were readily resolved from excess FMOC because of their high negative mobility. The peak indicated by an asterisk in *Figure 3.3(a)* represents a minor FMOC hydrolysis product that is also present in the blank. It was observed that P-Tyr generated two peaks in the electropherogram, which correspond to P-Tyr-FMOC (peak 2) and unlabelled P-Tyr (peak 5). The identity of P-Tyr was confirmed by performing separations using different borate buffers with a pH range from 9 to 10, which clearly indicated P-Tyr due to its

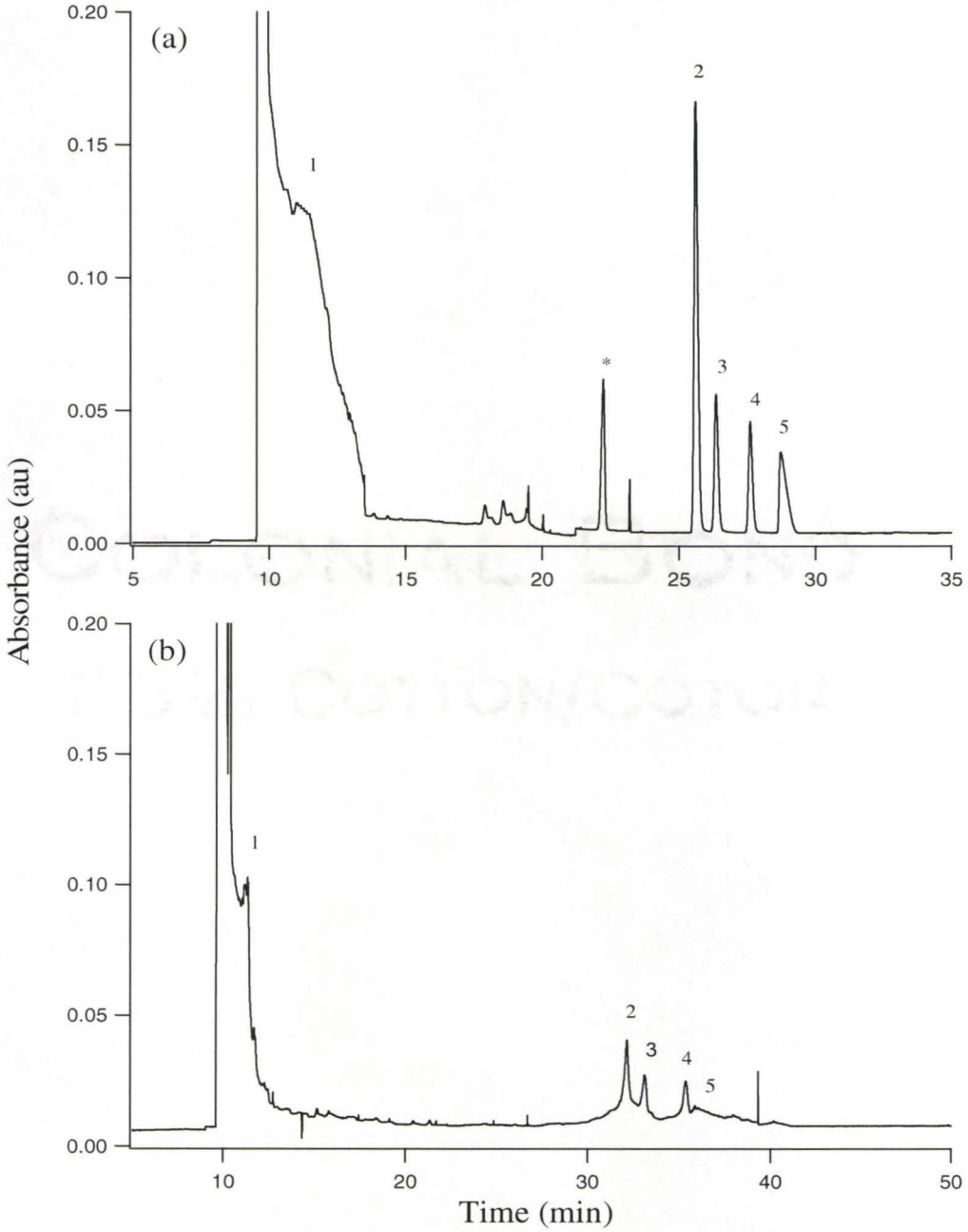

Figure 3.3: Electropherograms demonstrating on-line preconcentration of phosphoamino acids with FMOC derivatization by CE using (a) dynamic pH junction and (b) control without buffer pH junction. Sample solutions contained 20 μM P-Tyr, P-Thr and P-Ser in either (a) 40 mM phosphate, pH 6.5 or (b) 140 mM borate, pH 9.6. Injection sequence: 150 s, sample; 10 s, borate buffer; 5 s, 100 mM FMOC. Conditions 140 mM borate buffer, pH 9.6; voltage 25 kV; capillary length 87 cm; UV at 214 nm. Analyte peak numbering corresponds to; 1, FMOC; 2, P-Tyr-FMOC; 3, P-Thr-FMOC; 4, P-Ser-FMOC; 5, P-Tyr; where * denotes FMOC hydrolysis product.

dramatic shift in migration time (apparent mobility) because of the presence of the free primary amino group (p*K*a ≈ 9.5) unlike P-Tyr-FMOC. In addition, it was noticed that the magnitude of the P-Tyr peak increased as a lower FMOC concentration was used for on-line derivatization, as will be discussed later. These observations indicate that FMOC labelling to P-Tyr is inhibited by steric hindrance even under favourable kinetic conditions operative in CE due to the presence of the bulky phenolic side group, in contrast to P-Ser and P-Thr. However, this does not represent a significant interference since the P-Tyr-FMOC and P-Tyr peaks generated are reproducible and easily resolved by CE. Moreover, FMOC labelling is primarily directed at P-Ser and P-Thr due to their lack of a useful chromophoric group for sensitive UV detection. *Figure 3.3(b)* is a control electropherogram that shows the influence of the dynamic pH junction on analyte focusing and FMOC labelling, which is similar to *Figure 3.3(a)* except that the sample is dissolved in borate, pH 9.6. It is evident that partial focusing and derivatization of phosphoamino acids still occurs without phosphate, pH 6.5 in the sample, which may be caused by a transient isotachophoretic effect[35] due to the injection of the low conductivity FMOC plug in acetonitrile behind the sample. Nevertheless, dynamic pH junction of FMOC-labelled phosphoamino acids in *Figure 3.3(a)* results in about a five-fold greater peak height response, improved resolution and shorter migration time compared to *Figure 3.3(b)*. Thus, the application of multiple yet additive electrokinetic focusing effects based on buffer pH and buffer co-ion mobility serves to maximize analyte band narrowing in CE.

3.4.3. Influence of buffer pH and ionic strength

Five major factors were examined to optimize analyte focusing and FMOC derivatization which included background buffer and sample pH, ionic strength, sample injection length, spacer length and FMOC concentration. *Figure 3.4* shows the influence of phosphoamino acid apparent electrophoretic mobility (μ_{ep}^{A}) as a function of borate pH (background buffer) ranging from 9.0 to 9.8. In general, as the pH of the borate buffer was increased from 9.0 to 9.8, the resolution and migration time of the three FMOC-labelled phosphoamino acids also increased. Although sharper peaks were achieved at lower borate pH because of the reduced time for diffusion, the phosphoamino acid peaks were only partially resolved. Optimum conditions in terms of phosphoamino acid focusing and resolution were achieved using borate pH 9.6 as shown in *Figure 3.4*. *Figure 3.4* also highlights the unique change in the mobility of P-Tyr (free 1^0 amino group) in contrast to the other FMOC-labelled phosphoamino acids, which undergoes a significant increase in mobility at higher borate pH resulting in a complete reversal of the migration order. The use of borate at pH > 10 resulted in longer analysis times and increased broadening for the phosphoamino acids, which can also increase the rate of hydrolysis for the FMOC label. Phosphate was selected as the sample buffer co-ion because of its wide pH buffering capacity and its compatibility to many biological samples. In this work, the pH of the 40 mM phosphate (sample) buffer was examined from 3.0 to 8.0. The use of strongly acidic phosphate (pH < 3) in the sample reduced the efficiency of the FMOC labelling for the phosphoamino acids (*i.e.*, lower peak heights) since the reaction is catalyzed ideally under alkaline conditions. In order to balance analyte focusing and by dynamic pH junction (favoured by acidic pH), a sample buffer

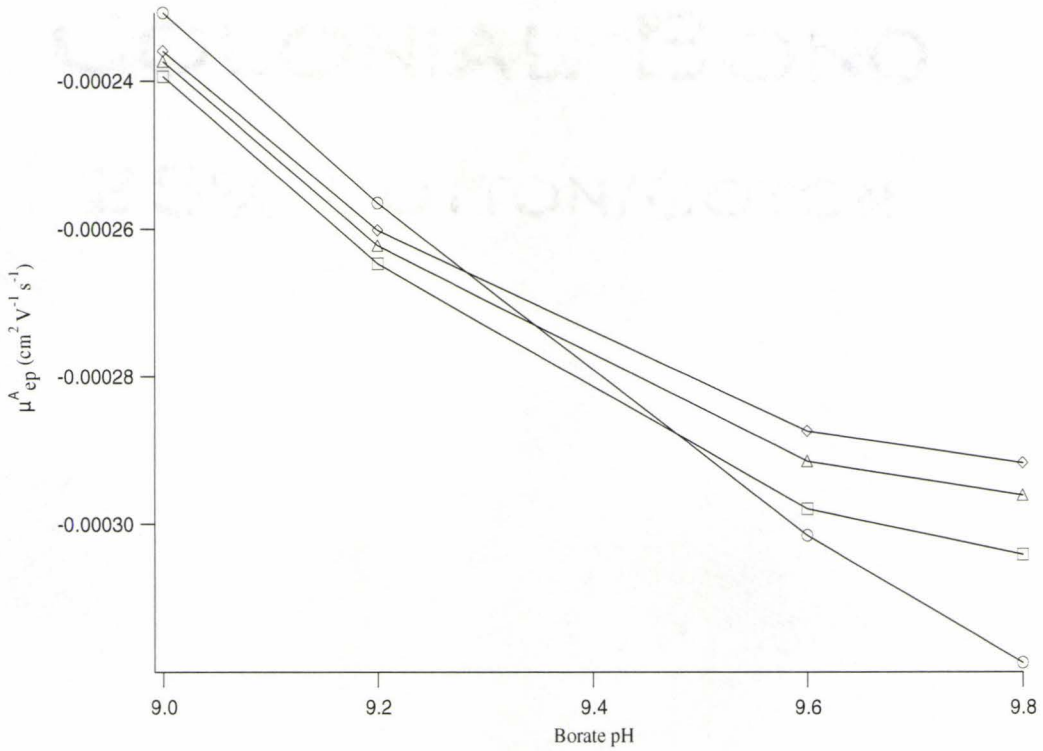

Figure 3.4: Graph depicting measures electrophoretic mobility of phosphoamino acids as a function of borate pH. Shapes on plot lines represent (◇) P-Tyr-FMOC, (Δ) P-Thr-FMOC, ([]) P-Ser-FMOC and (o) P-Tyr. Note the unique mobility profile of unlabelled P-Tyr.

consisting of phosphate, pH 6.5 was selected. Optimal focusing and resolution of the FMOC-labelled phosphoamino acids was achieved under non-stacking conditions when using 40 mM phosphate pH 6.5 in the sample, which was measured to have a slightly lower conductivity of 4.28 mS·cm^{-1} relative to 6.45 mS·cm^{-1} in 140 mM borate, pH 9.6, as similarly observed in previous reports[16]. The use of buffers with very low conductivity (*i.e.*, 10 mM phosphate) with the sample injection length generated unfavourable sample stacking due to the amplified local electric field with broad unresolved peaks. However, it was observed that this method was able to tolerate high ionic strength analyses (*e.g.*, 50 mM NaCl added) with-out significant deterioration of the phosphoamino acid peaks. Thus, analysis of phosphoamino acids by CE *via* on-line preconcentration with chemical

derivatization is amendable to real biological samples without labour-intensive sample pretreatment.

3.4.4. Influence of sample injection length

The influence of low pressure sample injection was also examined by varying the w_{inj} from 0.26 cm (3 s) to 25.7 cm (300 s) in order to determine the maximum sample injection that would allow for optimum analyte focusing with baseline resolution. In general, it was observed that an increase in sample injection length resulted in a linear increase in measured analyte peak area. This trend continued until the injection length reached w_{inj} 17.1 cm (200 s), at which the resolution between the P-Thr-FMOC, P-Ser-FMOC and P-Tyr peaks was reduced (co-migrating peaks). A sample injection length of w_{inj} 12.8 cm (150 s) generated the greatest sensitivity enhancement while maintaining baseline resolution. Since analyte focusing and analyte separation occur within the same capillary, the use of extremely large sample plugs reduces the effective capillary length required for adequate resolution. Moreover, since excess FMOC migrates as a broad band that spectrally interferes with lower mobility amino acid adducts (*e.g.*, P-Ser-FMOC), the effective separation window is restricted to primarily high mobility analytes. However, the use of alternative labels which form adducts that have unique photometric properties can expand the peak capacity of the technique for a wider range of analytes with different mobility. Thus, the magnitude of analyte enrichment achieved by on-line preconcentration and chemical derivatization in CE is limited by the inherent complexity of the sample and the choice of chemical label which impact the maximum injection length permitted.

3.4.5. Influence of FMOC concentration and spacer length

Next, the concentration of FMOC used as the derivatization agent for on-line phosphoamino acid labelling was varied from 0 to 100 mM, as depicted in *Figure 3.5*. When using 0 mM FMOC (*i.e.*, acetonitrile) *Figure 3.5(a)* reveals that only P-Tyr was detected at this concentration level. However, the addition of higher FMOC concentrations of 25 mM, 50 mM and 100 mM resulted in a significant increase in the peak area of all FMOC-labelled phosphoamino acids (including FMOC hydrolysis product), as well as a decrease in unlabelled P-Tyr. For instance, the relative peak area ratio of P-Tyr-FMOC : P-Tyr increased about 20-fold in *Figure 3.5(d)* relative to *Figure 3.5(b)*. The use of 100 mM FMOC also resulted in improved resolution of FMOC-labelled phosphoamino acids. These observations indicate that a high concentration of FMOC is required for efficient in-capillary labelling of phosphoamino acids by favouring the kinetic of the reaction *via* zone passing in CE. Although higher concentration of the label (> 100 mM) can be used to further enhance P-Tyr labelling, this was not feasible due to the limited aqueous solubility of FMOC which resulted in frequent current error due to precipitation. The FMOC labelling efficiency was also influenced by the length of time between the sample injection and the injection of the label (*i.e.*, spacer length). When the time between the sample plug and the FMOC label was less than 20 s (w_{inj} < 1.7 cm), the spacer length had minimal influence on analyte peak area. However, spacer lengths greater than 20 s resulted in the production of larger FMOC hydrolysis products, reduced resolution, as well as decreased peak areas for P-Ser-FMOC, P-Thr-FMOC and P-Tyr-FMOC. Thus, a spacer length of 10 s (w_{inj} 0.86 cm) was selected since it offered

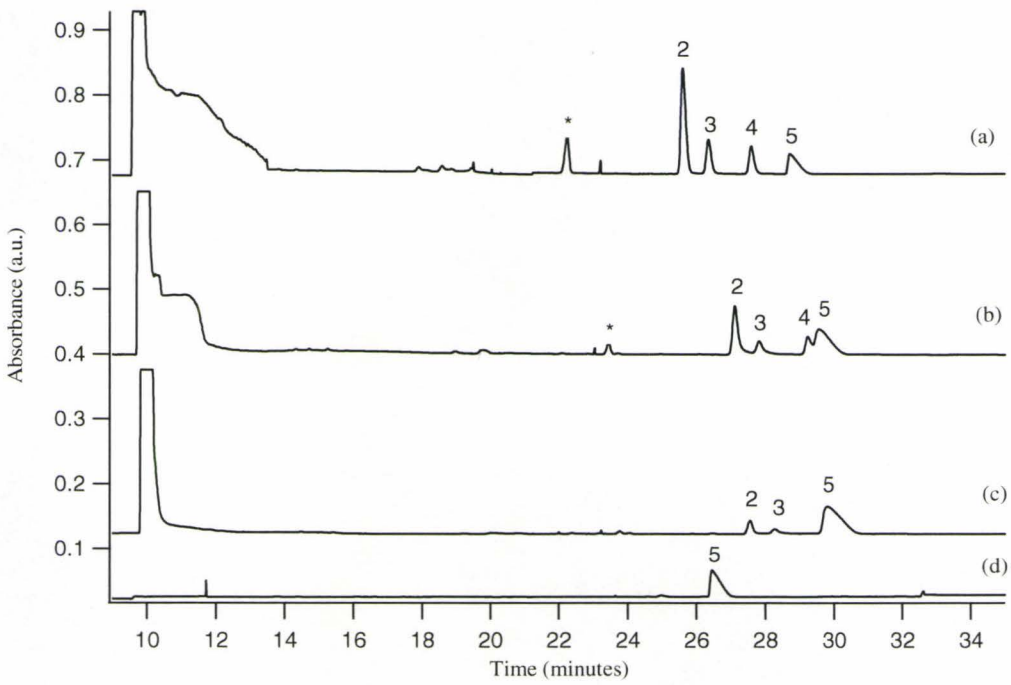

Figure 3.5: Influence of FMOC concentration on on-line preconcentration and derivatization of phosphoamino acids using (a) 0 mM FMOC, (b) 25 mM FMOC, (c) 50 mM FMOC and (d) 100 mM FMOC. Sample solutions contained 20 μM P-Tyr, P-Thr and P-Ser in 40 mM phosphate, pH 6.5. Injection sequence, conditions and analyte peak numbering are the same as *Figure 3.3*.

adequate resolution with maximum sensitivity, while ensuring good reproducibility by minimizing sample and FMOC zone mixing prior to separation.

3.4.6. Method validation

Under optimum conditions, about a 200-fold enhancement in concentration sensitivity for phosphoamino acids was achieved by on-line sample preconcentration and derivatization relative to off-line derivatization with conventional (3 s) injection in CE as demonstrated in *Figure 3.6*. This large boost in sensitivity for the "in-capillary" method can be attributed to several factors including a 50-fold larger sample injection, a 3-fold sharper analyte peak width, as well as enhanced kinetics for the reaction in the nanolitre volume dimensions inside the capillary. *Figure 3.6(b)* demonstrates that off-line FMOC

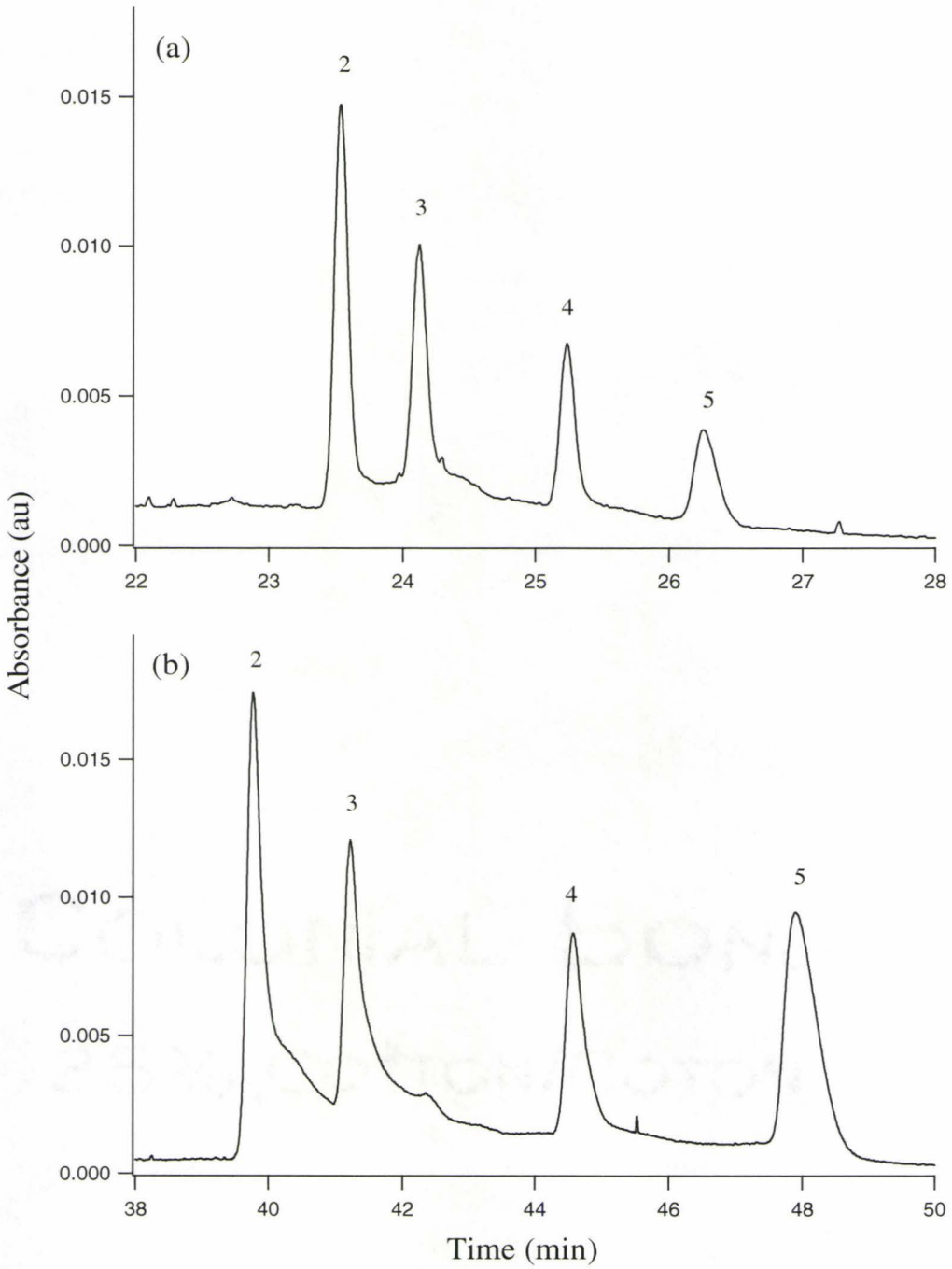

Figure 3.6: Phosphoamino acid analysis by CE using (a) on-line sample preconcentration with FMOC derivatization and (b) conventional off-line FMOC derivatization. Sample solutions contained either (a) 4 μM phosphoamino acids in 40 mM phosphate, pH 6.5 or (b) 1 mM phosphoamino acids which were derivatized with 100 mM FMOC. Injection sequence: (a) 150 s, sample; 10 s, borate buffer; 5 s, 100 mM FMOC, or (b) 3 s, sample.

derivatization of phosphoamino acids also generated two P-Tyr peaks (*i.e.*, P-Tyr-FMOC and unlabelled P-Tyr). In fact, the ratio of labelled P-Tyr-FMOC : P-Tyr is produced to a lower extent when using off-line chemical derivatization. In addition *Figure 3.6(b)* suffered from severe peak broadening and longer migration times as compared to *Figure 3.6(a)*. The intra-day repeatability (n = 5) for the analysis of FMOC-labelled phosphoamino acids using on-line preconcentration with chemical derivatization compared to off-line derivatization revealed a dramatic improvement in the precision of the method in terms of quantitation (analyte peak area) with an average CV of 3.1 % and 28.3 % respectively. The improvement in precision is related to automation of the sample preconcentration and chemical derivatization with a commercial thermostatted CE instrument. Further improvement in precision can also be achieved by using a suitable internal standard during routine analysis. The reproducibility of analyte migration time using the optimized method was also determined to be acceptable with a CV under 5 %. Calibration curves were obtained for the three phosphoamino acids based on duplicate measurements of six points over a 100-fold concentration range from 0.4 μM to 40 μM with excellent linearity, as reflected by the R^2 of 0.996. The limit of detection (S/N ≈ 3) for the FMOC-labelled phosphoamino acids was estimated to be approximately 0.1 μM. In fact, the sensitivity for phosphoamino acid analysis achieved by this technique using CE with UV detection in comparable to a previous method based on off-line fluorescence labelling and CE-LIF[28]. Because of the higher negative mobility of the phosphoamino acids, the selectivity of the method was excellent with no interferences observed upon the addition of 20 other common amino acid metabolites. *Table 3.1* summarizes the major

Table 3.1: Validation of single-step analysis of phosphoamines *via* on-line preconcentration with FMOC labelling by CE with UV detection.

Parameter	P-Tyr	P-Thr	P-Ser
A. Precision (n = 5)			
Peak Area/CV	1.7	2.2	5.5
Migration Time/CV	3.8	3.9	4.2
B. Calibration curve[a]			
Linearity/R^2	0.9979	0.9991	0.9918
C. Detection Limit			
S/N ≈ 3/μM	0.06	0.10	0.13

[a] Duplicate measurements of six concentrations from 0.4 μM to 40 μM

validation parameters that were examined in this report for the determination of phosphoamino acids *via* on-line preconcentration and derivatization. The major disadvantages of the present method are the limited aqueous solubility of FMOC, as well as the spectral overlap of both label and adduct peaks, this restricts it applicability to native and modified acidic amino acids, such as glutamic acid. Overall, this single step methodology based on CE using on-line sample preconcentration with chemical derivatization offers significant advantages over conventional methods in terms of greater automation, improved reproducibility, enhanced sensitivity, as well as shorter analysis times, which can be useful in high-throughput analytical strategies for metabolomics[17] based on capillary of microchip electrophoresis platforms. It is anticipated that the enhanced kinetics of this technique will be even more relevant when labelling nanomolar levels of analytes by CE-LIF, which typically requires higher temperatures and longer reaction times when performing off-line.

3.5. Summary and conclusion

The analysis of phosphoamino acids by CE using on-line sample preconcentration with chemical derivatization represents a highly sensitive, rapid and reproducible method

in which the capillary functions as a concentrator, chemical reactor and separator. This method can be used to electrokinetically focus and effectively label sub-micromolar levels of low abundance metabolites without intrinsic chromophore moieties using nanolitre volumes of reagents in a single unmodified capillary. Over a 200-fold enhancement in concentration sensitivity was realized by this technique as compared to conventional off-line methods. Future work will study the kinetics of analyte focusing and zone passing during electromigration, as well as the use of alternative labels for trace analysis of other classes of low abundance metabolites by CE.

3.6. References

1. T. Soga, Y. Ohahsi, Y. Ueno, H. Naraoka, M. Tomita and T. Nishioka, *J. Proteome Res.*, 2003, **2**, 488-494.
2. P. Britz-McKibbin and S. Terabe, *J. Chromatogr. A*, 2003, **1000**, 917-934.
3. J. Allen, H. M. Davey, D. Broadhurst, J. K. Heald, J. J. Rowland, S. G. Oliver and D. B. Kell, *Nat. Biotechnol.*, 2003, **21**, 692-696.
4. S. Waidyanatha, N. Rothman, G. Li, M. T. Smith, S. Yin and S. M. Rappaport, *Anal. Biochem.*, 2004, **327**, 184-199.
5. V. V. Tolstikov and O. Fiehn, *Anal. Biochem.*, 2002, **301**, 298-307.
6. O. Corcoran, R. W. Mortensen, S. H. Hansen, J. Troke and J. K. Nicholson, *Chem. Res. Toxicol.*, 2001, **14**, 1363-1370.
7. J. K. Nicholson, J. Connelly, J. C. Lindon and E. Holmes, *Nat. Rev. Drug Discovery*, 2002, **1**, 153-161.

8. J. Zhang, Y. Fang, J. Y. Hou, H. J. Ren, R. Jiang, P. Roos and N. J. Dovichi, *Anal. Chem.*, 1995, **67**, 4589-4593.

9. H. Lord and J. Pawliszyn, *J. Chromatogr. A*, 2000, **885**, 153-193.

10. C. X. Zhang and W. Thormann, *Anal. Chem.*, 1996, **68**, 2523-2532.

11. R. L. Chien and D. S. Burgi, *Anal. Chem.*, 1992, **64**, 1046-1050.

12. L. Krivakova, A. Vrana, P. Gebauer and P. Bocek, *J. Chromatogr. A*, 1997, **772**, 283-295.

13. T. J. Thompson, F. Foret, P. Vouros and B. L. Karger, *Anal. Chem.*, 1993, **65**, 900-906.

14. J. P. Quirino and S. Terabe, *Science*, 1998, **282**, 465-468.

15. J. P. Quirino and S. Terabe, *Anal. Chem.*, 1999, **71**, 1638-1644.

16. P. Britz-McKibbin and D. D. Y. Chen, *Anal. Chem.*, 2000, **72**, 1242-1252.

17. P. Britz-McKibbin, T. Nishioka and S. Terabe, *Anal. Sci.*, 2003, **19**, 99-104.

18. P. Britz-McKibbin, K. Otsuka and S. Terabe, *Anal. Chem.*, 2002, **74**, 3736-3743.

19. P. Britz-McKibbin, M. J. Markuszewski, T. Iyanagi, K. Matsuda, T. Niskioka and S. Terabe, *Anal. Biochem.*, 2003, **313**, 89-96.

20. P. Britz-McKibbin, T. Ichihashi, K. Tsubota, D. D. Y. Chen and S. Terabe, *J. Chromatogr. A*, 2003, **1013**, 65-76.

21. N. J. Reinhoud, U. R. Tjaden and J. v. d. Greff, *J. Chromatogr. A*, 1994, **673**, 255-266.

22. R. M. Lattore, J. Saurina and S. Hernandez-Cassou, *Electrophoresis*, 2001, **22**, 4355-4361.

23. S. Oguri, H. Tanagaki, M. Hamaya, M. Kato and T. Toyo'oka, *Anal. Chem.*, 2003, **75**, 5240-5245.

24. A. H. Ross, D. Baltimore and H. N. Eisen, *Nature*, 1981, **294**, 654-656.

25. P. Connelly, L. H. Parker-Botelho, R. B. Sisk and J. C. Garrison, *J. Biol. Chem.*, 1987, **262**, 4324-4332.

26. R. S. Annan, M. J. Huddleston, R. Verma, R. J. Deshaies and S. A. Carr, *Anal. Chem.*, 2001, **73**, 393-404.

27. J. C. Yang, J. M. Fujitaki and R. A. Smith, *Anal. Biochem.*, 1982, **122**, 360-363.

28. X. Liu, L. Ma and Y. T. Lu, *Anal. Chim. Acta*, 2004, **512**, 297-304.

29. M. Matzner, R. P. Kurkjy and R. J. Cotter, *Chem. Rev.*, 1964, **64**, 645-687.

30. P. G. Righetti and A. Bossi, *Anal. Chim. Acta*, 1998, **372**, 1-19.

31. *Handbook of Biochemistry: Selected Data for Molecular Biology*, H.A. Sober, CRC Press, Cleveland, OH. , 1970.

32. J. B. Kim, P. Britz-McKibbin, T. Hirokawa and S. Terabe, *Anal. Chem.*, 2003, **75**, 3986-3993.

33. S. Oguri, K. Yokoi and Y. Motohase, *J. Chromatogr. A*, 1997, **787**, 253-260.

34. A. Taga, A. Nishino and S. Honda, *J. Chromatogr. A*, 1998, **822**, 271-279.

35. Z. K. Shihabi, *Electrophoresis*, 2002, **23**, 1612-1617.

Chapter IV

On-line Sample Preconcentration with Chemical Derivatization of Bacterial Biomarkers by Capillary Electrophoresis: A Dual Strategy for Integrating Sample Pretreatment with Chemical Analysis

IV. On-line Sample Preconcentration with Chemical Derivatization of Bacterial Biomarkers by Capillary Electrophoresis: A Dual Strategy for Integrating Sample Pretreatment with Chemical Analysis

4.1. Abstract

Simple, selective yet sensitive methods to quantify low-abundance bacterial biomarkers derived from complex samples are required in clinical, biological, and environmental applications. In this *Chapter*, a new strategy to integrate sample pretreatment with chemical analysis is investigated using on-line preconcentration with chemical derivatization by CE and UV detection is presented. Single-step enantioselective analysis of muramic acid (MA) and diaminopimelic acid (DAP) was achieved by CE via sample enrichment by dynamic pH junction with *ortho*-phthalaldehyde/*N*-acetyl-L-cysteine labelling directly in-capillary. The optimized method resulted in up to a 100-fold enhancement in concentration sensitivity compared to conventional off-line derivatization procedures. The method was also applied toward the detection of micromolar levels of MA and DAP excreted in the extracellular medium of *Escherichia coli* bacterial cell cultures. Online preconcentration with chemical derivatization by CE represents a unique approach for conducting rapid, sensitive, and high-throughput analyses of other classes of amino acid and amino sugar metabolites with reduced sample handling, where the capillary functions simultaneously as a concentrator, microreactor, and chiral selector.

4.2. Introduction

Conventional methods used for analyzing complex biological samples often rely

on multiple sample pretreatment protocols prior to analysis, which include off-line sample preconcentration and chemical derivatization. These procedures are often critical for reliable and quantitative analyses as they serve to enhance method sensitivity and selectivity, as well as to reduce chemical interferences. However, off-line sample pretreatment steps are labour intensive, which can also additively result in greater bias, increased variance, as well as longer total analysis time. CE represents a promising technique for integrating sample pretreatment with analysis directly "in-capillary" because of the small sample/reagent requirements and its ability to control analyte band separation and diffusion properties via kinetic (mobility) and thermodynamic (equilibria) processes during electromigration. To date, several different techniques have been developed for either on-line sample preconcentration[1-3] or in-capillary derivatization[4-6] with separation by CE; however there have been only a few groups who have reported direct coupling of on-line sample enrichment with analyte labelling without significant loss in separation performenace[7-9]. Further work is necessary to design more effective in-capillary analyte focusing and chemical labelling strategies for low-abundance metabolites that lack intrinsic chromophores, which is required for rapid, sensitive, and high-throughput analyses by capillary array[10] and microfluidic[11] platforms.

There is growing interest in developing sensitive and specific methods to characterize unique metabolomic signatures from bacteria. Muramic acid (MA) and diaminopimelic acid (DAP) represent two important types of bacterial biomarkers derived from the peptidoglycan (PG) component of the bacterial cell wall[12]. MA is the stable acid-hydrolysate product of *N*-acetyl MA, which is utilized in the polysaccharide

backbone of the PG layer of most eubacteria, whereas DAP serves as a cross-linker between adjacent muropeptide side chains in Gram-negative bacteria to impart cell wall rigidity[13]. DAP contains two asymmetric carbons that result in the formation of three distinct stereoisomers: D,D-, L,L- and *meso*-configuration. The latter is the most prevalent in Gram-negative bacteria; however L,L-DAP has been reported in the cell wall belonging to the *Streptomyces* bacteria genus[14]. Several enzymes involved in DAP metabolism have been identified as promising targets for the development of new classes of drugs against antibiotic-resistant strains of bactaeria[15]. Bacterial biomarker analyses play important roles in estimating its biomass in dissolved organic matter in oceans[16], as well as detecting the presence of bacteria in ancient calcerous rocks[17] and extraterrestrial meteorites[18]. Analyses of these biomarkers in indoor air samples have also been used as clinical indicators of bacterial contamination and its association with respiratory illness[19].

Previous methods reported for the analysis of either MA or DAP have relied primarily on HPLC[20, 21] and GC-MS[22, 23]. Although GC-MS provides qualitative information for unambiguous structural identification, complex and time-consuming off-line sample pretreatment steps based on SPE and chemical derivatization are normally required. Surprisingly, there has only been one previous CE method for MA or DAP analysis despites its suitability for high resolution separations of weakly ionic and polar metabolites. Driouich *et al.*[24] described the use of salicylaldehyde-5-sulfonate as a precapillary derivatization agent for the analysis of DAP and other diamine metabolites by CE with UV detection. However, this method is limited by a long derivatization time that lacked full resolution of all three DAP stereoisomers. As discussed in *Chapter III,*

our group introduced a new single-step strategy for the analysis of low abundance phosphoamino acids using on-line sample preconcentration by dynamic pH junction with 9-fluorenylmethyloxycarbonyl chloride (FMOC) derivatization[25]. Over a 200-fold improvement in concentration sensitivity was achieved for acidic amino acid metabolites that lack intrinsic chromophores. However, the technique was limited to analytes that have a relative high mobility due to spectral interference with excess neutral FMOC that comigrates with the EOF. In this report, an improved strategy for the enantioselective analysis of MA and DAP is demonstrated by CE with UV detection via online preconcentration with chemical derivatization using *ortho*-phthalaldehyde (OPA) and *N*-acetyl-L-cysteine (NAC). On-line analyte focusing by dynamic pH junction with in-capillary OPA/NAC labelling *via* zone passing resulted in up to a 100-fold improvement in concentration sensitivity while using only nanolitre volumes of reagents. Moreover, this technique enabled rapid, automated, and reproducible analyses of MA and DAP under a single format with baseline resolution of all three DAP stereoisomers. The optimized method also demonstrated high selectivity without interference from more abundant amino acid metabolites present in the extracellular matrix of *Escherichia coli*. To the best of our knowledge, this work represents the first example of CE used for the simultaneous analysis of MA and DAP as unique bacterial biomarkers in biological samples.

4.3. Methods and materials

4.3.1. Chemicals and reagents

Deionized water used for buffer and sample preparations was obtained using a

Barnstead EASYpure ®II LF ultrapure water system (Dubuque, IA, USA). The sample buffer used was 40 mM phosphate, pH 6.5, which was prepared using sodium dihydrogen phosphate from Alfa Aesar (Ward Hill, MO., USA). The aqueous BGE was 140 mM borate that was prepared from sodium tetraborate decahydrate (borax) from Sigma-Aldrich (St. Louis, MO., USA). The pH of the borate was modified by 0.1 M NaOH to obtain a pH of 9.5. MA or 2-amino-3-O-(D-1-carboxyethyl)-2-deoxy-D-glucose, 2,6-DAP, glucosamine-6-phosphate (GlcN-6P), OPA, NAC, 3-mercaptopropinoic acid (MPA), and 2-mercaptoethanol (ME) were all obtained from Sigma-Aldrich. It is important to note that DAP is purchased as a mixture of the three stereoisomers in an approximate molar ratio of 1:2:1 for D,D-, *meso*-, and L,L-, respectively. Glucosamine hydrochloride (GlcN) was purchased from Alfa-Aesar. Twenty millimolar standard stock solutions of MA, DAP, GlcN and GlcN-6P were prepared in deionized water. Stock solutions were then diluted in sample or BGE buffer prior to analysis. Primary stock solutions of 400 mM OPA and 600 mM thiol were prepared fresh everyday in HPLC grade ACN and 140 mM borate, pH 9.5, respectively. OPA and thiol solutions were then mixed together and diluted in borate buffer to give a final concentration of 100 and 150 mM, respectively, which were used for off-line derivatization or on-line preconcentration with labelling studies by CE. All stock solutions were stored refrigerated at 4^0C when not in use.

4.3.2. Apparatus and procedure

Separations were performed on an MDQ CE system (Beckman-Coulter, Fullerton, CA., USA). Uncoated capillaries (Polymicro Technologies, Phoenix, AZ., USA) with 75

μm i.d., 365 μM o.d., and 90 cm total length were used. Each separation was preceded with a 5 min rinse of 0.1 M NaOH, followed by a 5 min rinse with BGE. Hydrodynamic injections were performed on all samples using a low pressure (0.5 psi or 3.5 kPa). The low pressure injection was measured to have an average (n = 5) velocity of 7.49×10^{-2} $cm\cdot s^{-1}$, which was used to estimate the sample injection bandwidth (w_{inj}). The detector bandwidth (w_{det}) of analyte zones was measured by transforming the measured base peak width in the time to the distance domain by multiplying with the analyte migration velocity. The detector-to-injection bandwidth ratio (DIBR) was used as a measure of analyte band focusing[26]. All separations were thermostatted at 25^0C using a voltage of 25 kV and UV absorbance was monitored at 340 or 214 nm.

4.3.3. *E. Coli* incubation

E. coli strain BL-21 (DE3) used in this study was a gift from Dr. Eric Brown of the Department of Biochemistry at McMaster University. *E. coli* was initially grown for 24 h in Luria-Bertani (LB) medium agar-treated plate (BioShop Canada, Burlington, ON., Canada). A single *E. coli* colony was then selected from the plate and used to inoculate a 500 mL flask containing 100 mL of liquid LB Miller broth (BioShop Canada), where the bacteria were grown on rotary shakers for an additional 24 h at 37^0C. This broth was then used to inoculate three separate flasks containing LB medium with a 25% seeding volume. Immediately after inoculation the OD of the medium was measured using a DU® General Purpose UV/VIS Spectrometer (Beckman-Coulter) at 600 nm. The samples were then centrifuged for 10 min at 6000 rpm after which the supernatant containing the extracellular medium was removed and stored frozen for future analyses. This procedure

was repeated in 0.5 h intervals for 6 h, allowing for an *E. coli* growth curve to be measured. All equipments used for the bacterial growth were sterilized prior to usage, and the bacterial cultures were handled safely in microbiological facility until discarded in 10 % bleach (sodium hypochlorite) solution.

4.4. Results and discussion

4.4.1. Optimum thiol coreactant using off-line chemical derivatization

Chemical derivatization serves two functions in CE in terms of modifying the intrinsic electrophoretic mobility of an analyte for enhanced selectivity, as well as incorporating a useful chromophoric or fluorescent moiety for improved detection[27]. In this study, OPA was selected as the label since it reacts rapidly with primary amines in the presence of a thiol coreactant under alkaline conditions to form a 1-thio-2-amino substituted isoindole adduct with unique spectral properties[28]. In addition, the chemical properties of the isoindole adduct can be readily tuned by altering the type of coreagent, such as the use of an optically active thiol to form diastereomeric adducts. *Figure 4.1* depicts the chemical structures of MA and DAP. Note that MA is a monocarboxylic acid glucosamine derivative with an additional chiral center derived from D-lactic acid, whereas DAP is a diamino acid metabolite with two chiral centers that are synthesized *via* a lysine pathway in the bacteria[15]. First, off-line chemical derivatization of MA, DAP, GlcN and GlcN-6P with OPA was performed in order to determine the thiol that generates the highest absorbance response with maximum resolution. Three different thiol coreactants were investigated, namely, ME (neutral), MPA (anionic) and NAC (chiral/anionic). *Figure 4.2* illustrates the influence of the three thiol coreactants on the

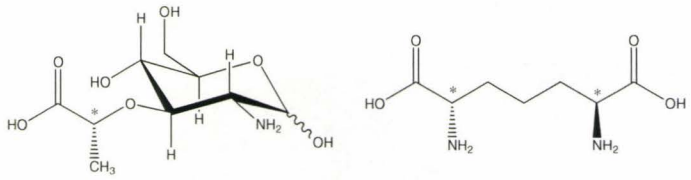

Figure 4.1: Chemical structures of two unique biomarkers associated with the PG component of the bacterial cell wall: (1) MA and (2) DAP. Asterisk * represents an asymmetric carbon center (not indicated on the D-glucosamine moiety of MA).

mobility, resolution, and absorbance response (monitored at 340 nm) of the isoindole adducts under the same reaction and separation conditions. Although the OPA/ME reaction generated the greatest response in terms of peak height due to reduced band broadening as a result of the lower analyte negative mobility (shorter migration time), it was inadequate to resolve the three stereoisomers of DAP. The use of increasing concentrations of β-CD as a neutral chiral selector to the run buffer was unsuccessful at further improving DAP resolution (data not shown). *Figure 4.2(b)* depicts the effect of using OPA/MPA for off-line derivatization in which all analytes have significantly larger negative mobilities with improved resolution. However, it was observed that DAP did not form stable isoindole adducts with OPA/MPA as reflected by the extremely small responses, as well as extraneous peaks associated with DAP that varied in magnitude from run to run. The stability of the isoindole adduct has been observed to be relatively sensitive to the type of substituent on both the primary amine reactant and thiol coreactant[28]. Moreover, diamine analytes have been previously reported to undergo more rapid degradation when using OPA/MPA[29]. In contrast, *Figure 4.2(c)* highlights optimal resolution and detection of all test analytes in this study with baseline resolution of the three DAP stereoisomers when using OPA/NAC. Tentative peak assignment for DAP

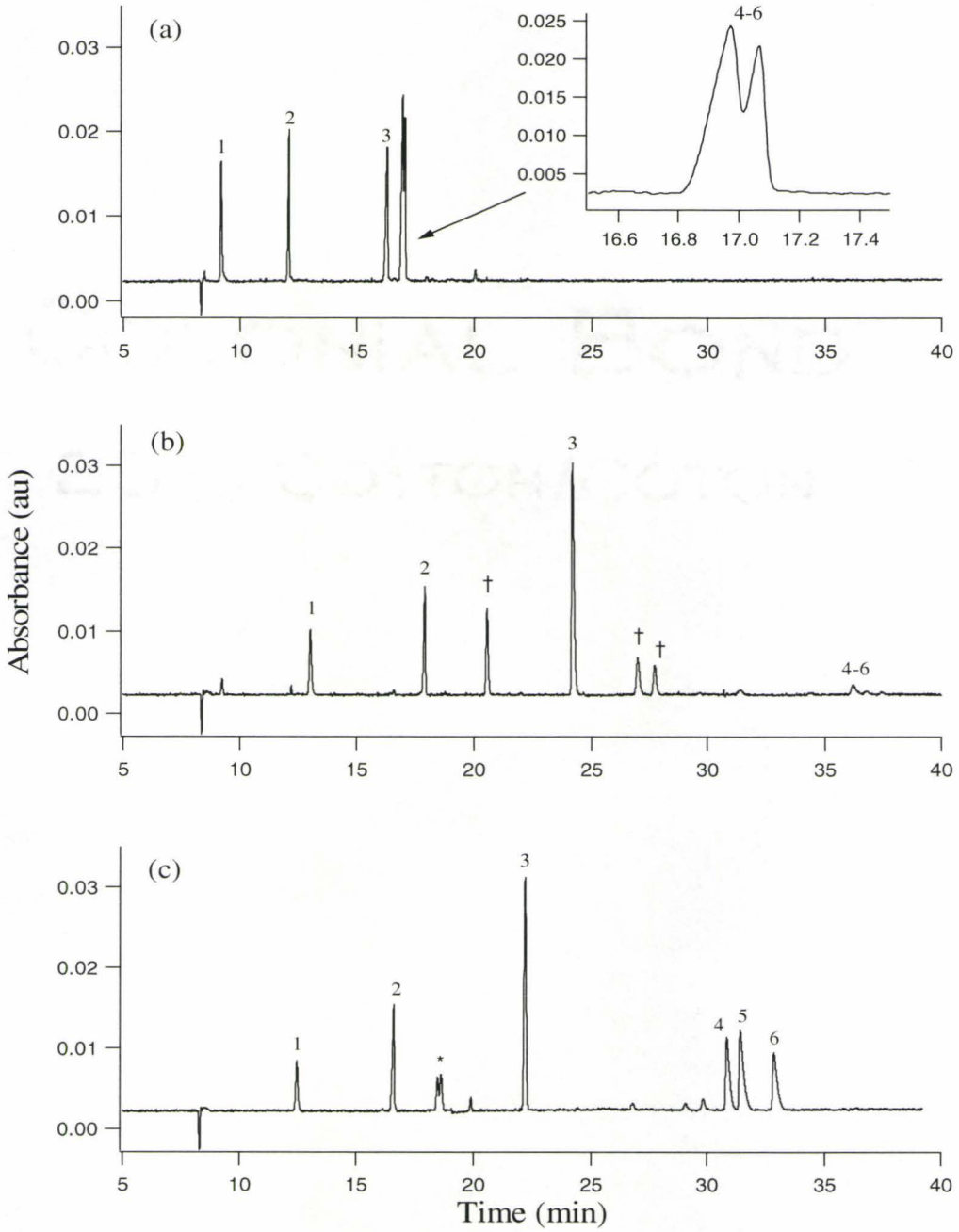

Figure 4.2: Electropherograms comparing the influence of thiol coreactant on analyte separation and peak response using offline OPA derivatization. Sample solutions contained 2 mM Glu, GluP, MA and DAP in 140 mM borate, pH 9.5. All derivatization reactions using 100 mM OPA and 150 mM (a) ME, (b) MPA, (c) NAC as the thiol coreactant. Conditions: 140 mM borate buffer, pH 9.5; voltage, 25 kV; capillary length, 90 cm; injection, 3 s; UV at 340 nm. Analyte peak numbering; 1, GlcN; 2, MA; 3, GlcN-6P; 4, D,D-DAP; 5, *meso*-DAP; and 6, L,L-DAP, where * signifies a OPA/NAC side product observed in blank, whereas † represents OPA/MPA degradation products.

isomers were deduced by the expected molar ratios in the commercial standard (*meso* in the most abundant), as well as comparing a similar elution profile in a previous HPLC assay[20]. *Figure 4.2(c)* also clearly demonstrates the analyte substituent effect (*i.e.*, acidic moiety) on the isoindole adduct stability with GlcN-6P generating over a four-fold greater response relative to GlcN, which was not observed with OPA/ME in *Figure 4.2(a)*. Hence, NAC was selected as the optimum thiol coreactant for chemical derivatization because of its ability to form relatively stable isoindole adducts with MA and DAP to improve detectability, as well as providing sufficient enantioselectivity due to the formation of anionic diastereomeric adducts with distinct electrophoretic mobilities.

4.4.2. Integration of on-line preconcentration with chemical derivatization

On-line chromatographic preconcentration with CE is promising due to the large sample enrichment capacity[30, 31], however, it is technically challenging to couple effectively since conditions used for analyte elution often result in significant band broadening that can deteriorate overall separation performance. In contrast, on-line sample preconcentration by dynamic pH junction in CE represents a simple method to electrokinetically focus large sample volumes of various weakly ionic metabolites directly in-capillary while retaining high resolution[2]. Analyte band-narrowing is generated by a moving transient pH boundary, which is initiated by a buffer pH discontinuity (pH junction) between the sample and BGE segments[32]. In this study, a modified electrokinetic based technique for integrating on-line preconcentration with chemical derivatization was examined based on our recent report for phosphoamino acid analysis using FMOC labelling[25]. The previous method was adapted such that a long

sample injection plug (100 s or 7.5 cm) was sandwiched by two short plugs (5 s or 0.4 cm) of OPA/NAC without the use of a spacer plug as depicted in *Figure 4.3*. Thus, the total length of the sample injection (w_{inj}) was approximately 8.3 cm or 14 % of the effective capillary length. A slight excess of NAC was mixed with OPA (*i.e.*, 1.5:1 molar ratio) in order to ensure formation of the activated hemithioacetal intermediate[28] similar to off-line derivatization experiments. Briefly, the injection sequence was carried out by first rinsing the capillary with borate buffer, pH 9.5 that serves as an optimal alkaline BGE for both analyte focusing and OPA/NAC derivatization. A premixed solution of 100 mM OPA/150 mM NAC was then hydrodynamically injected for 5 s as a short plug into the capillary. This was then followed by a 100 s low pressure injection of the same sample dissolved in phosphate, pH 6.5, which constitutes the buffer pH junction. The phosphate buffer serves to reduce the local electrophoretic mobility of the weakly ionic metabolites in the sample relative to the alkaline BGE to induce electrokinetic focusing[2]. A second short plug of the OPA/NAC was then introduced directly after the sample segment after which the borate buffer reservoir at the inlet is replaced prior to separation. It is important to note that chemical derivatization is not performed at the capillary inlet, which normally requires long times to ensure adequate mixing by diffusion, but rather it is performed in-capillary via zone passing[4] of the OPA/NAC bands through the sample zone. In order to enhance the kinetics of the reaction during electromigration, high concentrations of the chemical label (*i.e.*, OPA) is required, which was fixed at 100 mM similar to our previous report[25]. The major advantage of in-capillary derivatization via zone passing relative to through-capillary derivatization where the label is added to the

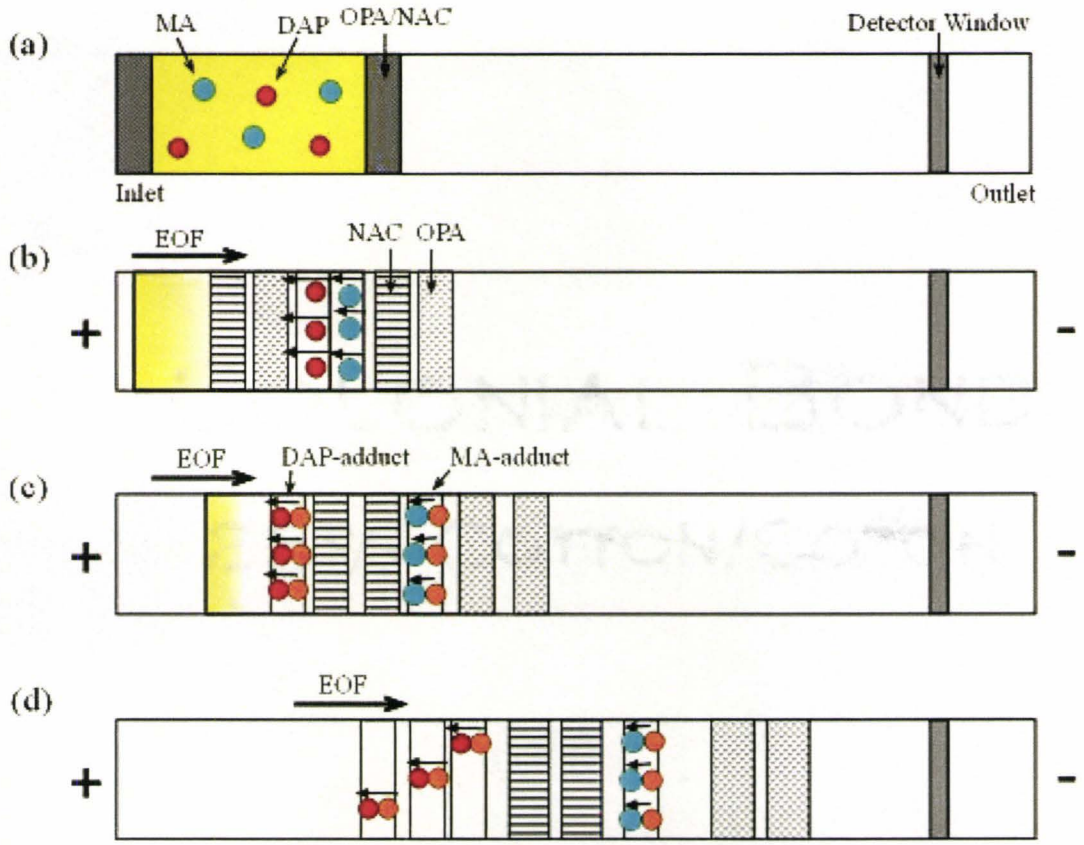

Figure 4.3: Schematic depicting single-step enenatioselective analysis of MA and DAP *via* on-line preconcentration with chemical derivatization by CE: (a) injection sequence consisting of a long sample plug sandwiched by two short label (OPA/NAC) zones; (b) application of voltage with rapid electrokinetic focused of weakly ionic analytes by dynamic pH junction; (c) zone passing of OPA/NAC through focused MA and DAP zones with chemical labelling; and (d) zone separation of excess OPA and NAC reagents with chiral resolution of MA and DAP-adducts. Note focusing of MA and DAP zones toward the front boundary of the buffer pH junction (sample; phosphate, pH 6.5) with gradual dissipation of the pH discontinuity during separation. Also, original injection of the two label zones results in the formation of four distinct migrating zones that undergo increasing band diffusion.

BGE is that only small volumes (< 10 nL) of reagent is needed without significantly altering the separation performance in terms of higher background noise and increased Joule-heating current.

4.4.3. Capillary functioning as a concentrator, microreactor and chiral selector

Preliminary experiments were performed using several different injection formats, including OPA/NAC plugs injected either in the front of back end of the sample zone. It

was observed that DAP generated about a two-fold enhancement in peak height response when the OPA/NAC plug was injected at both ends of the sample relative to injecting it as a single plug behind the sample zone. In this case, a sandwich injection sequence as shown in *Figure 4.3(a)* is preferable to ensure that both OPA (neutral) and NAC (anionic) migrate through the focused sample zone despite their different intrinsic mobilities. Surprisingly, this injection format did not generate skewed, broadened or multiple peaks caused by the analyte labelling at different positions within the long sample segment injected between two separate reagent zones. Thus, this implies that sample preconcentration by dynamic pH junction precedes chemical derivatization in order for the OPA/NAC zone passing and labelling to occur efficiently through single focused analyte zones, as depicted in *Figure 4.3(b)* and *(c)*. Note that the original two mixed label zones migrate as four distinct bands containing residual OPA and NAC that undergo increasing band diffusion after zone passing, as illustrated in *Figure 4.3(d)*. Further work will be carried out to better understand the mechanism and kinetics of in-capillary analyte focusing when used in conjunction with chemical labelling by CE. *Figure 4.4(a)* demonstrates on-line preconcentration by dynamic pH junction with OPA/NAC labelling using 20 μM of analytes by CE with UV detection at 214 nm. Note that all previous off-line derivatization experiments shown in *Figure 4.2* were performed using an analyte concentration of 2 mM. It is apparent that the use of high concentrations of OPA/NAC results in elution of extremely broad zones associated with excess OPA, which comigrated with the EOF and NAC, which migrates in between MA and GlcN-6P adducts. In order to improve selectivity and reduce background noise, *Figure 4.4(b)*

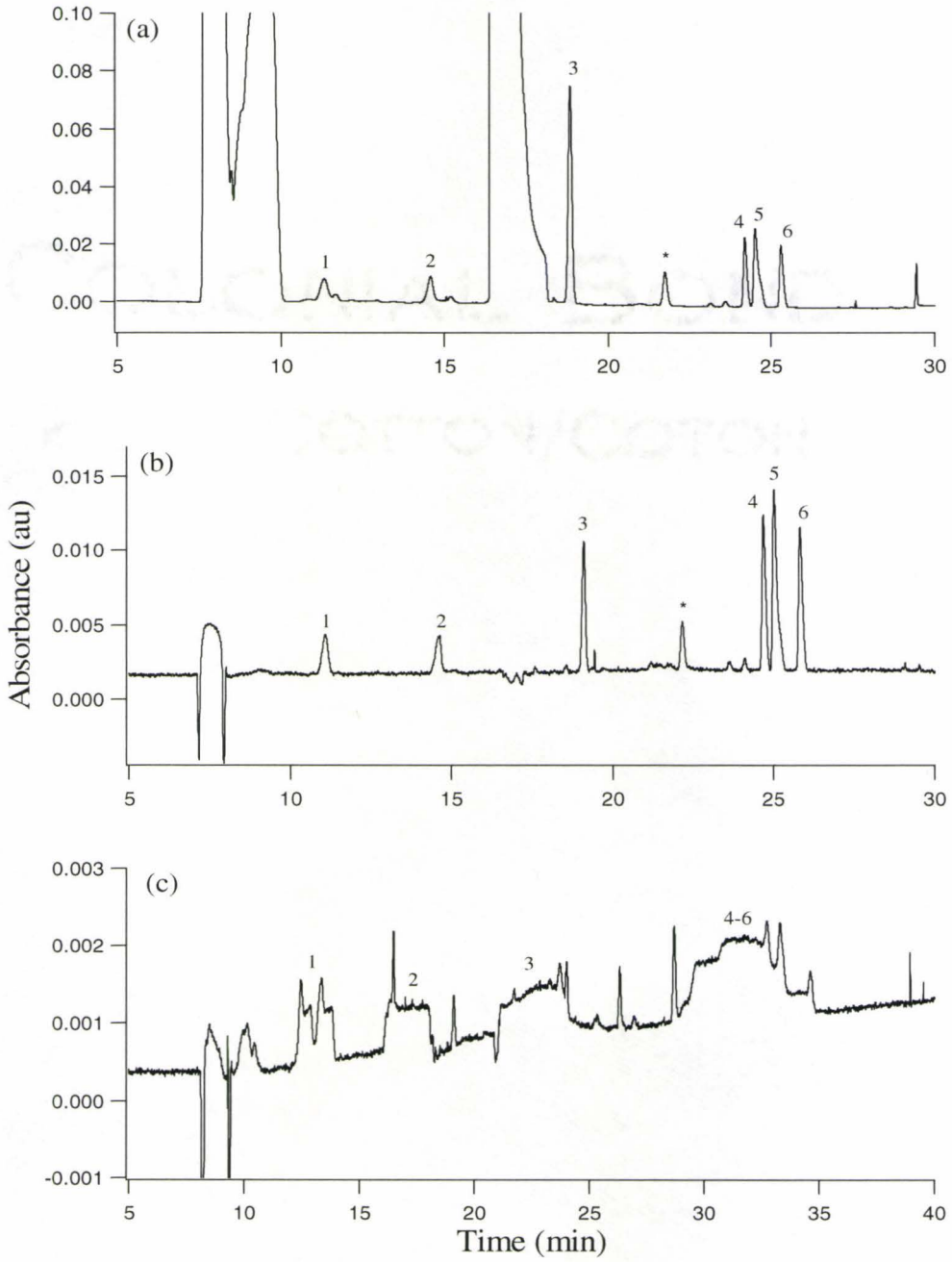

Figure 4.4: Electropherograms highlighting the influence of UV wavelength and buffer pH junction for specific and sensitive analyses of bacterial biomarkers using on-line preconcentration with chemical derivatization. Separations were monitored at (a) 214 nm and (b), (c) 340 nm. Sample solutions contained 20 μM analytes dissolved in either (a), (b) 40 mM phosphate, pH 6.5 or (c) 140 mM borate, pH 9.5. Conditions are similar to *Figure 4.2* except that OPA/NAC derivatization was performed in-capillary via zone-passing using an injection sequence shown in *Figure 4.3*.

shows the same procedure monitored at 340 nm. Since the isoindole adducts have a unique absorption band centered at around 340 nm where OPA or NAC do not absorb, there is a dramatic improvement in the baseline noise of the electropherogram with minimal spectral interference. Despite the lower molar absorptivity of the isoindole adduct at 340 nm relative to 214 nm, there was only about a two-fold lower signal, except in the case of GlcN-6P. It was observed that the efficiency of analyte focusing and labelling was enhanced for the more acidic (larger negative mobility) metabolites, GlcN-6P and DAP relative to GlcN or MA. For example there was about a 100- and 30-fold improvement in concentration sensitivity achieved for DAP and MA, respectively, when comparing conventional off-line chemical derivatization in *Figure 4.2(c)* and on-line preconcentration with labelling in *Figure 4.4(b)*. In the case of DAP, the large boost in concentration sensitivity is due to several additive factors including a 33-fold larger sample volume injected and a 1.5-fold more narrow peak width associated with reduced diffusion. In addition enhanced reaction kinetics due to zone passing of excess OPA/NAC through concentrated analytes bands confined within nanolitre volumes can also contribute to lower detection limits. This latter effect may become even more relevant when performing on-line labelling of nanomolar levels of analytes because of the slow pseudo first-order kinetics and the tendency to generate extraneous peaks caused by sample or reagent impurities, which can increase detection limits when using conventional off-line derivatization prior to CE-LIF analysis[33]. In *Figure 4.4(b)*, DAP was measured to have a w_{det} of about 0.1 cm, which is equivalent to a DIBR of 0.12 or about a eight-fold band-narrowing relative to the initial injection plug. In contrast, MA

had about a 2.5-fold broader w_{det} than DAP despite its shorter migration time for diffusion. Thus, on-line preconcentration by dynamic pH junction was more effective at focusing DAP compared to MA under these conditions due to a greater pH-dependent mobility change since it has two weakly basic amine moieties with a p*K*a ≈ 9.5[2]. In fact, w_{det} of DAP is approximately 50 % sharper in *Figure 4.4(b)* relative to *Figure 4.2(c)* despite using over a 33-fold longer sample injection. At the same time, baseline resolution of the three DAP stereoisomers was still retained. Nevertheless, the use of longer sample injection lengths (> 100 s) resulted in a gradual loss of DAP resolution. Thus, there is a compromise between the extent of sensitivity enhancement and resolution required when analyzing complex sample mixtures by CE. As a control experiment, *Figure 4.4(c)* highlights the impact of on-line analyte focusing with labelling when using a continuous buffer system in which both sample and BGE zones are the same (*i.e.*, borate, pH 9.5). It is clear that injection of such long sample plugs will normally result in detrimental band broadening in CE when there does not exist a specific electrokinetic focusing mechanism to overcome sample overloading and longitudinal diffusion prior to in-capillary chemical derivatization.

4.4.4. Enhanced method performance

Besides improving concentration sensitivity and lowering detection limits, on-line preconcentration with chemical labelling also serves to enhance method performance in terms of reduced sample handling, improved reliability, and automation. This is particularly relevant for OPA/NAC derivatization reactions that can form relatively unstable isoindole adducts with certain analytes, which can lead to large variability in

quantification. High-throughput analyses can be realized using this technique since the online preconcentration with derivatization technique can be fully integrated of commercial CE and microchip devices. For instance, the repeatability (intraday, n = 5) for the analysis of MA and DAP based on migration time and analyte peak area resulted in average CV of 1.7 and 6.0 %, respectively. The reproducibility (interday, n = 10) of the method was performed on two consecutive days using fresh OPA, NAC, and buffer reagents was also consistent with average CV of 1.6 and 8.0 % for migration time and peak area, respectively. Further improvements in the reproducibility of quantification can be realized by using appropriate internal standard. Note that the apparent analyte electrophoretic mobility can be measured with high precision (CV < 0.5 %) by this technique when corrected for changes in EOF using the broad injection plug (EOF marker) that migrates at about 8 min in *Figure 4.5*. *Table 4.1* summarizes the validation parameters for the determination of bacterial biomarkers by CE *via* on-line preconcentration with chemical derivatization. Calibration curves for MA and the three DAP stereoisomers were generated using duplicate measurements of six different concentrations over a 50-fold (5 - 250 μM) and a 40-fold (1 - 40 μM) concentration range for MA and DAP, respectively. Excellent linearity was achieved for quantification as reflected by an R^2 of 0.9994 and 0.9929 for MA and DAP, respectively. The measured detection limits were about 2 and 0.2 μM for MA and DAP (each stereoisomer), respectively, based on S/N ≈ 3. The lower detection limit achieved for DAP relative to MA by this technique is based on the greater focusing efficiency for highly acidic metabolites when using on-line preconcentration by dynamic pH junction.

Table 4.1: Validation of the optimized on-line preconcentration with OPA/NAC derivatization technique for bacterial biomarker analysis by CE with UV detection.

Parameter	MA	D,D-DAP	*meso-DAP*	L,L-DAP
A. Intraday precision (n = 5)				
Migration Time /CV	0.6	1.8	1.9	2.1
Peak Area[a] /CV	5.8	7.8	4.1	6.2
B. Interday precision (n = 10)				
Migration Time /CV	0.8	1.7	1.8	1.9
Peak Area[a] /CV	9.8	7.8	6.4	7.7
C. Calibration curve[b] (n = 5)				
Linearity/R^2	0.9994	0.9942	0.9972	0.9872
D. Detection limit (S/N ≈ 3)				
Concentration/μM	2	0.2	0.2	0.2
E. Apparent mobility				
$\mu_{ep}{}^{A} \times 10^{-4}/cm^2 \cdot V^{-1} \cdot s^{-1}$	-2.784	-3.866	-3.886	-3.938
CV/n=5	0.2	0.4	0.4	0.4

[a] Peak area precision measurements performed using 20 μM of MA and DAP

[b] Duplicate measurements of six different concentrations ranging from 5 to 250 μM for MA and 1 to 40 μM for DAP

4.4.5. Selective extracellular bacterial biomarker detection

The optimized method was next applied to the analysis of MA and DAP in the extracellular medium of *E. coli* BL-21 bacterial cultures with minimal sample pretreatment. Since the LB nutrient broth used to grow bacteria is derived from bacteria and yeast extracts in high salt, it serves as a complex real sample matrix (containing essential amino acids) to properly assess method selectivity. In addition, bacterial culture experiments were performed to investigate whether *E. coli* excreted MA and DAP metabolites could be detected in the extracellular medium during cell growth. All bacterial extracellular samples were diluted 20-fold in phosphate buffer prior to CE analyses due to the extremely high concentrations of many amino acids present in the

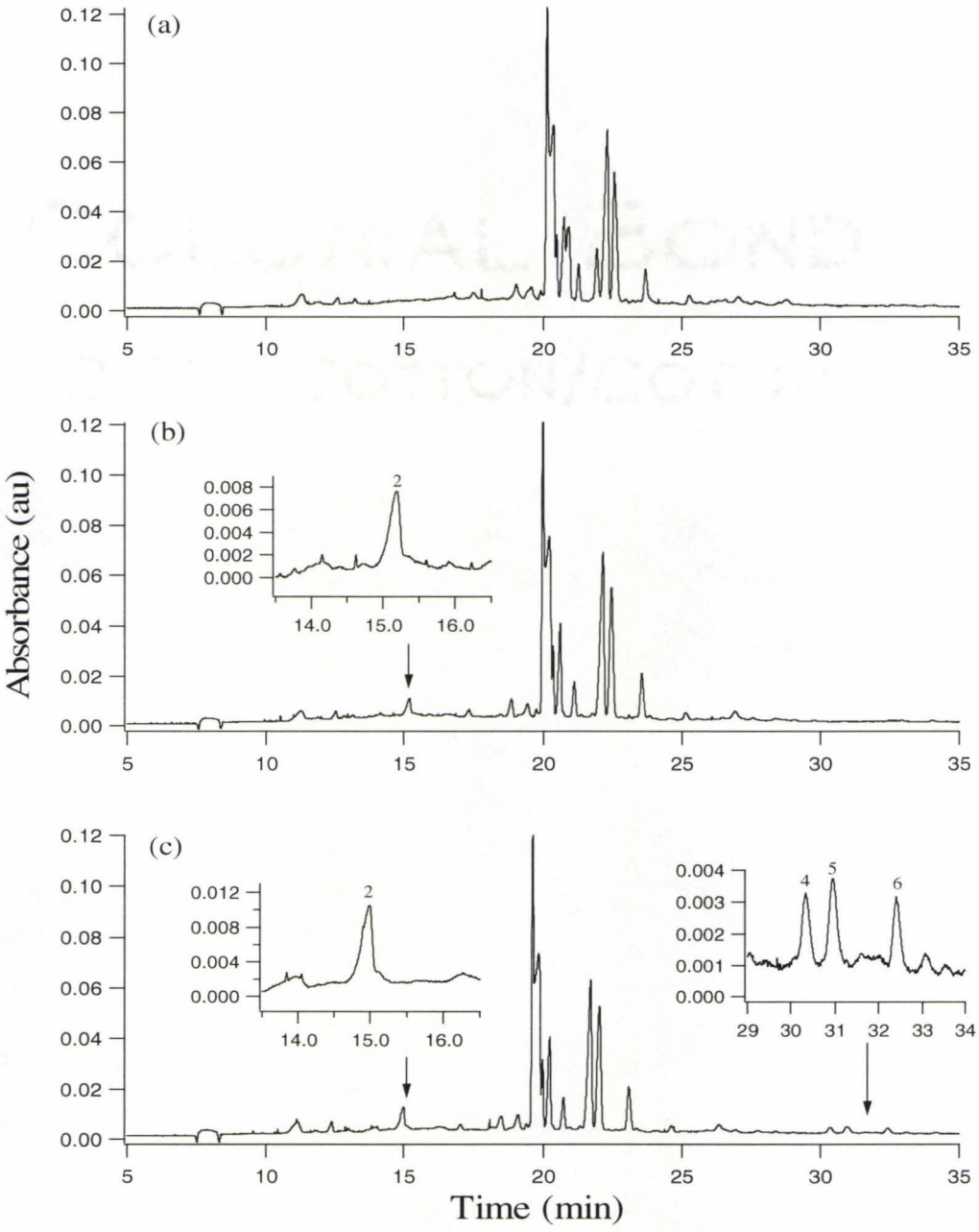

Figure 4.5: Selective analysis of MA and DAP in the extracellular matrix of *E. Coli* bacteria by CE using on-line preconcentration with chemical derivatization. Electropherograms represent (a) LB medium (no bacteria added), (b) extracellular medium of bacteria grown with 25% seeding volume for 360 min, and (c) same sample as (b) but spiked with 6 μM of MA and DAP. Sample solutions were diluted 20-fold with 40 mM phosphate buffer, pH 6.5 prior to analysis. Conditions are the same as *Figure 4.4(b)*.

broth medium, which increase baseline noise. However, it was observed that the optimized online preconcentration with derivatization technique was also applicable to bacterial cell extract sample injected directly even without prior dilution. *Figure 4.5(a)* shows a control electropherogram, which represents the metabolite profile in the LB medium prior to inoculation with bacteria. It was determined that no detectable level of MA or DAP was measured in the original broth medium by this technique. It is important to note that this method can be used to analyze changes in other amino acid and amino sugar metabolites present in the broth although it was not the focus in this work. *Figure 4.5(b)* demonstrates that after 6 h of bacterial incubation (stationary growth phase) in LB medium, a significant change in the metabolite profile was observed due to the specific nutrient uptake and metabolite excretion in the matrix. Notably, a new peak associated with MA was detected in *Figure 4.5(b)*, which was not originally present in *Figure 4.5(a)*. Tentative peak assignment of MA based on electrophoretic mobility in comparison with standard (-2.784×10^{-4} $cm^2 \cdot V^{-1} \cdot s^{-1}$), as well as spiking experiments performed in *Figure 4.5(c)*. However, DAP was not detected in the sample under these conditions. The method was considered to be highly selective for MA and DAP analyses based on spiking experiments depicted in *Figure 4.5(c)*, as well as performing a separation using a 20 standard amino acid mixture (data not shown), which confirmed that there was no known comigrating amino acid interference. Longer apparent migration times of MA and DAP were observed in *Figure 4.5(c)* relative to standard solution in *Figure 4.4(b)* due to sample matrix effects in the growth medium, which influence the magnitude of the EOF in CE separations. Nevertheless, precise measurements of analyte

mobility or corrected migration times can be achieved when injecting different sample matricies by normalizing for changes in EOF. The potential of this technique to accurately quantify micromolar levels of bacterial biomarkers in complex biological samples was assessed by performing recovery studies (n = 3) using 20 μM of DAP spiked in the LB broth growth medium of *E. coli*, which resulted in an average recovery of 94% for all three stereoisomers. It is unclear why free MA and not *meso*-DAP was detected in this study since the PG component of *E. coli* is known to undergo significant turnover during bacterial growth by the enzymatic actions of transglycosidases, endopeptidases and amidases[34]. However, given the higher abundance of MA relative to *meso*-DAP in the PG, as well as efficient bacterial recycling of hydrolyzed metabolites, this can reflect *meso*-DAP levels below the detection limit of the present method when using UV detection. Future work will apply on-line preconcentration with chemical derivatization techniques by CE with LIF detection to further enhance detection limits for trace analysis of low-abundance bacterial biomarkers in complex biological samples.

4.5. Summary and conclusion

A new on-line preconcentration with chemical derivatization technique has been developed for the enantioselective analysis of MA and DAP associated with the bacterial PG by CE. Up to a 100-fold improvement in concentration sensitivity has been achieved while retaining high-resolution chiral separations by integrating sample enrichment with chemical labelling steps directly within a single capillary during electromigration. High-throughput separations with submicromolar detection limits can be realized by this technique using commercial CE instruments with UV detection. The detection of unique

bacterial biomarkers excreted in the extracellular matrix of *E. coli* bacteria has also been demonstrated. Further work will involve the application of this technique to other classes of bacterial biomarkers in biological and environmental samples by CE.

4.6 References

1. J. P. Quirino, J. B. Kim and S. Terabe, *J. Chromatogr. A*, 2002, **965**, 357-373.
2. P. Britz-McKibbin and S. Terabe, *J. Chromatogr. A*, 2003, **1000**, 917-934.
3. C. H. Lin and T. Kaneta, *Electrophoresis*, 2004, **25**, 4058-4073.
4. A. Taga, A. Nishino and S. Honda, *J. Chromatogr. A*, 1998, **822**, 271-279.
5. Y. Zhang and F. A. Gomez, *Electrophoresis*, 2000, **21**, 3305-3310.
6. S. v. Dyck, E. Kaale, S. Novakova, Z. Glatz, J. Hoogmarten and A. v. Schepdael, *Electrophoresis*, 2003, **24**, 3868-3878.
7. N. J. Reinhoud, U. R. Tjaden and J. v. d. Greff, *J. Chromatogr. A*, 1994, **673**, 255-266.
8. R. M. Lattore, J. Saurina and S. Hernandez-Cassou, *Electrophoresis*, 2001, **22**, 4355-4361.
9. S. Oguri, H. Tanagaki, M. Hamaya, M. Kato and T. Toyo'oka, *Anal. Chem.*, 2003, **75**, 5240-5245.
10. P. Britz-McKibbin, T. Nishioka and S. Terabe, *Anal. Sci.*, 2003, **19**, 99-104.
11. K. Sato, A. Hibara, M. Tokeshi, H. Hisamoto and T. Kitamori, *Anal. Sci.*, 2003, **19**, 15-22.
12. N. O. G. Jorgensen, R. Stepanaukas, A. G. U. Pedersen, M. Hansen and O. Nyrobe, *FEMS Microbiol. Ecol.*, 2003, **46**, 269-280.

13. A. Atrih, G. Bacher, G. Allmaier, M. P. Williamson and S. J. Foster, *J. Bacteriol.*, 1999, **181**, 3956-3966.

14. M. Zanol and L. Gastaldo, *J. Chromatogr. A*, 1991, **536**, 211-216.

15. R. J. Cox, A. Sutherland and J. C. Vederas, *Bioorg. Med. Chem.*, 2000, **292**, 917-920.

16. H. Ogawa, Y. Amagi, I. Koike, K. Kaiser and R. Benner, *Science*, 2001, **292**, 917-920.

17. G. Borruat, C. A. H. Roten, R. Marchant, L. B. Fay and D. Karmata, *J. Chromatogr. A*, 2001, **922**, 219-224.

18. A. Fox, *Anat. Rec.*, 2002, **268**, 180-185.

19. R. T. v. Strien, R. Engel, O. Holst, A. Bufe, W. Eder, M. Waser, C. Braun-Fahrlaender, J. Riedler, D. Nowak, E. v. Mutius and A. S. Team, *J. Allergy Clin. Immunol.*, 2004, **113**, 860-867.

20. T. Nagasawa, J. R. Ling and R. Onodera, *J. Chromatogr.*, 1993, **653**, 336-340.

21. R. Puchala, H. Pior, G. W. Kulasek and J. A. Shelford, *J. Chromatogr.*, 1992, **623**, 63-67.

22. A. Sebastian and L. Larsson, *Appl. Environ. Microbiol.*, 2003, **69**, 3103-3109.

23. M. P. Kozar and A. Fox, *J. Chromatogr. A*, 2002, **946**, 229-238.

24. R. Driouich, T. Takayanagi, M. Oshima and S. Motomizu, *J. Pharm. Biomed. Anal.*, 2003, **30**, 1523-1530.

25. A. S. Ptolemy and P. Britz-McKibbin, *Analyst*, 2005, **130**, 1263-1270.

26. P. Britz-McKibbin and D. D. Y. Chen, *Anal. Chem.*, 2000, **72**, 1242-1252.

27. W. J. M. Underberg and J. C. M. Waterval, *Electrophoresis*, 2002, **23**, 3922-3933.

28. M. C. G. Alvarez-Coque, M. J. M. Hernandez, R. M. V. Camanas and C. M. Fernandez, *Anal. Biochem.*, 1989, **178**, 1-7.

29. D. Kutlan, P. Presits and I. Molnar-Perl, *J. Chromatogr. A*, 2002, **949**, 235-248.

30. E. Bonneil and K. C. Waldron, *Tatlanta*, 2000, **53**, 687-699.

31. F. W. A. Tempels, J. Teeuwsen, I. K. Kyriakou, G. Theodoridis, W. J. M. Underberg, G. W. Somsen and G. J. d. Jong, *J. Chromatogr. A*, 2004, **1053**, 263-268.

32. J. B. Kim, P. Britz-McKibbin, T. Hirokawa and S. Terabe, *Anal. Chem.*, 2003, **75**, 3986-3993.

33. B. W. Boyd and R. T. Kennedy, *Analyst*, 1998, **123**, 2119-2124.

34. W. Vollmer and J. V. Holtje, *J. Bacteriol.*, 2004, **186**, 5978-5987.

Chapter V

Single-step Enantioselective Amino Acid Flux Analysis by Capillary Electrophoresis Using On-line Sample Preconcentration with Chemical Derivatization

V. Single-step Enantioselective Amino Acid Flux Analysis by Capillary Electrophoresis Using On-line Sample Preconcentration with Chemical Derivatization

5.1. Abstract

Capillary electrophoresis (CE) represents a versatile platform for integrating sample pretreatment with chemical analysis because of its ability to tune analyte electromigration and band dispersion properties in discontinuous electrolyte systems. In this *Chapter*, a single-step method that combines on-line sample preconcentration with in-capillary chemical derivatization is developed for rapid, sensitive, and enantioselective analysis of micromolar levels of amino acids that lack intrinsic chromophores by CE with UV detection. Time-resolved electrophoretic studies revealed two distinct stages of amino acid band narrowing within the original long sample injection plug occurring both prior to and after in-capillary labeling via zone passing by *ortho*-phthalaldehyde/*N*-acetyl-L-cysteine (OPA/NAC). This technique enabled direct analysis of D-amino acids in a 95% enantiomeric excess mixture with sub-micromolar detection limits and minimal sample handling, where the capillary functions as a preconcentrator, microreactor, and chiral selector. On-line sample preconcentration with chemical derivatization CE (SPCD–CE) was applied to study the enantioselective amino acid flux in *Escherichia coli* bacteria cultures, which demonstrated a unique L-Ala efflux into the extracellular medium. New strategies for high-throughput analyses of low-abundance metabolites are important for understanding fundamental physiological processes in bacteria required for screening the efficacy of new classes of antibiotics as well as altered metabolism in

genetically modified mutant strains.

5.2. Introduction

Conventional analytical techniques that are directed at low-abundance metabolites in complex biological samples typically require several distinct off-line sample pretreatment procedures prior to analysis. Two of the most widely used sample pretreatment protocols are sample preconcentration and chemical derivatization. There is increasing interest in developing new techniques that integrate multiple sample pretreatment steps during analysis under a single format, as exemplified by chip-based micro-total analysis systems (μ-TAS)[1, 2]. Although there have been a number of techniques reported for either on-line sample preconcnetraion[3-7] or on-line chemical labelling[8-11] in capillary electrophoresis (CE), their integration within a single capillary has been relatively unexplored[12-14]. Recently, Zare and co-workers[15] demonstrated a new method to analyze the intercellular amino acid content of a single cell that integrated cell selection, cell lysis, chemical derivatization, and electrophoretic separation steps within a microchip device. However, the major obstacle for integrating multiple functions on-line relative to off-line sample pretreatment remain extra-column band broadening and chemical interferences that result in poor separation efficiency when combining multiple steps sequentially within a capillary or microchannel. As previously discussed, our group introduced a new hyphenated strategy that effectively integrates on-line sample preconcentration with chemical derivatization in CE using 9-fluorenylmethyloxycarbonyl chloride (FMOC)[16] or *ortho*-phthalaldehyde (OPA)[17] labelling. On-line preconcentration not only is important for sample enrichment to enhance concentration detection limits but

also is useful for ensuring narrow peak shapes for high-efficiency separations. Moreover, effective coupling of on-line sample preconcentration with chemical derivatization is useful for enhancing reaction kinetics in free solution as is required when labelling dilute samples containing sub-micromolar levels of analytes. On-line sample preconcentration with chemical derivatization (SPCD-CE) is based on discontinuous electrolytes systems that serve to improve method reliability, reduce total analysis times, and facilitate high-throughput analyses because it can be readily automated with commercial capillary arrays[18]. Further research is needed to better understand the mechanism and applicability of SPCD-CE for the analysis of different classes of metabolites in biological samples.

D-amino acids represent an important class of low-abundance chiral metabolites with biological significance ranging from unique components of the bacterial cell wall (*e.g.*, D-Ala and D-Glu) to recently indentified mammalian neurotransmitters (*e.g.*, D-Ser). There is growing interest in developing enantioselective and ultrasensitive methods for their analysis in complex biological matrices in the presence of high levels of corresponding L-amino acids. Because of this need for sufficient resolution and low detection limits in chiral amino acid separations, previous methods have included off-line chemical derivatization in conjunction with HPLC fluorescence[19], GC-MS[20], CE-MS[21], and CE[22] or microchip electrophoresis[23] with laser-induced fluorescence detection. In the current work, an integrated SPCD-CE technique is applied to study the amino acid flux in the extra-cellular matrix of *Escherichia coli* bacterial cultures as an extension of our recent report involving the analysis of the bacterial biomarkers muramic acid and 2,6-diaminopimelic acid[17]. Flux analysis[24] plays an important role in metabolic engineering

for understanding fundamental metabolic pathways in bacteria as a way to maximize the conversion of nutrients into biomass yield and specific by-products such as recombinant protein[25] and amino acids[26]. Single-step enantioselective analysis of amino acids that lack intrinsic chromophores in complex nutrient broth solutions was realized by SPCD-CE with UV detection. On-line sample preconcentration with chemical derivatization provided approximately a 40-fold enhancement in concentration sensitivity in CE with sub-micromolar detection limits, and this is amendable to resolve 95 % enantiomeric excess mixture. Of note, our studies revealed enantioselective efflux of L-Ala during the exponential growth phase of *E. coli* BL-21 bacteria that was also verified enzymatically. To the best of our knowledge, this is the first reported CE method used to assess the amino acid flux in the extracellular medium of bacteria. In addition, this article provides further insight into the mechanism of SPCD-CE, which revealed distinct time-dependent electrokinetic focusing events that were mediated by a dual transient isotachophoresis (t-ITP) and dynamic pH junction process.

5.3. Materials and methods

5.3.1. Chemicals and reagents

Deionized water used for buffer and sample preparations was obtained using a Barnstead EasyPure®II LF ultrapure water system (Dubuque, IA., USA). Borate buffer (140 mM) was prepared using sodium tetraborate decahydrate from Sigma-Aldrich (St. Louis, MO. USA) that serves as the aqueous background electrolyte (BGE). All phosphate buffers were prepared using sodium dihydrogen phosphate from Alfa-Aesar (Ward Hill, MA., USA). The pH values of the borate and phosphate buffers were

adjusting using 0.1 M NaOH solution to 9.5 and 6.0, respectively unless otherwise noted. All D-amino acids used in this study were purchased from Alfa-Aesar. The L-amino acids, OPA, NAC, taurine, L-Ala dehydrogenase (53 $U \cdot mg^{-1}$), L-Lys oxidase (36 $U \cdot mg^{-1}$) and oxidized β-nicotinamide adenine dinucleotide (NAD^+) were purchased from Sigma-Aldrich. Individual 50 mM standard solutions of D/L-ser (D-Ser, L-Ser), D/L-alanine (D-Ala, L-Ala), D/L-glutamic acid (D-Glu, L-Glu) and D/L-aspartic acid (D-Asp, L-Asp) initially were prepared in deionized water. Stock solutions of the amino acids were then prepared in BGE or sample buffer prior to analysis. Primary stock solutions of 600 mM NAC and 400 mM OPA were prepared fresh every day in 140 mM borate (pH 9.5) and HPLC-grade acetonitrile, respectively. Individual 150 mM NAC and 100 mM OPA solutions were then prepared in borate buffer prior to either on-line derivatization of on-line sample preconcentration with chemical derivatization analyses by CE.

5.3.3. Apparatus and procedure

All separations were performed on an automated P/ACE 2100 or P/ACE MDQ CE system (Beckman Instruments, Fullerton, CA., USA). Uncoated fused-silica capillaries with 50 μm i.d., 360 μm i.d. and 67 or 90 cm length were used for analyses. All separations began by rinsing the capillary for 5 min with 0.1 M NaOH followed by 5 min rinse with BGE. Labelling reagents and samples were introduced sequentially into the capillary using a low-pressure injection (0.5 psi or 3.5 kPa). The low pressure injection was measured to have an average (n = 9) velocity of $5.50 \times 10^{-2}\ cm^2 \cdot V^{-1} \cdot s^{-1}$. This velocity was used to estimate the sample injection bandwidth (w_{inj}) and to position the front boundary of the sample plug at various distances from the detector window for time-

resolved electrokinetic focusing studies. On-line sample preconcentration with OPA/NAC derivatization was performed in-capillary by first injecting 150 mM NAC for 5 s. Then a 3 or 100 s injection of the sample (amino acid mixture) was performed immediately followed by a 5 s injection of 100 mM OPA. The total w_{inj} is approximately 6.1 cm, which is equivalent to a sample plug that fills approximately 10.2 % of the effective capillary length. It is important to note that this injection procedure was modified from to simplify the setup relative to our previous report, where the OPA and NAC were manually premixed together and injected as two identical plugs in a sandwich format[17]. Separations were performed thermostatted at 25^{0}C using 25 kV, and UV absorbance was monitored at either 214 nm or 340 nm. Analyte detector bandwidths (w_{det}) were determined by measuring base-peak widths and converting this time measurement into the distance domain by multiplying it by the measured migration velocity. This allows for the detector/injection bandwidth ratio (DIBR) to be calculated as a quantitative measure to assess analyte band focusing[6].

5.3.4. Escherichia coli bacteria incubation

The incubation procedure for batch cultures of the *E. Coli* BL-21 (DE3) strain used in this study has been described previously[17]. Briefly, after the selection of a single *E. coli* colony from a Luria-Bertani (LB) medium agar-treated plate (BioShop Canada, Burlington, ON., Canada), a 500 mL flask containing 100 mM of liquid LB Miller broth (BioShop Canada) was inoculated. Bacteria were grown in this medium on rotary shakers for 24 h at 37^{0}C and then were used to inoculate three separate flask containing LB broth with 5 % seeding volume. The optical densities of these samples were then measured

with a DU General Purpose UV/Vis Spectrometer (extracellular medium) to be removed and frozen at -78^{0}C for future use. This procedure was repeated in 30 min intervals over 5 h to generate a bacterial growth curve. All bacteria were handled safely in a microbiological facility until discarded in 10 % sodium hypochlorite solution.

5.3.5. Enzymatic treatment of *E. coli* extracellular broth samples

Initial stock solutions of 30 mM NAD^+ and 0.2 U L-Ala dehydrogenase were prepared in deionized water and 50 mM carbonate buffer (pH 10.0), respectively. A stock solution of 2.6 U L-Lys oxidase was also prepared in deionized water. Selective enzymatic transformations of L-Ala (products: pyruvate and reduced in NADH) and L-Lys (product: 6-amino 2-oxo-hexanoate) substrates contained within a 100-fold diluted 5 h extracellular *E. coli* sample was then performed separately with each enzyme at room temperature in 50 mM carbonate buffer (pH 10.0) with 1 mM NAD^+ and 0.2 U L-Ala dehydrogenase and in 70 mM phosphate buffer (pH 8.0) with 0.1 U L-Lys oxidase, respectively. After approximately 4 h of enzyme incubation, the samples were dilute six-fold with 40 mM phosphate buffer (pH 6.0) and then analyzed directly by SPCD-CE. A comparison of enzymatically treated samples with controls allowed for qualitative identification of L-Ala as well as the absence of D-Ala in the bacteria extracellular matrix. The latter was deemed necessary due to chemical interference caused by co-migration of a minor doubly labelled L-Lys OPA adduct peak in the electropherogram.

5.4. Results and discussion

5.4.1. Online sample preconcentration with in-capillary chemical derivatization

Chemical derivatization[27] can serve two major functions in CE: (i) incorporate a

useful moiety on the analyte for improved photometric detection and (ii) to alter chemical properties for enhanced selectivity. The latter property is particularly useful for separating amino acid enantiomers by CE via the formation of diastereomeric adducts using a chiral reagent. In general, on-line chemical derivatization techniques in CE can be performed electrophoretically in two different formats: (i) discrete zone passing of a label through a migrating analyte zone (in-capillary) and (ii) zone passing of a migrating analyte through a label that is contained continuously in the separation buffer (through-capillary)[9]. The former discontinuous procedure is preferred in CE because only small volumes (< 10 nL) of reagent are required for in-capillary derivatization without significant modification to BGE conditions. In either case, the method is limited to labels that undergo rapid kinetics at room temperature for selected analytes. OPA and the chiral thiol co-reactant NAC was selected as the label in this study because it reacts rapidly with primary amino acids enantiomers under alkaline conditions to form charged diasteromeric 1-thio-2-amino substituted isoindole adducts with unique spectral properties[28]. On-line sample preconcentration by dynamic pH junction is an effective way to enhance concentration sensitivity of weakly ionic, metabolites in CE via electrokinetic focusing of large sample injection volumes due to pH dependent mobility changes in discontinuous buffer systems[6]. When using mixed buffer junctions in CE, analyte focusing can be extended to both weakly and strongly ionic analytes based on optimal selection of buffer pH and co-ion mobility differences in sample and BGE as mediated by dynamic pH junction and t-ITP[29]. Recently, our group introduced SPCD-CE as a single-step hyphenated platform that combines in-capillary sample preconcentration with chemical

labelling for improved detection and resolution of analytes that lack chromophoric or fluorescent moieties[30]. Selective chiral resolution of three major stereoisomers of gram-negative bacteria cell wall crosslinker, 2,6-diaminopimelic acid, was demonstrated previously by SPCD-CE with a 100-fold improvement in concentration sensitivity relative to conventional off-line derivatziation[17].

Figure 5.1 highlights the general principle of SPCD-CE for chiral amino acid analysis using a discontinuous electrolyte system where sample preconcentration, OPA/NAC labelling and chiral resolution of amino acid adducts occur within a single capillary during electromigration. Note that after initial conditioning of the capillary with BGE, a multiple sample injection sequence is performed consisting of short concentrated plugs of NAC and OPA reagents positioned in between a long plug of dilute sample, as shown in *Figure 5.1(a)*. OPA is injected at the back end of the sample plug because it is neutral and co-migrates with the electroosmotic flow (EOF), unlike the anionic chiral NAC coreagent that migrates with a slower apparent mobility. A weakly acidic phosphate buffer is used in the sample relative to an alkaline borate buffer as BGE to enhance amino acid focusing by a dynamic pH junction and t-ITP mode at the front edge of the sample-BGE interface. As depicted in *Figure 5.1(b)*, in-capillary OPA labelling occurs optimally after sample preconcentration when analyte OPA and NAC zones co-migrate at the same position in space prior to irreversible zonal separation. Zone passing of OPA and NAC reagents through the preconcentrated amino acid zone results in the formation of diastereomeric adducts as highlighted in *Figure 5.1(c)*. Afterward, enantiomeric resolution of amino acid adducts is realized along with increasing band

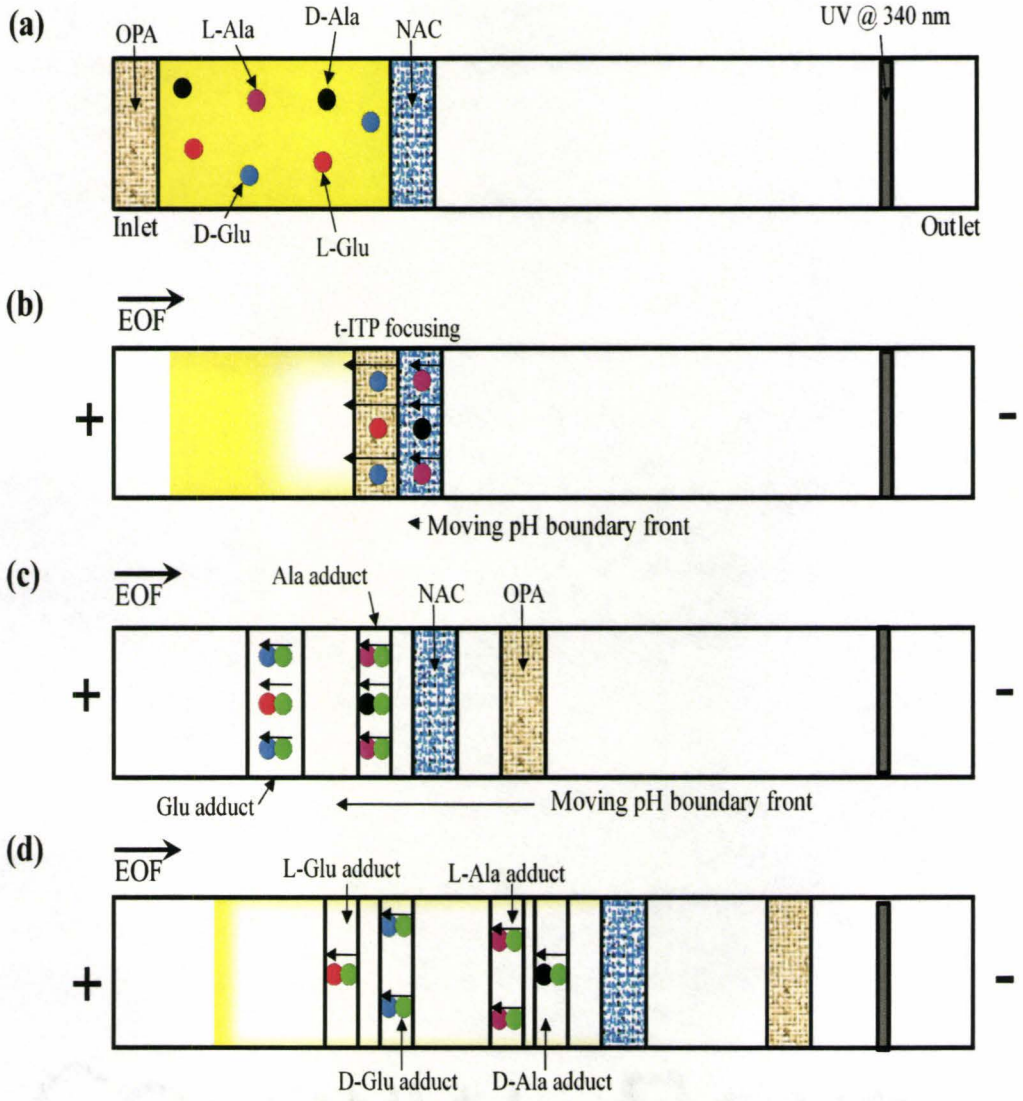

Figure 5.1: General principle of SPCD-CE for single-step enantioselective analysis of sub-micromolar levels of amino acids: (a) multiple hydrodynamic injection sequence; (b) on-line sample preconcentration; (c) in-capillary chemical labelling by zone passing of OPA/NAC; (d) chiral separation of diastereomeric amino acid adducts. Note that amino acid focusing occurs at different stages during electromigration both prior to and after in-capillary derivatization. Noncovalent dynamic complexation of amino acid adducts using cyclodextrins or other additives in the buffer can also be used to improve the enantioselectivity by SPCD-CE.

separation of all species, including excess labelling reagents, as shown in *Figure 5.1(d)*. Further insight into the kinetics of band narrowing relative to chemical labelling process in SPCD-CE is addressed later to support the general scheme described in *Figure 5.1*.

The major advantage of SPCD-CE is that sample preconcentration, chemical derivatization, and chiral resolution all are performed electrophoretically within a single automated instrumental format.

Figure 5.2(a) depicts in-capillary derivatization of micromolar levels of biologically relevant D-amino acids (D-Ser, D-Ala, D-Glu and D-Asp) and their L-enantiomers by CE with UV absorbance when using a conventional sample injection of 3 s (0.2 cm). Because of selective detection of the amino acid-isoindole adducts at 340 nm, there is minimal baseline noise or spectral interferences despite using high concentrations of OPA/NAC as discrete zones in the buffer. Because of the small injection volume, narrow optical path length, and band broadening caused by longitudinal diffusion, all amino acid adduct peaks are near the detection limit due to poor concentration sensitivity when using UV absorbance. It is evident that the use of OPA/NAC permitted baseline resolution of D/L-Ala and D/L-Glu and partial resolution of D/L-Ser due to the formation of diastereomeric adducts with unique mobilities. Surprisingly, D/L-Asp was not resolved under these conditions given a difference of only a methylene group relative to Glu. Minor OPA hydrolysis products (noted by [*] in *Figure 5.2(a)*) were observed in all electropherograms. *Figure 5.2(b)* is a control experiment that depicts the deleterious effects of normal band broadening ($w_{det} > 8.2$ cm) caused by sample overloading when using a continuous buffer system (borate in sample and BGE) with a long sample injection $w_{inj} \approx 6.1$ cm. Thus, increasing sample injection volumes beyond 1 % of the capillary length in CE normally results in poor separation efficiency and higher detection limits unless there exists a mechanism for effective

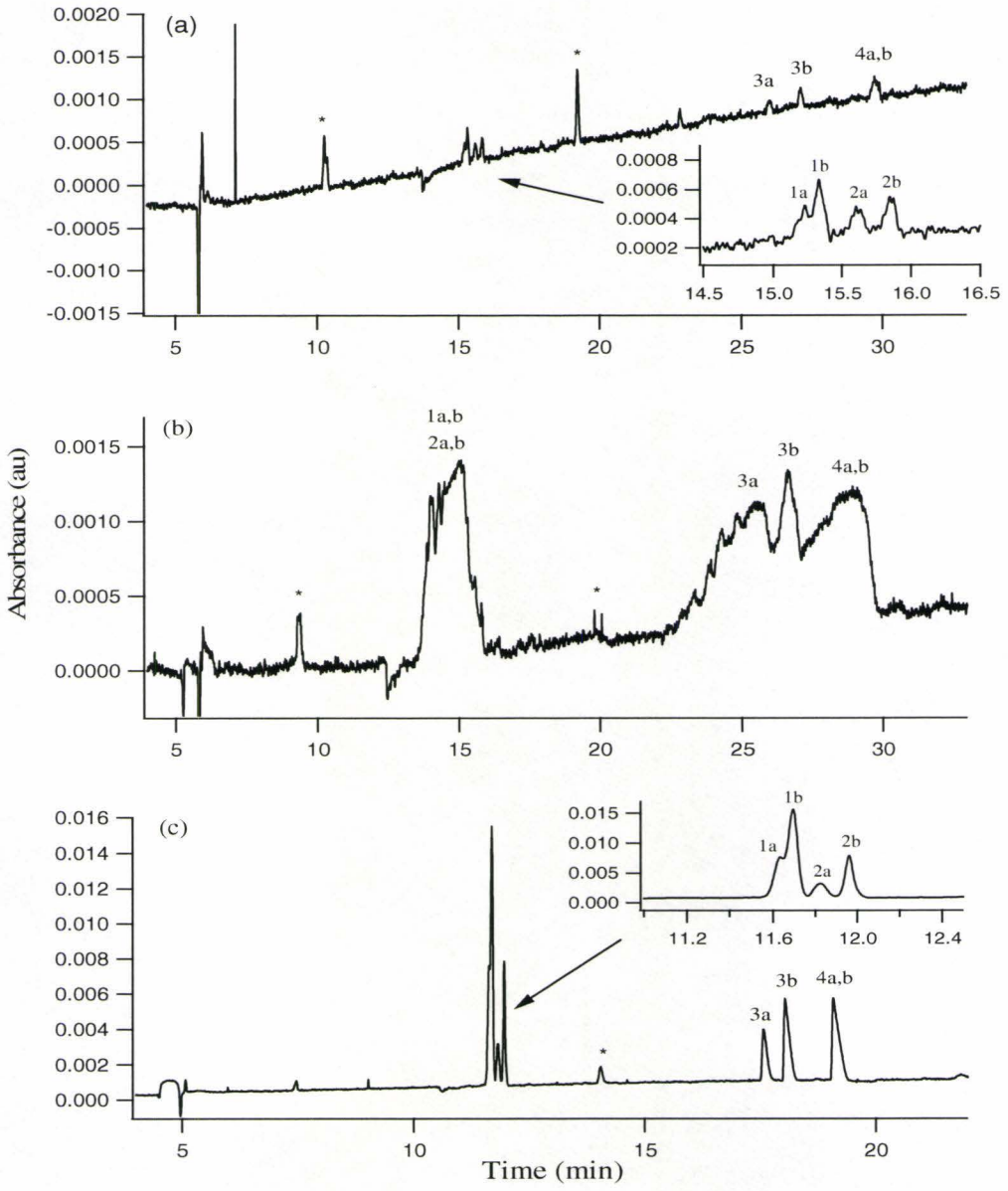

Figure 5.2: Electropherograms comparing CE separations for the analysis of eight amino acid enantiomers using in-capillary OPA/NAC derivatization (a) and on-line preconcentration with OPA/NAC derivatization using a continuous buffer junction (b) and a discontinuous buffer junction (c). Sample solutions contained 25 and 50 µM of the D- and L-amino acids, respectively, prepared in 140 mM borate (pH 9.5) ((a) and (b)) or 40 mM phosphate (pH 6.0) (c) using sample injection lengths of 3 s (a) and 100 s ((b) and (c)). Conditions: 140 mM borate, pH 9.5; voltage, 25 kV; effective capillary length, 65 cm; internal diameter, 50 µm; UV, 340 nm. Analyte peak numbers correspond to amino acid-isoindole adducts; 1a, D-Ser; 1b, L-Ser; 2a, D-Ala; 2b, L-Ala; 3a, D-Glu; 3b, L-Glu; 4a, D-Asp; 4b, L-Asp; *, OPA hydrolysis products.

analyte focusing prior to chemical labelling and detection. In contrast, *Figure 5.2(c)* demonstrates effective on-line sample preconcentration with in-capillary OPA/NAC derivatization of micromolar levels of D/L-amino acids using the same long sample injection plug of $w_{inj} \approx 6.1$ cm within a buffer junction[17]. It is apparent that approximately a 40-fold improvement in concentration sensitivity was achieved by SPCD-CE in *Figure 5.2(c)* relative to *Figure 5.2(a)*. In fact, *Figure 5.2(c)* clearly indicates that this technique also permitted shorter total analysis times while maintaining chiral resolution due to the lower average mobility of zwitterionic amino acids in the weakly acidic sample plug as well as the reduced effective capillary length for separation caused by the long injection plug. In the case of D-Ala, the measured w_{det} was approximately 0.60 cm in both *Figure 5.2(a)* and *Figure 5.2(c)*. This is reflected by a DIBR of 0.062 or a 16-fold band narrowing of the original sample plug. Further improvements in concentration sensitivity by SPCD-CE can be realized using larger injection volumes with wider and longer capillaries; however, this is limited by the complexity of the analyte mixture and the requirement for chiral resolution.

5.4.2. Dynamic noncovalent complexation and enantiomeric resolution

One of the inherent advantages of CE is the ability to tune the selectivity of a separation based on multiple equilibria and electrokinetic parameters in free solution via the use of additives in BGE. Cyclodextrins are chiral oligosaccharide macrocycles that are commonly used additives in chiral and achiral CE separations capable of dynamic inclusion complexation during electromigration with suitable guest analytes[31, 32]. In this study, a combination of in-capillary covalent OPA/NAC derivatization with noncovalent

dynamic complexation using β-cyclodextrin (β-CD) was examined to further enhance amino acid chiral resolution without the deterioration of band narrowing and sample enrichment properties of the technique. *Figure 5.3(a)* demonstrates the effect of the addition of 1 mM β-CD to the BGE using the SPCD-CE procedure described in *Figure 5.2(c)*. It is apparent that strong binding of the isoindole-labelled amino acids with β-CD is achieved, as reflected by differential analyte mobility shifts towards shorter migration times as a result of the increase in hydrodynamic radius of the complex. *Figure 5.3(a)* reveals that baseline resolution of D/L-Asp was achieved at the expense of co-migration of D/L-Ser with D-Ala. However, baseline resolution of D/L-Ala, D/L-Glu and D/L-Asp enantiomers were realized without the Ser interference, as shown in *Figure 5.3(a)* inset. Recently, Ciriacks and Bowser[33] demonstrated dynamic on-line microdialysis with CE laser-induced fluorescence (CE-LIF) analysis of D-Ser directly sampled from rat striatum using precolumn OPA labelling and hydroxypropyl-β-CD (HP-β-CD) as the chiral additive. Further studies (data not shown) using higher concentrations of β-CD and HP-β-CD were unsuccessful at simultaneous resolution of all eight amino acid enantiomers under these conditions. Improved resolution in CE can be achieved using multiple additives in the buffer such as the use of charged and neutral CD additive simultaneously[34]. Nevertheless, because D-Ala and D-Glu represent the major D-amino acid monomers associated with the peptidoglycan component of the bacterial cell wall, the original conditions used in *Figure 5.2(c)* without β-CD were used in subsequent work. *Figure 5.3(b)* demonstrates that under optimal conditions, this technique can be applied for micromolar-level analysis of trace levels of D-Ala and D-Glu in the presence of 95%

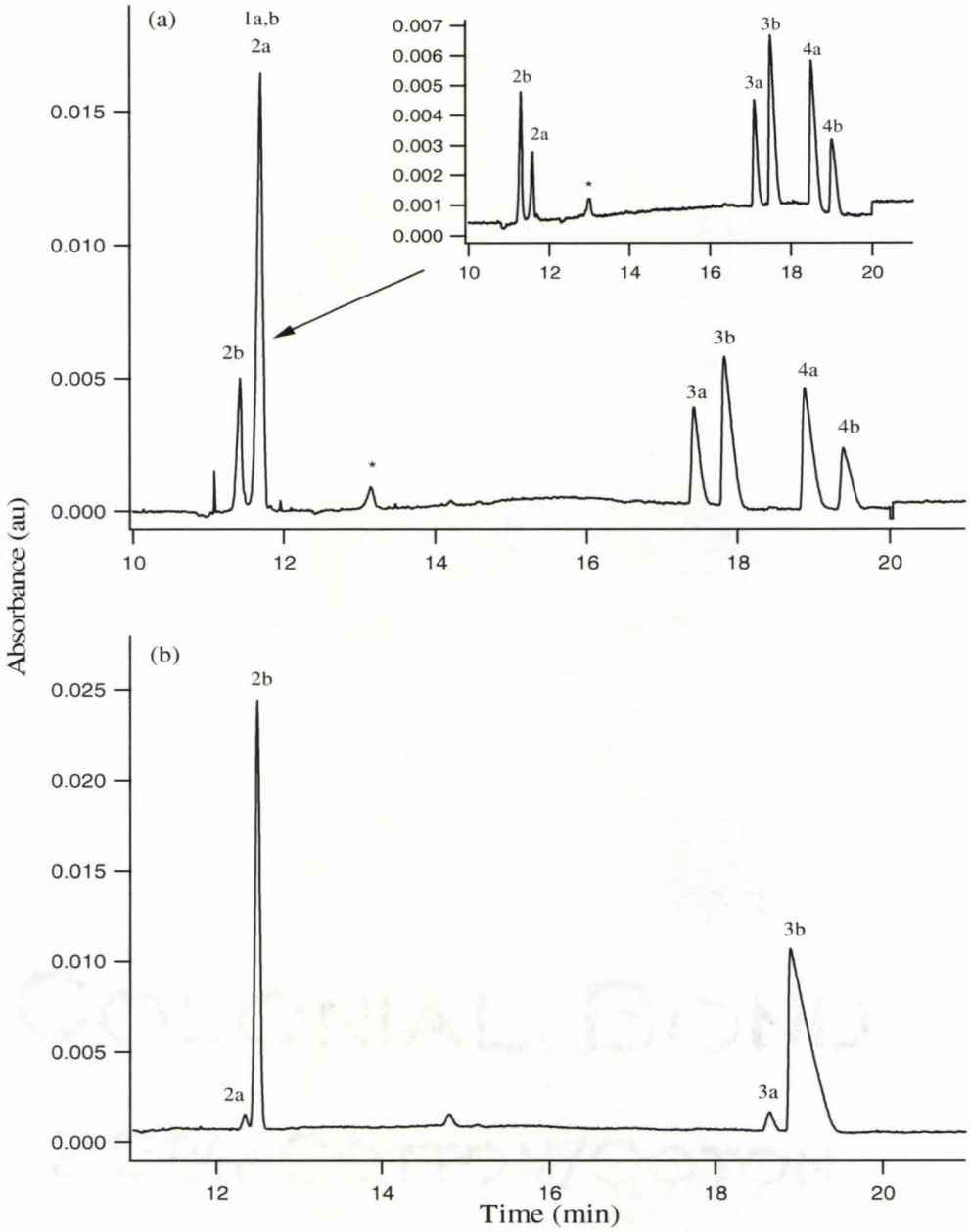

Figure 5.3: (a) Electropherogram demonstrating the use of 1 mM β-CD as a chiral additive to enhance enantioselectivity by dynamic inclusion complexation of amino acid adducts by SPCD-CE. Inset electropherograms shows the separation without D/L-Ser interference. (b) Enantioselective resolution of micromolar levels of D-amino acids from a 95% enantiomeric excess of their respective L-enantiomers without β-CD additive. Sample solutions contained 5 and 200 μM D- and L-Ala/Glu, respectively. All conditions are the same as in *Figure 5.2(c)* except panel (a), which uses 1 mM β-CD in the borate buffer.

Table 5.1: Validation parameters for integrated on-line preconcentration with in-capillary OPA/NAC derivatization technique for amino acid analysis by CE with UV detection.

Validation parameter	D-Ala	L-Ala	D-Glu	L-Glu
A. Interday precision (n = 5)				
Peak height/CV	4.3	5.6	9.2	10.3
Migration time/CV	1.0	1.0	1.8	1.1
B. Calibration curve[a] (n = 6)				
Linearity/R^2	0.9988	0.9983	0.9716	0.9907
C. Detection limit (S/N ≈ 3)				
Concentration/μM	0.4	0.4	0.6	0.6

[a] Duplicate measurements of six different concentrations over a 50-fold concnetraion range from 2 to 100 μM for D/L-amino acids using 6 μM taurine as the internal standard

enantiomeric excess of the corresponding L-amino acid with baseline resolution. *Table 3.1* summarizes the validation parameters examined in this study for SPCD-CE with UV detection. Linear calibration plots (R^2 of 0.990) were obtained for D/L-Ala and D/L-Glu using taurine as an internal standard over a 50-fold concentration range with a limit of detection of approximately 0.4 μM. The reproducibility (n = 5) of the integrated technique was acceptable with average coefficients of variation of approximately 7.4 and 1.3 % for quantitation (peak height) and apparent migration time, respectively. Additional improvement in detection limits can be realized when using SPCD-CE with LIF detection for automated, ultrasensitive and high-throughput metabolomics studies using capillary array platforms[35].

5.4.3. Electrokinetics of on-line sample preconcentration with in-capillary derivatization

Next, further insight into the mechanism of SPCD-CE was investigated by performing time-resolved electrophoretic experiments in which the effective capillary

length was change incrementally under otherwise identical conditions. The front boundary of the sample injection plug was placed at various positions from the detector window ($L_d \approx 0$ - 53 cm) by applying a low-pressure rinse for specific time intervals prior to voltage application, thereby providing a series of snapshots of analyte and reagent electromigrative processes as a function of capillary length[36]. The electropherograms in *Figure 5.4* were measure separately at 214 nm (i) and 340 nm (ii) to monitor changes in peak width (*i.e.*, extent of focusing) and peak area (*i.e.*, extent of chemical derivatization) of labelled amino acid adducts as well as residual OPA and NAC reagents, The series of wide-scale electropherograms serve to illustrate the relative positions of OPA and NAC reagents, whereas their zoomed insets highlight the distinct focusing process of amino acids during electromigration. *Figure 5.4(a)* clearly demonstrates that amino acid labelling by zone passing of OPA and NAC occurs rapidly (< 1 min) on voltage application despite the long sample plug placed near the detector window because both D-Ala and D-Glu isoindole adducts are detected at 340 nm. Moreover, it is apparent that significant focusing of D-Ala and D-Glu adduct peaks have already occurred at this interval relative to the initial w_{inj} of approximately 6 cm. It is important to note that due to the lower negative mobility of the D-Ala adduct, it has not yet zone separated from the broad NAC band, as shown in the 214 nm inset trace of *Figure 5.4(a)*. At this stage of the separation, the D-Ala adduct peak is more than 2.4-fold more narrow than the D-Glu peak. However, maximum band narrowing of the D-Ala adduct zone was observed to occur at a later stage in *Figure 5.4(b)*, whereas the D-Glu continued to broaden normally by diffusion reflected by a 4-fold broader w_{det} relative to D-Ala. Interestingly, D-Glu was

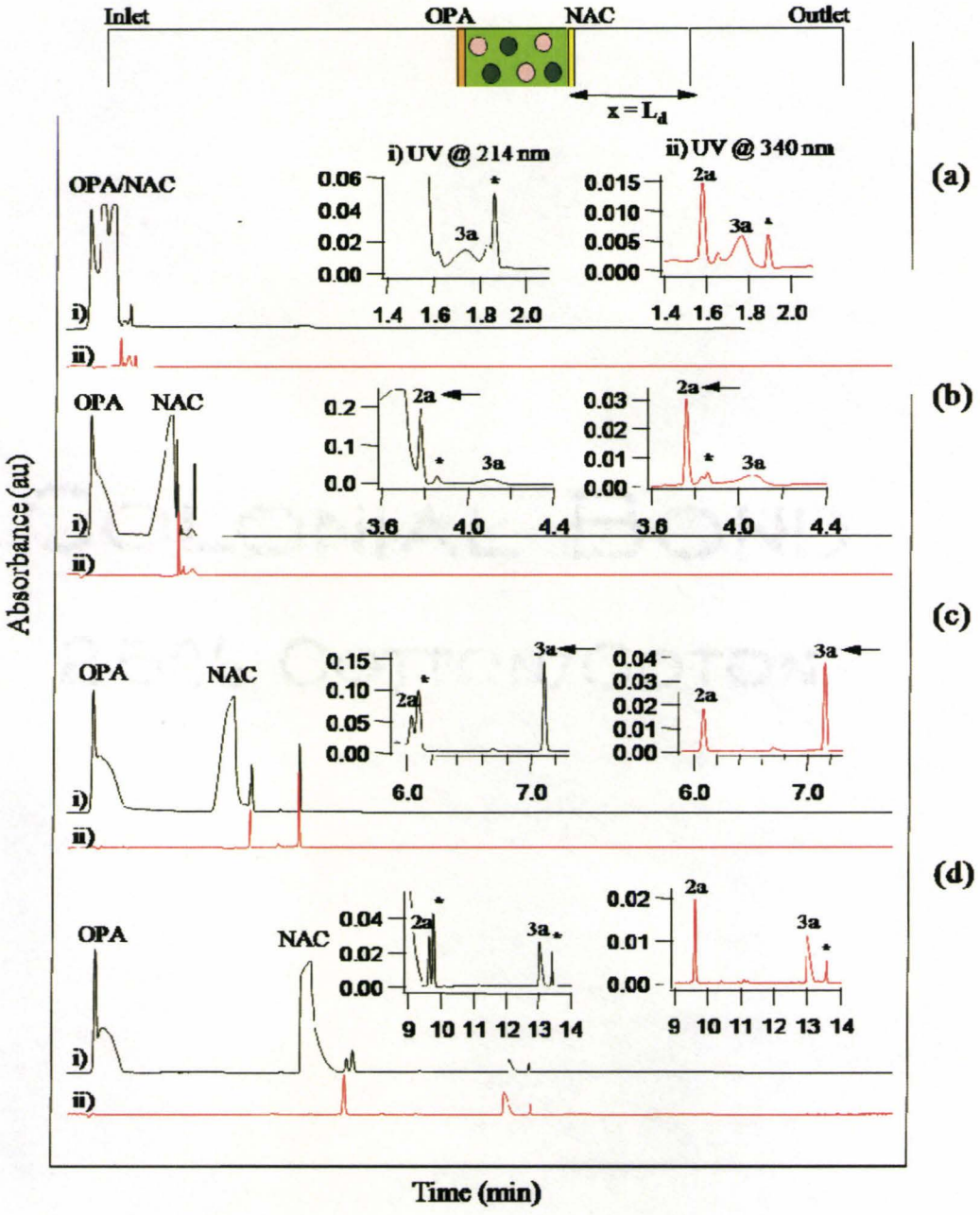

Figure 5.4: Series of electropherograms showing distinct time-dependent processes of amino acid focusing with in-capillary OPA/NAC derivatization by SPCD-CE electropherograms monitored with UV absorbance at 214 nm (i) and 340 nm (ii). Arrows note time-delayed amino acid adduct electrokinetic focusing associated with a moving pH boundary. All samples contained 20 μM D-Ala and D-Glu in 40 mM phosphate (pH 6.0). A long sample plug (6.1 cm) was placed at different positions from the capillary window using a low pressure rinse (0.5 psi or 3.5 kPa) to change the effective capillary length (L_d) from approximately 0 cm (a), 11.4 cm (b), 22.8 cm (c), and 30.5 cm (d). Other conditions are as described in *Figure 5.2(c)*.

then observed to undergo a discrete band narrowing transition in *Figure 5.4(c)* when using a longer effective capillary length of approximately 23 cm. Thereafter, both D-Ala and D-Glu adducts continue to broaden by normal diffusion with increasing zonal separation by CE. These observations suggest that two discrete yet additive band narrowing processes are operative in SPCD-CE: (i) an initial t-ITP focusing of the amino acids mediated by hydrogen phosphate and borate co-anions in the sample and BGE and (ii) a time-delayed focusing of amino acid adducts (after OPA labelling) via a moving pH boundary zone generated by dynamic pH junction[37, 38]. Previous computer modeling studies[37] demonstrated that the rate at which the moving pH boundary migrates across the sample zone is dependent on several experimental factors, including sample injection length, sample/buffer pH, and ionic strength, as well as on the intrinsic mobility of a weakly ionic analyte. *Figure 5.2(b)* and *(c)* clearly demonstrate that the buffer junction is crucial for reducing band dispersion of weakly ionic amino acid adducts prior to detection. To the best of our knowledge, this is the first reported example of a dual electrokinetic focusing procedure that permits chemical derivatization and band narrowing of dilute solutions of analytes that lack intrinsic chromophores by CE. Further work is necessary to better understand the mechanism of SPCD-CE when using discontinuous electrolyte systems that can also be applied to other classes of analytes.

5.4.4. Enantioselective amino acid flux analysis in the extracellular matrix of *E. coli*

Next, SPCD-CE was applied to assess changes in the composition of nutrients and metabolites in the extracellular matrix of *E. Coli* BL-21 (DE3) cultures. Mutants of this strain of *E. coli* are routinely used for protein expression in molecular biology because it

lacks specific proteases and proliferates well under a variety of conditions. The bacteria were cultured in complex nutrient-rich LB broth media (derived from yeast extracts) that contain all essential nutrients to sustain maximum bacterial growth. Metabolite flux analyses in bacteria often involve simple chemically defined medium based on a single carbon source tracer (*e.g.*, ^{13}C-labelled D-glucose) to selectively track substrate uptake and transformation into various intracellular metabolite pathways by GC-MS[39] or NMR[40]. However, these studies do not necessarily reflect bacterial metabolic fluxes in real complex media. Although *E. coli* bacteria are not considered to be amino acid auxotrophs, co-metabolism of amino acid substrates (*e.g.*, L-Ser) in complex media[40] previously has been demonstrated to enhance bacterial growth and biomass conversion, notably in the biosynthesis of recombinant protein. Moreover, *E. coli* mutants with enhanced amino acid catabolism confer significant growth advantage in stationary phase when conventional carbon sources have been depleted. In the current study, SPCD-CE was applied as a new method to directly analyze the time-dependent amino acid flux (uptake/release) in a complex broth medium. *Figure 5.5* highlights the specific changes in the selected amino acids during *E. coli* at 3 and 5 h relative to the control at 0 h, when bacteria were just inoculated in the medium. Because of the high concentration of most amino acid nutrients in the extracellular medium, a 20-fold dilution of the sample in phosphate buffer was performed prior to SPCD-CE analyses to maintain adequate resolution, as well as to stay within the linear range of the method. It is important to note that the high salt content of the broth solution did not affect the efficiency of SPCD-CE because analyte focusing, unlike conventional sample stacking, ideally operates using

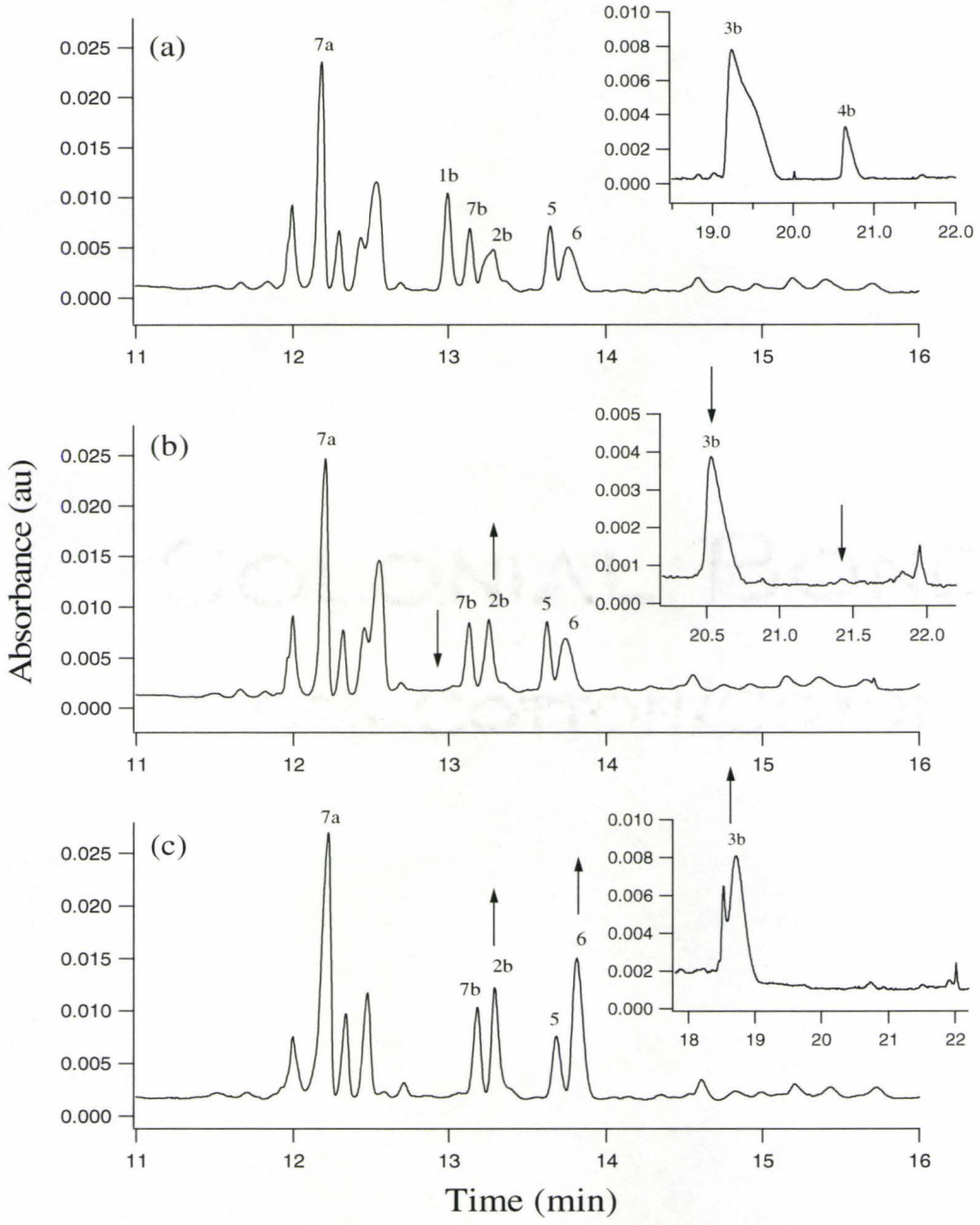

Figure 5.5: Single-step enantioselective amino acid flux analysis in the extracellular medium of *E. coli* by SPCD-CE. Electropherograms represent the extracellular media with 5 % seeding volume incubated for 0 h (control) (a), 3 h (b) and 5 h (c). Conditions and analyte peak labelling are described in *Figure 5.2(c)* except for the following: 5, taurine (6 μM, internal standard); 6, glycine; 7a, L-Lys; 7b, L-Lys side product. The direction of the arrow indicates that a net release (↑) or uptake (↓) of amino acid has been observed in the extracellular medium during bacterial growth. Note the rapid uptake of L-Ser and L-Asp and the steady-state enantioselective release of L-Ala, where as the doubly labelled L-Lys interference co-migrates with D-Ala.

conductive solutions[4]. *Figure 5.5* demonstrates qualitatively that specific uptake or release of amino acid metabolites is occurring in the extracellular medium of *E. coli* during bacterial growth. The time-dependent changes in amino acid concentration are indicated by the corresponding arrows in the *Figure* that highlight whether there is a net uptake/influx (down) or release/efflux (up). Metabolite flux analysis by SPCD-CE provides significant lower detection limits and higher peak capacities for enantiomeric resolution of complex sample mixtures relative to NMR as well as reduced sample handling and shorter total analysis times relative to GC-MS, which often requires off-line chemical derivatization (up to 1 h) at elevated temperatures for polar amino acid analyses[39].

5.4.5. Enzymatic assays for CE analysis for D/L-Ala identification in broth medium

As shown in *Figure 5.5*, it was observed that the basic amino acid L-Lys generated two peaks associated with singly and doubly labelled isoindole adducts. The latter minor peak comigrated with a similar mobility D-Ala, which was confirmed by comparing amino acid standards. *Figure 5.6* shows that two selective enzyme assays were performed on diluted broth samples prior to SPCD-CE analysis to confirm the identity of L-Ala as well as the lack of D-Ala. Note the selective loss of the L-Ala adduct peak and the increase in NADH (absorbance at 340 nm) generated as the product in the assay using L-Ala dehydrogenase in *Figure 5.6(b)* relative to the control in *Figure 5.6(a)*. Similarly, *Figure 5.6(c)* demonstrates that a significant reduction in the first major L-Lys adduct peak, as well as a complete loss of the second minor L-Lys adduct, was achieved when using L-Lys oxidase compared with the control in *Figure 5.6(a)*. The latter

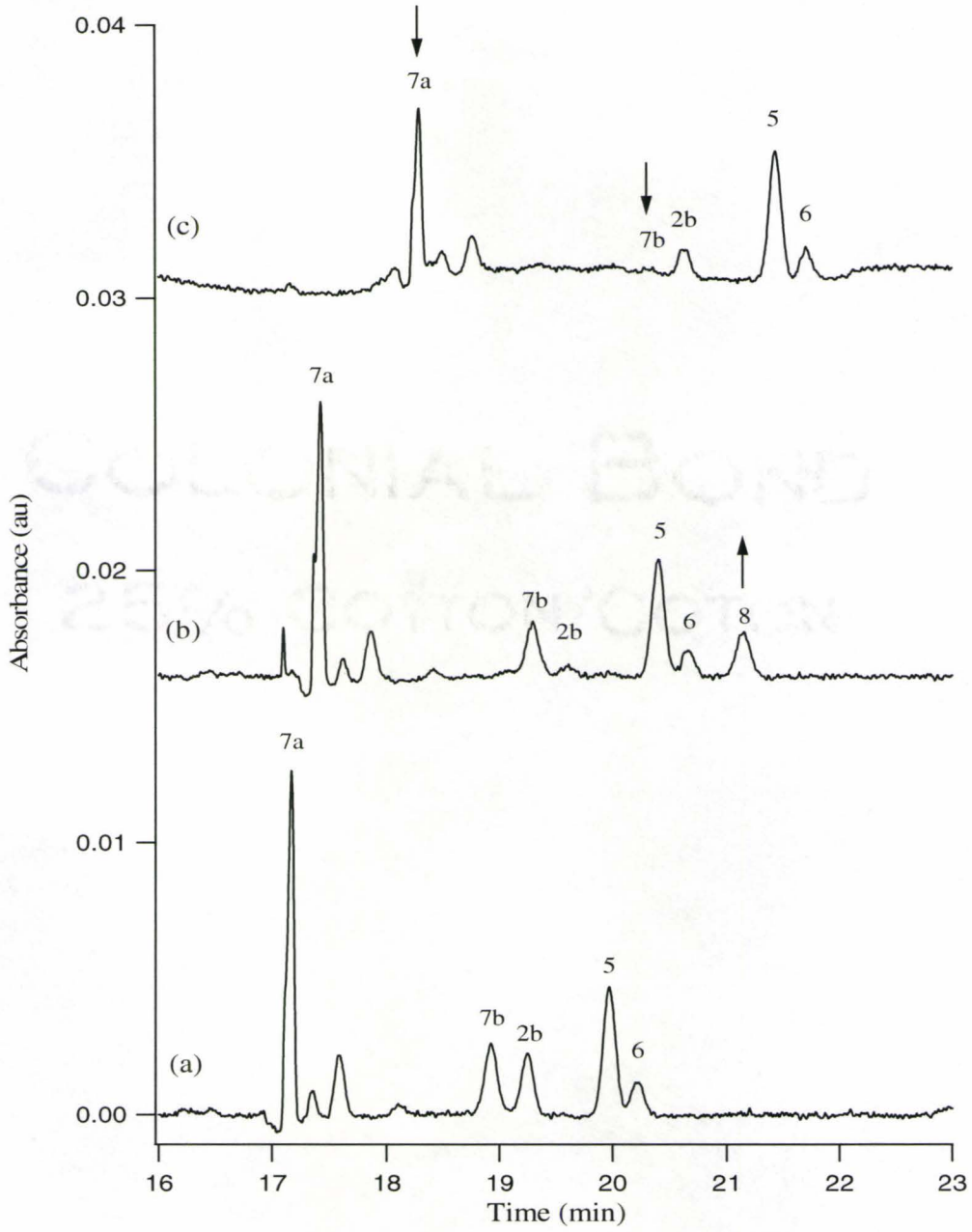

Figure 5.6: Analysis of selective enzymatic treatment of *E. coli* extracellular samples by SPCD-CE. Electropherograms represent the extracellular medium after 5 h of bacterial growth with no enzymatic treatment (a) and after 4 h treatment with L-Ala dehydrogenase (b) and L-Lys oxidase (c). Samples initially were diluted 100-fold in their respective buffer matrix, followed by a 6-fold dilution in phosphate buffer prior to CE. Conditions and analyte peak numbering are as described in *Figure 5.5* except for the following; 8, NADH, generated as a by-product by L-Ala dehydrogenase. Note that all separations have longer apparent times because they were performed using a 90 cm capillary for improved resolution to confirm enantioselective L-Ala efflux.

enzymatic assay did not require NAD^+ as a cofactor and so no NADH was generated in *Figure 5.6(c)*. Thus SPCD-CE analyses in conjunction with selective enzymatic assays provide qualitative evidence of L-Ala efflux without any known interference in the complex broth matrix and also confirmed the lack of D-Ala either in the original sample or released during bacterial growth.

5.4.6. Linear enantioselective L-Ala efflux during exponential bacterial growth

Figure 5.7(a) depicts the bacterial growth curve generated from optical density (turbidity) measurements in this study that reflect the total number of cells. It is apparent that the transition between initial lag phase and active cell division during the exponential (logarithmic) growth phase occurs at approximately 1.0 h. The generation time (doubling time) of *E. coli* in this study during exponential growth (1.5 - 5.0 h) was determined by linear regression to be 1.46 ± 0.08 h (R^2 of 0.9951). *Figure 5.7(b)* highlights quantitatively the major amino acid flux in the extracellular medium derived from SPCD-CE analyses as depicted in *Figure 5.5*. It is important to note the specific and rapid uptake (co-metabolism) of amino acids during *E. coli* growth in the preference order of L-Ser and L-Asp that corresponds to a recent report[41]. For example, L-Ser is considered as a vital intermediate of central metabolism[40] because it can serve as an alternative carbon substrate for pyruvate and energy production in several species of bacteria. However, it was noticed that L-Ala underwent a unique linear net efflux (release) that occurred discretely during the exponential growth phase of *E. coli*. Figure 5.7(c) demonstrates that a linear correlation (R^2 of 0.9990) was determined for net L-Ala efflux during exponential growth with a rate of 2.45 ± 0.07 $\mu M \cdot min^{-1}$. Moreover, there was a direct correlation

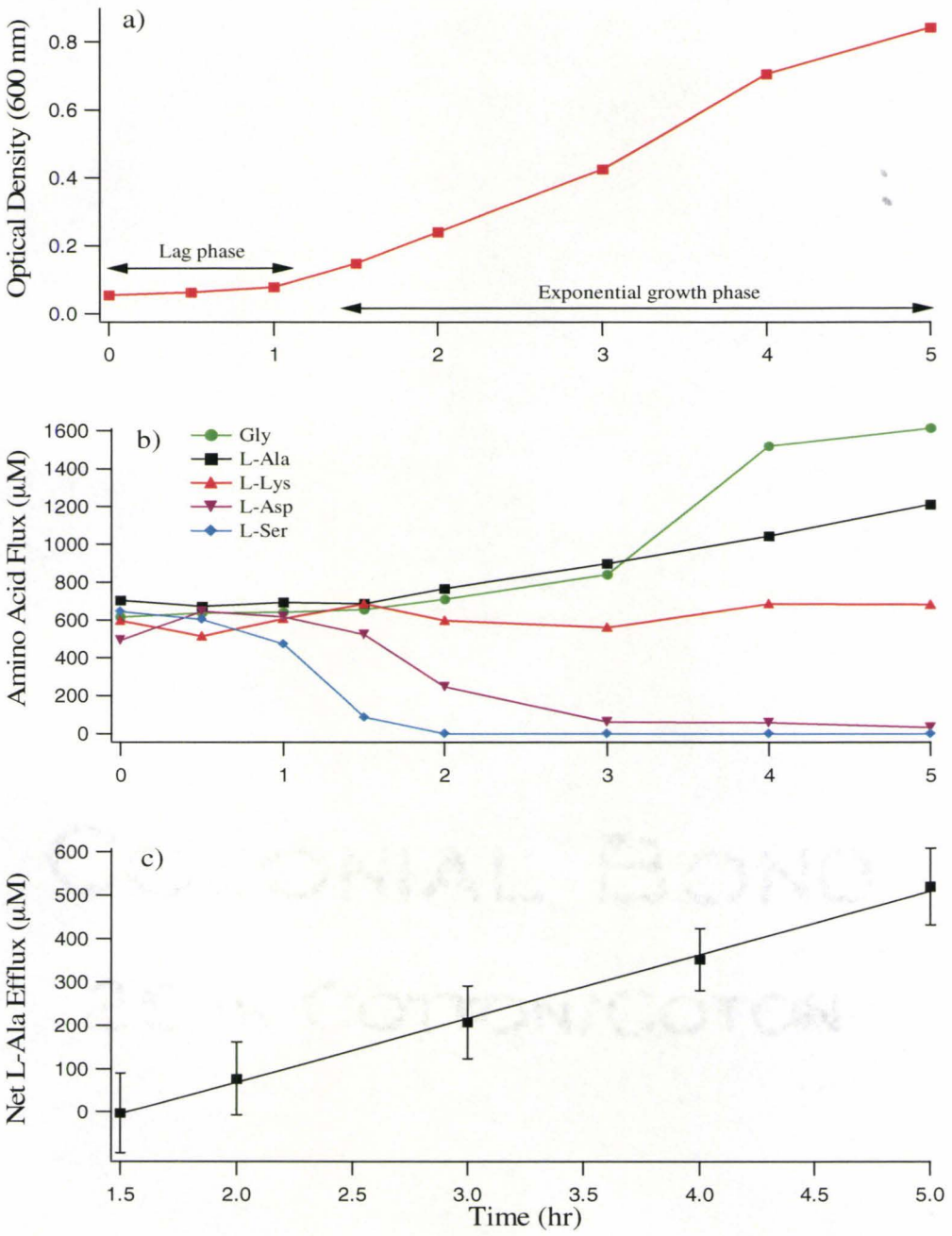

Figure 5.7: (a) *Escherichia coli* bacterial growth curve in this study obtained from optical density measurements at 600 nm. (b) Plots showing differential amino acid flux in the extracellular medium of *E. coli* bacteria batch cultures. Note the unique enantioselective efflux of L-Ala during exponential growth phase in contrast to other amino acids. (c) Linear L-Ala efflux correlation plot (R^2 = 0.9994) based on triplicate measurements as a function of incubation time during exponential growth of *E. coli*.

between net L-Ala efflux with measured optical density (R^2 of 0.9982) during exponential growth, indicating that L-Ala excretion is associated with bacterial cell division and increasing semilogarithmically with total number of cells. In contrast, there was no detectable level of D-Ala or D-Glu released by the *E. coli* during bacterial growth despite their relatively high intracellular concentrations associated with the peptidoglycan component of the cell wall, which undergoes significant turnover during bacterial growth by the enzymatic actions of transglycosidases, endopeptidases and amidases[42]. Thus, there exists specific intracellular bacterial pathways for recycling and converting D-amino acids into other metabolites that can be transported for excretion such as L-Ala. An earlier report had observed differential D/L-Ala distribution in *E. coli* bacteria, with more that 85 % of the free intracellular Ala in the D- configuration, whereas L-Ala was found exclusively in the extracellular matrix[43]. However, there was no information regarded the kinetics of L-Ala transport relative to other amino acids in the broth medium. Interestingly, other types of Gram-negative bacteria, such as *Helicobacter pylori*, recently have been shown to metabolize D-Ala as carbon substrates because of the presence of genes encoding for D-amino acid dehydrogenase[44]. *Figure 5.7(b)* also demonstrates that Gly was observed to undergo a specific nonlinear efflux at later stages of bacterial growth that is quite distinct from L-Ala, whereas there was no significant change observed in L-Lys. Further studies will be performed to better understand amino acid metabolism in wild-type and mutant strains of *E. coli* over longer incubation times (stationary phase) in which metabolic fluxes are normalized to total cell and viable (colony-forming unit) cell densities. In addition, the impact of limiting nutrient levels and the reproducibility of

different bacterial batches will be examined to determine whether L-Ala efflux also occurs under nutrient-stressed conditions during bacteria stringent response. These fundamental investigations are relevant for understanding the efficacy of new classes of antibiotics that inhibit specific enzymatic activity involving peptidoglycan biosynthesis and amino acid metabolism such as alanine racemase.

5.5. Summary and conclusion

A new strategy for integrating on-line sample preconcentration with in-capillary chemical derivatization by CE and UV detection was developed for enantioselective analysis of micromolar levels of amino acids that lack intrinsic chromophores in complex biological samples. Time-dependent electrophoretic studies of long sample injection plugs revealed two additive electrokinetic processes occurring both prior to and after chemical labelling by zone passing of OPA/NAC reagents during electromigration. Efficient analyte band narrowing was essential for realizing high-resolution chiral amino acid analyses with sub-micromolar detection limits. SPCD-CE was directly applied to assess the extracellular amino acid flux in the complex broth media of *E. coli* cultures with minimal sample handling. Enantioselective amino acid influx was observed at different stages of co-metabolism of L-Ser and L-Asp, where as linear efflux of L-Ala was noticed during the exponential growth phase of *E. coli* despite the high intrinsic intracellular levels of D-Ala. SPCD-CE offers a unique format for performing rapid, sensitive, and enantioselective analyses of amino acids, compared with conventional analytical techniques, and is amendable for high-throughput screening using capillary array or microfluidic platforms.

5.6. References

1. A. R. Wheeler, W. R. Throndset, R. J. Whelan, A. M. Leach, R. N. Zare, Y. H. Liao, K. Farrell, I. D. Manger and A. Daidron, *Anal. Chem.*, 2003, **75**, 3581-3586.
2. H. Hisamoto, Y. Nakashima, C. Kitamura, S. Funano, M. Yasuoka, K. Morishima, Y. Kikutani, T. Kitamori and S. Terabe, *Anal. Chem.*, 2004, **76**, 3222-3228.
3. L. Krivankova, A. Vrana, P. Gebauer and P. Bocek, *J. Chromatogr. A*, 1997, **772**, 283-295.
4. R. L. Chien and D. S. Burgi, *Anal. Chem.*, 1992, **64**, 1046-1050.
5. J. P. Quirino and S. Terabe, *Science*, 1998, **282**, 465-468.
6. P. Britz-McKibbin and D. D. Y. Chen, *Anal. Chem.*, 2000, **72**, 1242-1252.
7. P. Britz-McKibbin, K. Otsuka and S. Terabe, *Anal. Chem.*, 2002, **74**, 3736-3743.
8. S. Oguri, K. Yokoi and Y. Motohase, *J. Chromatogr. A*, 1997, **787**, 253-260.
9. A. Taga, A. Nishino and S. Honda, *J. Chromatogr. A*, 1998, **822**, 271-279.
10. Y. Zhang and F. A. Gomez, *Electrophoresis*, 2000, **21**, 3305-3310.
11. S. v. Dyck, E. Kaale, S. Novakova, Z. Glatz, J. Hoogmarten and A. v. Schepdael, *Electrophoresis*, 2003, **24**, 3868-3878.
12. N. J. Reinhoud, U. R. Tjaden and J. v. d. Greff, *J. Chromatogr. A*, 1994, **673**, 255-266.
13. R. M. Lattore, J. Saurina and S. Hernandez-Cassou, *Electrophoresis*, 2001, **22**, 4355-4361.
14. S. Oguri, H. Tanagaki, M. Hamaya, M. Kato and T. Toyo'oka, *Anal. Chem.*, 2003, **75**, 5240-5245.

15. H. Wu, A. Wheeler and R. N. Zare, *Proc. Natl. Acad. Sci. USA*, 2004, **101**, 12809-12813.

16. A. S. Ptolemy and P. Britz-McKibbin, *Analyst*, 2005, **130**, 1263-1270.

17. A. S. Ptolemy, M. LeBihan and P. Britz-McKibbin, *Electrophoresis*, 2005, **26**, 4206-4214.

18. P. Britz-McKibbin, T. Nishioka and S. Terabe, *Anal. Sci.*, 2003, **19**, 99-104.

19. N. O. G. Jorgensen, R. Stepanaukas, A. G. U. Pedersen, M. Hansen and O. Nyrobe, *FEMS Microbiol. Ecol.*, 2003, **46**, 269-280.

20. M. D. McCarthy, J. I. Hedges and R. Benner, *Science*, 1998, **281**, 231-234.

21. C. Simo, A. Rizzi, C. Barbas and A. Cifuentes, *Electrophoresis*, 2005, **26**, 1432-1441.

22. K. B. O'Brien, M. Esguerra, R. F. Miller and M. T. Bowser, *Anal. Chem.*, 2004, **76**, 5069-5074.

23. A. M. Skelley and R. A. Mathies, *J. Chromatogr. A*, 2003, **1021**, 191-199.

24. H. Holmes, *FEMS Microbiol. Rev.*, 1996, **19**, 85-116.

25. H. H. Wong, Y. C. Kim, S. Y. Lee and H. N. Chang, *Biotechnol. Bioeng.*, 1988, **60**, 271-276.

26. A. Galkin, L. Kulakova, T. Yoshimura, K. Soda and N. Esaki, *Appl. Environ. Microbiol.*, 1997, **63**, 4651-4656.

27. W. J. M. Underberg and J. C. M. Waterval, *Electrophoresis*, 2002, **23**, 3922-3933.

28. M. C. G. Alvarez-Coque, M. J. M. Hernandez, R. M. V. Camanas and C. M. Fernandez, *Anal. Biochem.*, 1989, **178**, 1-7.

29. P. Britz-McKibbin and S. Terabe, *J. Chromatogr. A*, 2003, **1000**, 917-934.

30. A. S. Ptolemy and P. Britz-McKibbin, *J. Chromatogr. A*, 2006, **1006**, 7-18.

31. C. L. Cooper, J. B. Davis, O. O. Cole and M. J. Sepaniak, *Electrophoresis*, 1994, **15**, 785-792.

32. P. Britz-McKibbin and D. D. Y. Chen, *Electrophoresis*, 2002, **23**, 880-888.

33. C. M. Ciriacks and M. T. Bowser, *Anal. Chem.*, 2004, **76**, 6582-6587.

34. A. R. Kranack, M. T. Bowser, P. Britz-McKibbin and D. D. Y. Chen, *Electrophoresis*, 1998, **19**, 338-346.

35. H. J. Crabtree, S. J. Bay, D. F. Lewis, L. D. Coulson, G. Fitzpatrick, D. J. Harrison, S. L. Delinger, J. Z. Zhang and N. J. Dovichi, *Electrophoresis*, 2000, **21**, 1329-1335.

36. J. Palmer, N. Munro and J. Landers, *Anal. Chem.*, 1999, **71**, 1679-1687.

37. J. B. Kim, P. Britz-McKibbin, T. Hirokawa and S. Terabe, *Anal. Chem.*, 2003, **75**, 3986-3993.

38. M. Stedry, M. Jaros, K. Vcelakova and B. Gas, *Electrophoresis*, 2003, **24**, 536-547.

39. E. Fischer, N. Zamboni and U. Sauer, *Anal. Biochem.*, 2004, **235**, 308-316.

40. R. Netzer, P. Peters-Wendisch, L. Eggeling and H. Sahm, *Appl. Environ. Microbiol.*, 2004, **70**, 7148-7155.

41. A. J. Wolfe, *Microbiol. Mol. Biol. Rev.*, 2005, **69**, 12-50.

42. W. Vollmer and J. V. Holtje, *J. Bacteriol.*, 2004, **186**, 5978-5987.

43. J. M. Manning, N. E. Merrifield, W. M. Jones and E. C. Gotschlich, *Proc. Natl. Acad. Sci. USA*, 1974, **71**, 417-421.

44. K. Nagata, Y. Nagata, T. Sato, M. A. Fujino, K. Nakajima and T. Tamura, *Microbiology*, 2003, **149**, 2023-2030.

Chapter VI

Future Applications and Prospects for SPCD-CE

VI. Future Applications and Prospects for SPCD-CE

Our preliminary studies have demonstrated efficient integration of sample preconcentration with chemical derivatization in CE (SPCD-CE), which represents a convenient platform for realizing high-throughput, ultra-sensitive and enantioselective analyses of low abundance polar metabolites in complex biological samples. Since multiple sample pretreatment steps are performed during electromigration directly in-capillary, via inexpensive discontinuous electrolyte systems, complicated off-line sample handling can be avoided. Single-step analysis by SPCD-CE is a feature particularly significant in bioanalytical chemistry since sample pre-treatment often represents the most time-consuming, labour-intensive and critical step that influences the overall success of an assay. To this end, it is envisioned that future SPCD-CE protocols will be offer a rapid, automated and reproducible platform for directed metabolomic studies of low abundance metabolites that are biologically relevant yet difficult to quantify by traditional spectroscopic or chromatographic methods. This thesis has also contributed to a deeper understanding of the fundamental thermodynamic and electrokinetic parameters influencing separations in CE. The minimum criteria necessary for achieving enantiomeric resolution was investigated when using chiral selectors that exploit differential weak interactions with stereoisomers in CE. In fact, the work in this thesis illustrated for the first time a unique multivariable approach for high resolution chiral separations that combined covalent chemical modifications (diastereomeric adduct formation OPA/NAC labelling by SPCD-CE) with specific non-covalent interactions (inclusion complexation by β-CD) directly in-capillary for enantiomeric excess

determination of sub-micromolar amounts of low abundance D-amino acids.

6.1. Future research directions: Single-step analysis for glutathione - an elusive biomarker of oxidative stress

The overproduction of reactive oxygen or nitrogen species (ROS and RNS respectively) leads to a relative imbalance with the human body's natural anti-oxidants. This oxidative stress is thought to be associated with normal ageing processes, as well as a risk factor for the development of several chronic human diseases including various neurological disorders (e.g. Parkinson's, Alzheimer's and Huntington's Disease), cardiovascular disease, atherosclerosis, ischemic stroke, diabetes, low birth weight, cystic fibrosis and Eales' disease[1]. However, a direct causal relationship between the onset and/or progression of these diseases and oxidative stress has yet to be established. This deficiency is in part related to the lack of a suitable biomarker in which changes in its concentration can be directly correlated to the early onset of disease. Recently, there has been much interest in the development of reliable analytical methods for determination of the redox status of patients as an indicator of oxidant stress for early detection of atherogenesis, cardiovascular and other vascular diseases[2]. This has prompted researchers to quantify the relative amounts of reduced glutathione (GSH), oxidized glutathione (GSSG) and other physiologically relevant thiols in biofluids, since the ratio of GSH:GSSG can be applied as a useful indicator of cellular oxidative stress[3, 4].

To date, reliable analysis of GSH:GSSG levels is plagued with technical challenges due to the chemical lability of GSH and its high intra-cellular concentration. Indeed, Rossi *et al.* recently concluded that the vast majority of the reported analytical

methods for ratiometric glutathione analyses in the literature are biased due to a significant amount of auto-oxidation that occurs during off-line sample handling[5]. Given that GSH and GSSG exist in human red blood cells at low mM and μM concentration levels, respectively, a small amount of auto-oxidation of GSH can lead to a significant underestimation of the apparent GSH:GSSG ratio with increased variability[5]. Therefore, efficient and rapid sample processing strategies that minimize auto-oxidation is a critical for reliable analysis of GSH:GSSG[6, 7]. Despite numerous techniques developed for the measurement of GSH:GSSG reported in literature, such as GC-MS[8, 9], HPLC with electrochemical[10] and fluorescence detectors[11-13], and CE-LIF[2, 14], rapid yet reliable methods for an *accurate* measurement of this ratio relative to nicotinamide dinucleotide coenzymes within a single format is still lacking. This is particularly relevant since GSH:GSSG levels are regulated by the NADPH-dependent enzyme glutathione reductase. SPCD-CE represents an attractive strategy for the simultaneous analysis of multiple redox biomarkers of interest for accurate assessment of cellular redox-status that is applicable for early detection of oxidative stress associated with chronic and degenerative disorders. Presented within the remaining portions of this section are preliminary results demonstrating the feasibility of SPCD-CE for the selective preconcentration and chemical labelling of GSH and NADPH in complex sample mixtures. For this work the general sample injection procedure used for previous SPCD-CE studies was modified slightly (*Figure 6.1*), as no thiol co-reactant is required for OPA labelling of GSH due to the unique heterobifunctional reaction with the free primary amine and thiol functional groups of the tripeptide[12]. *Figure 6.2* demonstrates on-line preconcentration of

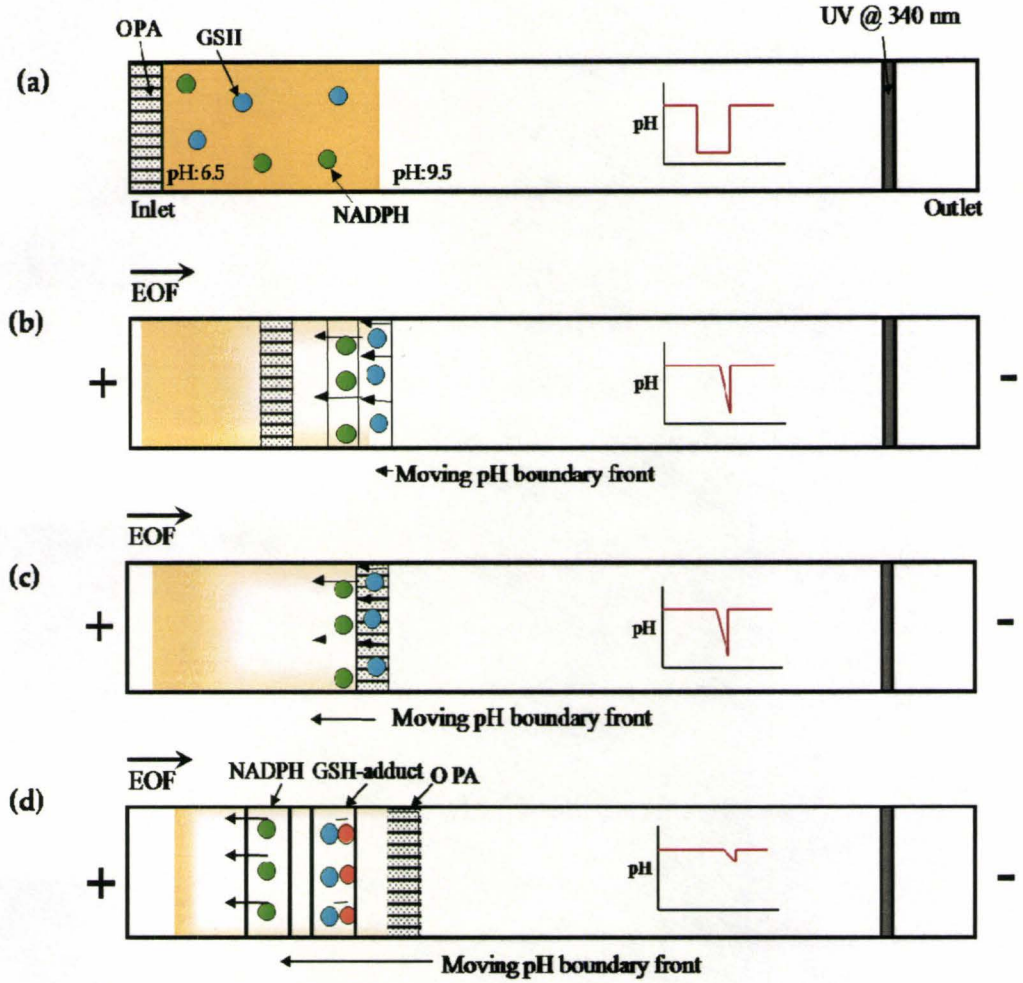

Figure 6.1: General principle of SPCD-CE for single-step analysis of GSH and NADPH: (a) multiple hydrodynamic injection sequence; (b) on-line sample preconcentration; (c) in-capillary chemical labelling of GSH by zone passing of OPA; (d) chiral separation of GSH-isoindole adduct and NADPH. Note that only GSH is labelled by OPA as NADPH is un reactive and natively UV absorbant at 340 nm.

micromolar levels of the two reduced nicotinamide dinucleotides with in-capillary labelling of glutathione (GSH), γ-GluCys (the biosynthetic precursor to GSH), and an ethyl ester GSH derivative (GSH-OEt) , using *o*-phthalaldehyde (OPA). This single-step analysis of multiple redox-active metabolites (*i.e.,* GSH, NADPH) can be realized without interferences due to the sensitivity enhancement provided by on-line sample preconcentration with selective chemical labelling and UV detection at 340 nm. Proper

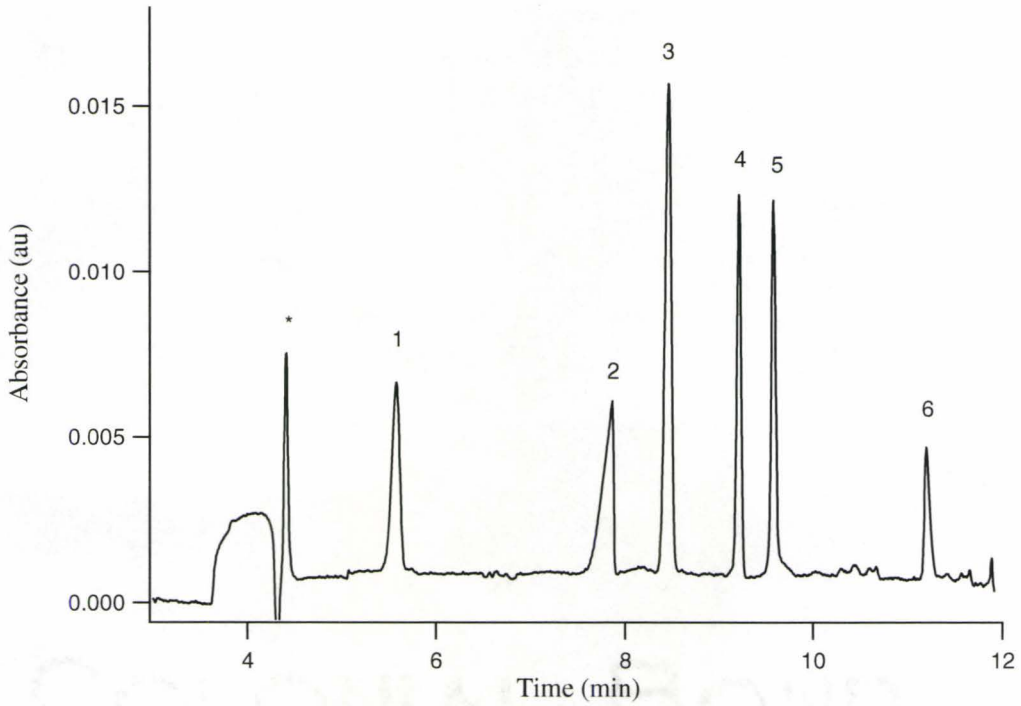

Figure 6.2: Single-step analysis of micromolar levels (10 μM) of redox-active metabolites by SPCD-CE using dynamic pH junction with in-capillary OPA labelling for selective chemical labelling of glutathione metabolites, GSH, γ-GluCys and GSH-OEt. Conditions: Background electrolyte, 100 mM borate buffer with 1 mM EDTA, pH 9.5; Sample buffer, 30 mM phosphate buffer with 1 mM EDTA, pH 6.5; Sample injection sequence consisted of a 100 s hydrodynamic injection of the sample followed by a 10 s injection of 100 mM OPA; voltage, 30 kV; capillary length, 67 cm; UV, 340 nm. Analyte peak numbering corresponds to; 1, GSH-OEt; 2, p-nitrophenol; 3, GSH; 4, γ-GluCys; 5, NADH; 6, NADPH; where 1, 3 and 4 correspond to OPA-isoindole adducts and * refers to excess OPA that co-migrates with the electroosmotic flow.

validation and expansion of this SPCD-CE procedure, to the selective analysis of GSSG in the presence of excess GSH, is required for the protocol to be considered viable alternative to conventional analytical techniques.

6.2. Future prospects of SPCD-CE

SPCD-CE represents a single-step strategy for the on-line integration of sample pretreatment allowing for sub-micromolar detection of metabolites lacking intrinsic chromophores by CE. In essence, the capillary in CE can serve as a unique

multifunctional analytical tool, namely as preconcentrator, microreactor, chiral selector and separator. If used in concert with multiplexed capillary array systems, SPCD-CE can provide a massively parallel and integrated platform for high-throughput metabolomic analyses unparalleled to conventional techniques.

In order to advance SPCD-CE, further improvements in the enantioselectivity for chiral separations that are directly applicable in complex biological matrices should be examined to minimize interferences seen in the earlier studies. The potential to achieve sub-nanomolar detection limits using SPCD-CE with LIF detection should also be investigated using near-UV laser excitation using inexpensive solid-state lasers. The application of SPCD-CE using alternative labels and complementary electrokinetic focusing techniques[15] should be explored as a way to provide greater selectivity for targeted analysis of different classes of metabolites, including peptides and protein. In addition, better quantitative understanding of the mechanism of SPCD-CE via computer modeling of fundamental electromigration processes[16] is needed for rapid virtual method development based on electrophoretic simulations. It is anticipated that this work will stimulate further interest in developing more integrated analytical strategies that take advantage of selective covalent and non-covalent interactions in CE when using discontinuous electrolyte systems.

In a larger context, the ease of integrating sample pretreatment processes directly in-capillary by SPCD-CE represents a truly unique, relatively unexplored feature of CE for realizing high-throughput analyses of low abundance metabolites in complex sample matrices. Additionally, the principles and philosophy of SPCD-CE, in terms of the

integration of multiple sample pretreatment steps typically required for challenging targeted metabolite analyses, may also be translated to emerging micro-chip based CE platforms, such as the recently introduced μ-TAS protocol[17, 18]. A specific example in which the SPCD-CE may offer clear benefits over existing labour intensive protocols can be found in the recent efforts to determine the amino acid enantiomeric excess of the Martian surface, as potential indicator of the existence of extraterrestrial life, via microchip CE[19, 20].

5.6. References

1. A. S. Ptolemy, R. Lee and P. Britz-McKibbin, *Amino Acids*, 2007, **33**, 3-18.
2. C. Carru, L. Deiana, S. Sotogia, G. M. Pes and A. Zinellu, *Electrophoresis*, 2004, **25**, 882-889.
3. R. Brigelius, R. Lenzen and H. Sies, *Biochem. Pharmacol.*, 1982, **31**, 1637-1641.
4. W. A. Kleinman and J. P. R. Jr., *Biochem. Pharmacol.*, 2000, **60**, 19-29.
5. R. Rossi, I. Dalle-Donne, A. Milzani and D. Giustarni, *Clin. Chem.*, 2006, **52**, 1406-1411.
6. A. Andersson, A. Lindgren and B. Hultberg, *Clin. Chem.*, 1995, **41**, 361-366.
7. P. M. Ueland, H. Refsum, S. P. Stabler, M. R. Malinov, A. Anderson and R. H. Allen, *Clin. Chem.*, 1993, **38**, 1311-1315.
8. J. O. Saas and W. J. Endres, *J. Chromatgr. A*, 1997, **776**, 342-347.
9. H. Katoka, K. Takagi and M. Makita, *J. Chromatgr. B*, 1995, **662**, 421-425.
10. S. C. Martin, A. C. Hilton, W. A. Bartlett and A. F. Jones, *Biomed. Chromatogr.*, 1999, **13**, 81-82.

11. D. Tsikas, J. Sandmann, D. Holzberg, P. Pantazis, M. Raida and L. C. Frolich, *Anal. Biochem.*, 1999, **273**, 32-40.

12. C. Parmentier, P. Leroy, M. Wellman and A. Nicolas, *J. Chromatgr. B*, 1998, **719**, 37-46.

13. R. H. Williams, *Clin. Chem.*, 2001, **47**, 1031-1039.

14. A. Zinellu, S. Sotgia, M. F. Usai, R. Chessa, L. Deiana and C. Carru, *Electrophoresis*, 2005, **26**, 1963-1968.

15. A. S. Ptolemy and P. Britz-McKibbin, *Analyst*, 2008, *submitted.*

16. R. Lee, A. S. Ptolemy, L. Niewczas and P. Britz-McKibbin, *Anal. Chem.*, 2007, **79**, 403-415.

17. H. Hisamoto, Y. Nakashima, C. Kitamura, S. Funano, M. Yasuoka, K. Morishima, Y. Kikutani, T. Kitamori and S. Terabe, *Anal. Chem.*, 2004, **76**, 3222-3228.

18. A. R. Wheeler, W. R. Throndset, R. J. Whelan, A. M. Leach, R. N. Zare, Y. H. Liao, K. Farrell, I. D. Manger and A. Daidron, *Anal. Chem.*, 2003, **75**, 3581-3586.

19. J. L. Bada, *Proc. Natl. Acad. Sci. USA*, 2001, **98**, 797-800.

20. A. M. Skelley, J. R. Scherer, A. D. Aubrey, W. H. Glover, R. H. C. Ivester, R. P. Ehrenfreund, F. J. Grunthaner, J. L. Bada and R. A. Mathies, *Proc. Natl. Acad. Sci. USA*, 2005, **102**, 1041-1046.